

©Copyright 2016

Yury Dvorkin

Operations and Planning in Sustainable Power Systems

Yury Dvorkin

A dissertation
submitted in partial fulfillment of the
requirements for the degree of

Doctor of Philosophy

University of Washington

2016

Reading Committee:

Daniel S. Kirschen, Chair

Miguel A. Ortega-Vazquez

Richard D. Christie

Program Authorized to Offer Degree:
Electrical Engineering

University of Washington

Abstract

Operations and Planning in Sustainable Power Systems

Yury Dvorkin

Chair of the Supervisory Committee:
Professor Daniel S. Kirschen
Department of Electrical Engineering

Renewable generation, e.g., wind power and photovoltaic resources, and non-traditional energy providers, e.g, flexible loads and energy storage, have demonstrated their potential to eliminate or, at least, to alleviate dependency on costly and depletable energy resources, as well as to reduce gas emissions, thus fostering a transition toward a sustainable power sector. As result of this transition, future power systems will require new decision-making tools that would rigorously account for unique features of the renewable generation and non-traditional energy providers to adopt these means at socially acceptable costs. However, operational and long-term planning decision-making tools for power systems have not kept pace with this dramatic growth in renewable generation. Hands-on experience in real-life power systems has revealed the inefficiency of these tools and demonstrated the need for an overhaul of the current approaches to power system operation and planning.

This dissertation examines existing approaches to account for the stochasticity of renewable generation in short-term planning tools and proposes two new unit commitment models based on stochastic and interval optimization techniques. These models are demonstrated to maintain acceptable levels of reliability and reduce the system-wide operating cost, as well as to increase utilization of available renewable generation. Furthermore, this dissertation presents a new framework that

enables participation of renewable generation in providing ancillary services, e.g., active power reserve, that facilitates higher penetration levels of this generation.

This dissertation describes a new bilevel model that determines the optimal location and size of merchant storage devices to perform the spatiotemporal energy arbitrage. This method aims to simultaneously reduce the system-wide operating cost and the cost of investments in ES while ensuring that merchant storage devices collect sufficient profits to fully recover their investment cost. This model is used to demonstrate that existing power system with perspective renewable generation portfolios will have sufficient profit opportunities to install merchant storage.

TABLE OF CONTENTS

	Page
List of Figures	vi
Glossary	ix
Part I: Introduction to Sustainable Power Systems	1
Chapter 1: Introduction	2
1.1 Embracing a Sustainable Future	2
1.2 Challenges	4
1.2.1 Uncertainty and Variability	5
1.2.2 Reduced Controllability	7
1.2.3 Market Implications of Renewable Generation	8
1.2.4 Is Energy Storage a Panacea?	10
1.2.5 Modelling Accuracy and Computational Complexity	11
1.3 Reader’s Guide	12
Chapter 2: Literature Review	14
2.1 Short-term Operations	14
2.1.1 Objectives	14
2.1.2 Forecasting of Renewable Generation	17
2.1.2.1 Statistical Approaches	18
2.1.2.2 Numerical Weather Prediction	20
2.1.3 Unit Commitment	20
2.1.3.1 Deterministic Unit Commitment	20
2.1.3.2 Stochastic Unit Commitment	21
2.1.3.3 Interval Unit Commitment	24
2.1.3.4 Robust Unit Commitment	24
2.1.4 Optimal Power Flow	25
2.1.5 Energy Storage Technologies	27

2.2	Long-term Planning	29
2.2.1	Objectives	29
2.2.2	Long-term Planning in a Competitive Environment	31
2.2.3	Long-term Planning with Energy Storage	34
2.2.4	Modeling Short-term Operations in Long-term Planning	35
2.3	Contributions	37
2.3.1	Short-term operation	37
2.3.2	Long-term planning	38
2.3.3	Impact	38
Part II:	Short-term Planning in Sustainable Power Systems	40
Chapter 3:	Improved Interval Unit Commitment	41
3.1	Motivation	41
3.2	Contributions	44
3.3	Formulation	44
3.3.1	Formulation of the IIUC	45
3.3.1.1	Binary variables logic	45
3.3.1.2	Minimum up and down times	46
3.3.1.3	Stepwise generator start-up cost	46
3.3.1.4	Generator constraints	47
3.3.1.5	Transmission constraints	48
3.3.2	Formulation of the IUC	49
3.3.3	Formulation of the SUC	50
3.3.4	Formulation of the RUC	50
3.4	Test Results	51
3.4.1	Description of the Test Cases	51
3.4.2	Wind Data	53
3.4.3	Assessing Cost and Reliability Performance using Monte Carlo Simulations	54
3.4.4	Comparison of the IIUC model and the RUC model with different budgets of uncertainty	62
3.4.5	Computation Efficiency	64
3.5	Conclusions	66
Chapter 4:	Hybrid Stochastic/Interval Unit Commitment	68
4.1	Motivation	68

4.2	Formulation of the HUC	70
4.2.0.1	Constraints on Binary Decision Variables	72
4.2.0.2	Constraints on the SUC part	72
4.2.0.3	Constraints on the IUC part	72
4.2.0.4	Coupling Constraints between SUC and IUC	73
4.2.1	Optimal Switching Time	75
4.2.1.1	Parallel Computing Implementation	75
4.2.1.2	Single Processor Implementation	76
4.3	Case Study	77
4.3.1	Description of the Test Cases and Data	77
4.3.2	Day-Ahead Cost of the DUC, SUC, and IUC	78
4.3.3	Day-Ahead Cost of the HUC	79
4.3.4	Optimizing the Switching Time	81
4.3.4.1	Parallel computing implementation	82
4.3.4.2	Single processor implementation	82
4.3.4.3	Impact of the VOLL	82
4.3.4.4	Impact of the domain of the switching time	83
4.3.4.5	Impact of the switching time on committed capacity	84
4.3.5	Results of Monte Carlo Simulations	86
4.4	Conclusion	89
Chapter 5:	Wind Generation as a Reserve Provider	91
5.1	Motivation	91
5.2	Contributions	92
5.3	Formulation	93
5.3.0.1	Constraints on Binary Decision Variables	94
5.3.0.2	Dispatch Constraints on Conventional Generators	94
5.3.0.3	Transmission Constraints	95
5.3.0.4	Wind Power Deration Constraints	95
5.3.0.5	Reserve Constraints	98
5.4	Case Study	100
5.4.1	Description of the Test Cases and Data	100
5.4.2	Day-Ahead Cost	101
5.4.3	Wind Utilization	101
5.4.4	Validation using Monte Carlo simulations	105

5.5	Conclusion	106
Part III:	Long-term Planning in Sustainable Power Systems	108
Chapter 6:	Profit-constrained Energy Storage Siting and Sizing	109
6.1	Motivation	109
6.2	Contributions	110
6.3	Formulation	112
6.3.1	Upper-Level Problem	112
6.3.1.1	Investment constraints	113
6.3.1.2	Profit constraint	114
6.3.1.3	Binary constraints on generators	115
6.3.2	Primal Lower-Level Problem	115
6.3.2.1	Dispatch constraints	116
6.3.2.2	DC network constraints	116
6.3.2.3	ES constraints	116
6.3.2.4	Nodal power balance	117
6.4	Solution Method	117
6.4.1	Dual Lower-Level Problem	118
6.4.1.1	Dual Lower-Level Objective Function	118
6.4.1.2	Dual Lower-Level Constraints	119
6.4.2	Strong Duality Condition	119
6.4.3	Nonlinear Single-Level Equivalent	119
6.4.4	Linearization of the Nonlinear Single-Level Equivalent	120
6.4.4.1	Linearization of the ES profit constraint	120
6.4.4.2	Linearization of the strong duality equality	124
6.4.5	MILP Formulation	125
6.4.6	Computational Complexity	126
6.5	Case Study	126
6.5.1	Test System and Experimental Setup	126
6.5.2	Siting and Sizing Decisions	130
6.5.2.1	Impact of the ES profit constraint	130
6.5.2.2	Effect of the budget constraint	133
6.5.2.3	Effect of the operating policy	135
6.5.2.4	Impact of the capital cost	135
6.5.3	Evaluation of Costs and Profits	136

6.6	Conclusion	138
Part IV:	Conclusions	140
Chapter 7:	Conclusions	141
7.1	Conclusions	141
7.2	Future Work	143
7.2.1	General modeling enhancements	143
7.2.2	Suggested Enhancements to Operational Planning	145
7.2.3	Suggested Enhancements to Storage Siting and Sizing	147
Part V:	Supplementary Materials	150
	APPENDICES	150
Appendix A:	Notation	151
A.0.3.1	Sets	151
A.0.3.2	Binary variables	152
A.0.3.3	Continuous non-negative variables	152
A.0.3.4	Continuous variables	154
A.0.3.5	Dual Continuous Variables	154
A.0.3.6	Auxiliary variables	155
A.0.3.7	Parameters	155
Appendix B:	Map of the IEEE Reliability Test System	159
Appendix C:	Author's Vita	161
Appendix D:	Author's Bibliography	162
D.0.3.8	Selected Journal Publications	162
D.0.3.9	Selected Conference Publications	164
	Bibliography	165

LIST OF FIGURES

Figure Number	Page
2.1 Priorities of the system operator when using short-term planning decision-making tools.	17
2.2 Comparison of the deterministic forecast (pred.) and probabilistic forecasts with different forecast uncertainties (in %) against actual measurements (meas.) [77].	19
2.3 Comparison of the deterministic forecast (prediction) against statistical scenarios [77].	19
2.4 An illustration of the central forecast, upper and lower bounds, scenarios (black), and ramping requirements (gray).	21
2.5 An illustration of a typical bi-level transmission and generation expansion model.	33
3.1 An illustrative example of uncertainty modeling: (a) the scenarios used in SUC; (b) the bounds (lines), up ramp requirements (dotted lines), and down ramp requirements (dashed lines) used in IUC; (c) the central forecast (green line), bounds (thick grey lines), up ramp requirements (dotted lines), and down ramp requirements (dashed lines) used in IIUC.	42
3.2 Aggregated load and wind profiles used for the test cases.	52
3.3 Comparison of expected operating costs of the day-ahead schedules obtained with the SUC, IIUC, IUC and RUC ($\Gamma = \text{card}(\Omega^W)$) for different wind penetration levels - (A) generator dataset G1, favorable wind profile; (B) generator dataset G1, unfavorable wind profile; (C) generator dataset G2, favorable wind profile; and (D) generator dataset G2, unfavorable wind profile.	56
3.4 Increase in the expected costs of the schedules produced by IIUC, RUC ($\Gamma = \text{card}(\Omega^W)$), and IUC when compared to SUC for different wind penetration levels.	57
3.5 Difference in the expected costs of the schedules produced by the IIUC and RUC with different budgets of uncertainty Γ - (A) generator dataset G1, favorable wind profile; (B) generator dataset G1, unfavorable wind profile; (C) generator dataset G2, favorable wind profile; and (D) generator dataset G2, unfavorable wind profile.	63
3.6 Wall-clock times (in seconds) required to reach a 1% optimality gap for different wind penetration levels.	66
4.1 Schematic representation of the unhedged uncertainty associated with the SUC solution.	68

4.2	Schematic representation of the Hybrid Unit Commitment (HUC).	69
4.3	(a) Cost of unhedged uncertainty; (b) running cost of the HUC formulation; and (c) comparison of the total day-ahead costs of the IUC, SUC, and HUC formulations. The optimal switching time is highlighted with a square.	80
4.4	Comparison of the cumulative number of commitments by the HUC throughout the optimization horizon for different VoLLs.	81
4.5	Computation time of the HUC formulation with different switching times.	81
4.6	Convergence of the day-ahead cost (DAC) and the switching time of the HUC formulation in the single processor implementation	83
4.7	The optimal switching time as a function of the VoLL.	84
4.8	Comparison of the hourly committed capacity for the day-ahead schedules of IUC (dash-dot), SUC (dash-dash), and HUC (solid) formulations.	85
4.9	Comparison of the cumulative number of commitments by different UC approaches throughout the optimization horizon.	86
4.10	Cumulative distribution function (CDF) of the actual operating cost (AOC) obtained with MC simulations for different <i>VoLLs</i>	87
5.1	Empirical cumulative distribution function (CDF) of the net wind power injection. The central forecast is marked with a circle and the derated state is marked with a square.	96
5.2	Empirical and linearised CDF of the net wind power injection. Data: BPA.	97
5.3	Normalized central wind power forecast profiles with positive and negative correlations with load.	100
5.4	Wind usage for the positively correlated wind and load profiles with the “(3 + 5) %” reserve policy. The dark gray area denotes wind spillage, the light grey area represents wind deration, and the white area stands for the energy produced by WG.	103
5.5	Wind usage for the negatively correlated wind and load profiles with the “(3 + 5) %” reserve policy. The dark gray area denotes wind spillage, the light grey area represents wind deration, and the white area stands for the energy produced by WG.	103
5.6	Fulfillment of the reserve requirements for the positively correlated wind and load profiles under the “(3 + 5) %” reserve policy. The light grey area is the portion provided by conventional generators. The dark grey area is the portion provided by wind. The white area represents the reduction in the reserve requirement achieved with the proposed methodology.	104
5.7	Fulfillment of the reserve requirements for the negatively correlated wind and load profiles under the “(3 + 5) %” reserve policy. The light grey area is the portion provided by conventional generators. The dark grey area is the portion provided by wind. The white area represents the reduction in the reserve requirement achieved with the proposed methodology.	104

5.8	Expected Cost (EC) of the MC simulations for the (a) positively correlated wind profile and “ 3.5σ ”-rule, (b) positively correlated wind profile and “ $(3 + 5)\%$ ”-rule, (c) negatively correlated wind profile and “ 3.5σ ”-rule, and (d) negatively correlated wind profile and “ $(3 + 5)\%$ ”-rule.	106
6.1	An illustration of the proposed bilevel program and the interfaces between the upper- and lower-level problems. For the sake of clarity, the indices of the decision variables have been omitted.	113
6.2	A diagram of the ISO NE system described in [220].	127
6.3	The mean and standard deviation of hourly LMPs throughout the considered year in cases without ES.	128
6.4	The system-wide aggregated representative load (A), wind generation (B), and net load (C) profiles. The net load profile is the difference between the load and wind generation profiles.	129
6.5	Effect of the ES profit constraint (6.4) on the optimized ES siting and sizing decisions for the low capital cost scenario.	130
6.6	Effect of the ES profit constraint (6.4) under the low capital cost scenario on the: A) investment cost of ES (IC), B) expected profit of ES (P), and C) net monetary gain/loss of ES ($\Delta = P - IC$).	132
6.7	Effect of the budget constraint (6.3) under the low capital cost scenario on: A) The optimized ES siting and sizing decisions, B) the relationship between the investment cost and the investment budget. Black circles and squares indicate respectively the cases where the optimization is driven by the binding investment constraint (6.3) and the ES profit constraint (6.4).	133
6.8	Effect of the operating policy under the low capital cost scenario on: A) ES siting and sizing decisions, B) investment cost of ES (IC), and C) profit of ES (P).	134
6.9	Effect of the capital cost on the profit-constrained ES siting and sizing decisions under the coordinated policy.	136
B.1	A modified IEEE Reliability Test System (1996) as described in [185].	160

GLOSSARY

AC: Alternating Current

AOC: Actual Operating Cost

BP: Bilevel Program

CAISO: California Independent System Operator

CDF: Cumulative Distribution Function

DAC: Day-Ahead Cost

DC: Direct Current

DOE: Department of Energy

DUC: Deterministic Unit Commitment

EENS: Expected Energy Not Served

ERCOT: Electric Reliability Council of Texas

ES: Energy Storage

ESA: Energy Storage Association

EWS: Expected Wind Spillage

FACTS: Flexible AC Transmission System

FBES: Flow battery Energy Storage

FES: Flywheel Energy Storage

HUC: Hybrid Unit Commitment

IEEE: Institute of Electrical and Electronics Engineers

ISO NE: ISO New England, Inc.

IUC: Interval Unit Commitment

IIUC: Improved IUC

LMP: Locational Marginal Prices

LP: Linear Programming

MILP: Mixed-Integer Linear Programming

MC: Monte Carlo

NWP: Numerical Weather Prediction

OPF: Optimal Power Flow

PDF: Probability Distribution Function

PHES: Pumped Hydropower Energy Storage

PJM: PJM Interconnection, LLC

PV: Photovoltaic Generation

RTS: Reliability Test System

SO: System Operator

SSBES: Solid State Battery Energy Storage

SUC: Stochastic Unit Commitment

TES: Thermal Energy Storage

UC: Unit Commitment

US: United States

RUC: Robust Unit Commitment

VOLL: Value of Lost Load

VOWS: Value of Wind Spillage

WECC: Western Electricity Coordinating Council

ACKNOWLEDGMENTS

My mentor, Prof. Daniel S. Kirschen—of whom I am enormously grateful to for his generous support, thoughtful guidance, and seemingly inexhaustible patience during the years of my graduate study—has often criticized me for my rather voluminous style of writing; he has helped me appreciate concision in (technical) writing. Nevertheless, while recalling all of the people who have helped set me forth on my way to success and waltz me through the obstacles, I have come to the conclusion that, at this moment, I can hardly follow his advice and be short-spoken. Therefore, I hope that Prof. Kirschen will magnanimously forgive me if I deviate briefly from this precept below.

My sincerest thanks go to everyone who have helped me during my graduate study, directly or indirectly. To all of you I quote Joseph Brodsky's Nobel lecture acknowledging his mentors: “[...] *If it were not for them, I, both as a man and a ~~researcher~~ writer, would amount to much less; in any case, I wouldn't be standing here today.*”

I would like to thank my mentors, Prof. Daniel S. Kirschen and Prof. Miguel A. Ortega-Vazquez, for their thoughtful guidance and resourceful assistance during my study. Their balanced criticism and encouragement have always been helpful and stimulating; our three-way meetings at early stages of my study were not only intellectually stretching and demanding (for me), but they have revealed to me the true value of creative thinking. I gratefully acknowledge that Prof. Kirschen

and Prof. Ortega-Vazquez, despite their constantly tight schedules, were always available for me and gave me as much face-to-face time as I requested. Both Prof. Kirschen and Prof. Ortega-Vazquez served as exemplary role models for my career—as a junior faculty member, I will have to grow professionally to meet the bar so highly set by them. As Joseph Brodsky eloquently referred to his mentors in his Nobel lecture, *‘I humbly deem myself their sum total, though invariably inferior to any one of them individually’*. I would also like to thank Prof. Richard D. Christie and Prof. Allison Cullen for serving on my Ph.D. reading committee and for their enriching comments and remarks on my work. Finally, this dissertation would not have been possible had one man—Prof. Alex Mamishev—not believed in my potential to succeed; I truly appreciate the invaluable opportunity he offered to me to come to UW EE.

My Ph.D. experience would not have been as rich had I not interned at the Center for Nonlinear Studies at the Los Alamos National Laboratory, supervised by Dr. Scott Backhaus and Dr. Michael Chertkov. My summer of 2014 was exciting and full of learning and intellectual stimulation. In Los Alamos, I was lucky enough to spend my time with a great crew of young and vigorous people! This experience is one of the most defining reasons for why I chose academia among other alternatives, and for that, I am forever grateful to: Miles Lubin and Johnny Rabago (also, my roommates), Dr. Emre Yamangil, Dr. Deepjyoti Deka, Dr. Petr Vorobev and Zhenya, Thomas Catanach, Jonas Kersulis, Michael Fisher, Vladimir Frolov, Dmitry Semchenko, Irina Stolbova, Zhentao Wang, James Dama, Barbara Qunintella, and many others.

I am very grateful to many UW EE faculty members for offering cutting-edge courses that have helped me shape and pursue my research interests. I am especially grateful to Prof. Mohamed El-Sharkawi and Prof. Maryam Fazel for their unique teaching styles and invaluable knowledge that I acquired in their classes.

I also thank my colleagues from UW EE's Renewable Energy Analysis Lab (REAL). I would especially like to acknowledge REAL's postdocs—Prof. Hrvoje Pandzic, Dr. Pierre Henneaux, and Dr. Ricardo Fernandez-Blanco—who were always a source of optimism and knowledge, and who contributed to some of the work presented in this dissertation. I hope that I will eventually become more like them, at least on my best of days. I am also grateful to: Dr. Ahlmahz Negash (for serving to me as a reminder that *'no act of kindness [...] is ever wasted'*), Daniel Olsen (for being an interesting discussor), Kenneth Bruninx (for an interesting experience of transoceanic collaboration; it was fun), Matthias Bucher (for a lot of exciting moments), Marcel Chuma (for introducing Brazil cuisine to me), Dr. Tobias Haring (for gym advice that I still struggle to follow), Dr. Tu Nguen (for the best Vietnamese sandwiches in my life and for suggestions on professional development), and Yishen Wang (for years of friendship, for being an excellent arbitrageur, and for sharing his seemingly limitless gourmet expertise). I would also like to thank all of the REAL student and postdoc population for making my Ph.D. experience thoroughly less stressful and more enjoyable: Abeer, Adam, Ahmad, Anna, Augustina, Bolun, Drew, James, Jesus, Jingkun, Karen, Kelly, Kevin, Marco (thanks for hosting me in Hong King), Mohammed, Mush, Omar, Pan, Remy, Ryan, Ting, Rebecca, Weiling, Yang, Yao, Yushi, Zeyu, and so many more.

I also gratefully acknowledge my co-authors who were generous enough to share with me their criticisms and help me improve the quality of my papers: Prof. Mads Almassalkhi, Dr. Scott Backhaus, Kenneth Bruninx, Dr. Michael Chertkov, Prof. William D'haeseleer, Prof. Erik Delarue, Jenny Felder, Dr. Ricardo Fernandez-Blanco, Dr. Pierre Henneaux, Prof. Ian Hiskens, Prof. Daniel Kirschen, Dr. George Kychyakoff, Miles Lubin, Prof. Alex Mamishev, Jon Martin, Prof. Miguel Ortega-Vazquez, Prof. Hrvoje Pandzic, Eric Pepin, Ting Qiu, Mushfiq Sarker, Dr. Cesar Silva-Monroy, Dr. Maria Vrakopoulou, Yishen Wang, Dr. Jean-Paul Watson, Bolun Xu, and Dr. Megran Xue.

I also thank Aaron Zielinski for proofreading this dissertation and some of my early papers, as well as for his tips and advice on technical writing.

I would like to thank my Seattle friends Aaron, Abe, Anna, Anthony, Dr. Andrey, Benzion, Bob, Gabriela, Joseph, Israel, Kenneth, Kishore, Laura, Lizzy, Marc, Dr. Mendel, Michael, Moshe, Paula, Peter, Phillippe, Dr. Solly, Vincent, Vladimir, and many others. In particular, I would like to single out and express my gratitude to Dr. Pavel for being a great companion, an intelligent and wit discussor, and a designated driver. I have always had all of the support that I needed from my best school friend, Oles Savchuk, and my best college friends, Sergey Tuzhilov and Dmitry Rimorov. Thank you for always having time for me!

I would be a different person had I not been raised by my parents, Evgeniya and Yury Sr., and my maternal grandparents, Svetlana and Vladimir; I am deeply privileged to be a member of the Dvorkin Family. To my Family: there is no higher honor to me than to be one of you.

I am grateful to my parents for supporting my cognitive development since my very early days and for letting me explore and push the bounds of my intellectual freedom. I firmly believe that this very freedom paved my interest in constantly gaining new knowledge and built my (albeit, perhaps, notorious) resistance to accepting failures. I thank my *Dad* Yury Sr. for suggesting to pursue a STEM education and my *Mom* Evgeniya for making the best educational options available to me. I appreciate my *Babushka* Svetlana for taking a toll on her own prolific, 5-decades-long career to be able to take care of my siblings and me when we were in a tender age. It was my *Babushka* who encouraged my passion for reading and constantly supplied me with new books. I am grateful to my *Dedushka* Vladimir Sr. for being a brilliant role model of a researcher and a leader who—although he is in his early 80s—still manages to maintain the same work pace and dedication that he had

decades ago. I also thank my junior *siblings*—Vladimir Jr. and Dmitry, both of whom are also power system engineers—for always lending their hands to me when it has been crucially needed, and I wish them the best of luck as they consider beginning their own Ph.D. studies.

Furthermore, I would like to thank my *fiancee*, Olga, who has been nothing but supportive during all of the years of my Ph.D. study and who has helped me settle down and get used to permanently residing in a foreign, yet greatly admired, country. It was Olga who helped me (admittedly, a lot) improve my English and overcome my initial shyness. I would also like to thank Olga’s parents, for welcoming me into their family, as well as Olga’s sister and her family for cheering me up whenever it has been needed.

I thank all sponsors of my research, which was funded by in part by the difference divisions of the University of Washington, US Department of Energy and by Clean Energy Institute’s Graduate Fellowship and the Clean Energy Institute’s Student Training & Exploration Grant.

Thank you all, and I hope I will not let you down in my post-graduate life!

DEDICATION

To my *Babushka* and *Dedushka*:

“No two men were less the same

Like stone and water, ice and flame”.

Alexander Pushkin, “Eugene Onegin” (2:XIII).

Part I

INTRODUCTION TO SUSTAINABLE POWER SYSTEMS

Chapter 1

INTRODUCTION

1.1 Embracing a Sustainable Future

Traditionally, power systems in post-industrialized societies have been designed to produce electricity on a bulk scale using generation technologies with relatively high energy densities (e.g., fossil-fired, hydro, and nuclear generation) and to deliver electricity to distributed end-users via a mesh network with low connectivity. This paradigm assumes that the electricity injected by bulk, fully controllable generation resources flows downstream to the load buses. The process is centrally coordinated by the system operator (SO), which is responsible for maintaining the generation-load balance by continuously adjusting the output of the generators. This configuration takes advantage of the economy of scale achieved by operating large generators with relatively low per-MW capital costs.

Renewable generation options, although they have always been available, have not always been considered viable due to their scattered network allocation, low capacity ratings, and relatively high per-MW capital costs [1, 2, 3, 4]. Traditionally, these drawbacks (including low predictability and controllability of those resources) outweighed their advantages (e.g., emissions-free operation and near-zero production costs [4]). The limited interest in exploring renewable alternatives was rooted in a lack of public awareness of the environmental implications of traditional generation technologies. However, after the Three Mile Island accident in 1979, the Chernobyl disaster in 1986, the triple meltdown in Fukushima in 2011, and the recognition of the risks associated with global climate change, there has been an international push toward the integration of renewable generation to minimize the anthropogenic effects of the power sector and related industries [5, 6].

Since then, renewable generation resources—mainly based on wind and photovoltaic (PV) technologies—and non-traditional energy providers that facilitate the integration of renewable generation into existing power systems—mainly, ultra-flexible gas-fired generators, adjustable loads, and energy storage—have been developed as a promising means to alleviate dependency on costly and depletable energy resources, as well as to reduce gas emissions [7, 8, 9], thus fostering a transition toward a *sustainable* power sector. Motivated by [10], this dissertation defines this attitude as achieving a power system planning design that is flexible enough to adopt continuously new technological means to reduce the usage of non-renewable resources and gas emissions, yet still provides universal access to energy at socially acceptable costs. While this concept has been discussed since the early 1970s, the massive deployment of renewable generation resources has only become possible after the recent policy initiatives that provide generous incentives (in the forms of subsidies and tax credits [11, 12, 13, 14, 15]). As a result, by the end of 2014, renewable generation exceeded 10% penetration levels, in terms of annual electricity produced in some regions of the US, the European Union, and China [16]¹; even higher targets are expected to be reached in the forthcoming years [17]. However, power system operational tools and long-term planning decision-making tools have not kept pace with this dramatic growth in renewable generation. For the most part, these tools still assume that power systems are operated in the traditional ‘fossil’ paradigm, thus ignoring the unique stochastic nature of renewable generation. Hands-on experience in real-life power systems has revealed the inefficiency of these tools and demonstrated the need for an overhaul of the current approaches to power system operation and planning.

Given the anticipated growth of renewable penetration levels [17], the challenges imposed by renewable generation on power system operation and planning should be addressed in a systematic and rigorous manner. The goal of this research is to assist power system professionals and

¹It should be noted that, in some regions, hydropower generation resources installed decades ago are counted toward achieving more recent renewable penetration targets. This practice, of course, simplifies achieving these targets, but at the expense of reducing the amount of newly built renewable generation resources (e.g., wind and PV) to be installed.

stakeholders in identifying and answering these challenges to facilitate a cost-effective and reliable transition into a *sustainable* power system. This work, among other studies on the subject, aims to pave the way to this promised *sustainability* by means of revisiting existing approaches to short-term operation and long-term planning:

- **Short-term operation:** This work analyzes non-deterministic optimization frameworks applied to day-ahead and hour-ahead decision-making tools and quantifies their benefits. These frameworks aim to replace traditional ad-hoc reserve rules with an endogenous assessment of actual system-wide reserve needs. This assessment either relaxes the ad-hoc reserve rules (thus reducing operating costs) or tightens them (thus improving performance reliability). The numerical results presented in this work demonstrate that the value of these non-deterministic optimization frameworks increases with renewable penetration levels. Therefore, this work argues that the practical implementation of these techniques is imperative for achieving sustainability in power systems.
- **Long-term planning:** This work explores the technical and economic benefits that can be attained by installing battery energy storage, an emerging technology that can arbitrage energy production and consumption in power systems with high penetration levels of renewable generation. These benefits are quantified regarding system-wide operating cost savings and the increased utilization of renewable generation. Furthermore, this work is extended to enable economically viable energy storage procurement that ensures that energy storage owners can recover their investment costs.

1.2 Challenges

Over the past decade, two renewable generation technologies (i.e., wind and PV generation) have been installed in quantities that can affect power system operation. Therefore, the scope of this dissertation is limited to the challenges specific to these two renewable generation technologies.

1.2.1 Uncertainty and Variability

Power systems have always been exposed to different sources of uncertainty. For instance, there is always a chance that a generator or transmission line will trip. The former failure would require the deployment of spare generation capacity to maintain the generation-load balance while the latter contingency would use the spare generation capacity to avoid potential transmission line overloads. Similarly, real-time load values are likely to deviate from their forecasts; the generators must compensate for these deviations. The inability to predict exactly these events introduces uncertainty into power system operation.

This uncertainty is unavoidable; system operators deal with uncertainty by using a number of robust, computationally efficient, and affordable heuristics. For instance, to handle random generator and transmission outages, systems operators enforce the $(N - 1)$ security criterion, which specifies that the system should be able to sustain the loss of any k out of N elements. Usually, system operators set $k = 1$, which protects the system against the failure of the largest on-line generator [18]. However, in some cases (e.g., in ERCOT), $k = 2$, which is equivalent to a sudden loss of 2300 MW generation² [19]. Similarly, the uncertainty of load forecasts is relatively small and is typically estimated as a certain percentage of the hourly load. For example, PJM assumes a load uncertainty of 1% of the peak and load valley loads, for respective peak and off-peak hours [20]. The advantage of these heuristics is that they are intuitive and very easy to implement.

The key difference between the uncertainty caused by renewable generation and the uncertainties mentioned above is that the latter have been scrutinized over the past century and are therefore better understood. For example, load forecasts and their uncertainty exhibit roughly the same daily and seasonal features (e.g., morning upward and evening downward ramps [21]). Similarly, contingencies can be ‘forecast’ using historical data and advanced condition-based monitoring techniques [22, 23]. On the other hand, the outputs of wind and PV generation are weather-driven and, there-

²For example, 2300 MW is the size of two average nuclear power plant blocks.

fore, do not necessarily follow a ‘typical’ daily pattern [24]. Furthermore, the accuracy of existing forecasting tools [25] is sensitive to look-ahead horizons and drastically decreases for time horizons of 6 hours or longer [26]. Thus, dealing with uncertainty becomes challenging for time scales longer than several scheduling intervals³.

In addition to their uncertainty, wind and PV generation are notorious for their variability (i.e., their inability to maintain a stable output [28]). Although semantically the terms uncertainty and variability have similar meanings, in the context of this work, they denote entirely different physical phenomena. Unlike uncertainty, which is caused by the imperfection of forecasting tools, variability is caused by random atmospheric processes [29]. These processes, and thus, variability, are observed on shorter time scales than uncertainty [28], therefore affecting power system operation within given scheduling intervals. When compared to load patterns (which also exhibit some variability), the variability of renewable generation is characterized by higher magnitudes and frequency [28].

As penetration levels of wind and PV generation increase, these resources impose larger magnitudes of uncertainty and variability, thus requiring more flexibility from conventional generators to maintain load-generation balance [29]. For example, data-driven studies for ERCOT [29] and CAISO [31] show that the integration of renewable generation will need more reserve from conventional generators (in terms of spare capacity), as well as higher and more sustainable ramping rates. These larger reserve requirements are likely to affect the scheduling and dispatch decisions of conventional generators [32] and thus, cause additional costs [33].

This dissertation proposes to address certain challenges imposed by renewable generation on power system operation and long-term planning by accommodating for the stochastic nature of these resources using a combination of different optimization frameworks.

³Typically, the generation scheduling of all but ultra-flexible generators is performed with an hourly resolution; however, this practice is likely to change to accommodate high penetration levels of renewables, see [27] for further details.

1.2.2 *Reduced Controllability*

As explained in Section 1.2.1, dealing with the uncertainty and variability of renewable generation requires additional flexibility from conventional generators. However, renewable generation—especially when integrated in large quantities—tends to replace conventional generation, thus reducing the supply of flexibility [34]. Notably, reference [34] emphasizes that the units that are most able to provide this flexibility are most likely to be replaced by renewable generation. Therefore, the replacement effect of renewable integration should be coordinated with long-term resource adequacy studies to ensure that the conventional generation mix can provide sufficient flexibility to accommodate for high penetration levels of renewable generation [35, 36]. This coordination is of greater importance to power systems that have an inflexible generation mix [37].

Conventional generators unaffected by the aforementioned replacement effect are likely to face operational challenges caused by an increasing flexibility burden. Many of these generators were commissioned decades ago and are thus not designed (neither technically nor economically) to provide flexibility for mitigating the impacts caused by renewable generation uncertainty and variability. These units may have to be cycled⁴, leading to accelerated wear-and-tear (e.g., fatigue, erosion, corrosion, and, subsequently, more frequent forced outages [34]). As explained in [38], assessing the indirect costs caused by these mechanical effects is not straightforward. Ultimately, excessive cycling of some conventional generation may significantly reduce their expected lifetimes [34]. In addition to tear-and-wear effects, additional cycling of conventional generators is shown to reduce the long-term fuel efficiency of these units [39]. In turn, this can have undesirable environmental consequences. For example, reference [40] concludes that cycling conventional units in the US Western Interconnection could reduce the CO_x and NO_x benefits of renewable generation by 2% and 0.3%, respectively. Thus, transitioning to sustainable power systems requires a conventional generation mix that can provide sufficient controllability to avoid reducing the costs and

⁴Here, and in the following discussions, cycling is defined as the turning on/off and ramping up/down of generators.

environmental benefits of renewable generation.

This dissertation addresses the challenge of this reduced controllability on the supply side by exploring the ability of wind generation to provide some flexibility, in addition to the flexibility provided by conventional generation.

1.2.3 Market Implications of Renewable Generation

While conventional (thermal) generation typically carries significant fuel costs⁵, renewable generation (specifically, wind and PV) has near-zero production costs. On the one hand, this makes renewable generation an effective means to reduce the overall cost of supplying electricity. On the other hand, under high wind penetration levels, these near-zero production costs reveal a number of flaws in existing market-clearing designs [42], which affect the profit opportunities of conventional electricity market participants [43].

The effect of renewable generation on energy prices is two-fold. First, renewable generation leads to higher intra-day volatility in locational marginal prices (LMP) [44]. This volatility favors flexible market participants (such as emerging energy storage and demand response resources) who gain new opportunities to trade energy on short notice, but discriminate against inflexible generators (such as base-load, coal-fired, and nuclear generators) that may experience significant monetary losses during some operating intervals due to their intertemporal constraints [45]. Second, renewable generation tends to reduce the LMPs, thus reducing the profit streams of conventional generation, which may eventually force some fossil-fired generators out of business [42]. Furthermore, the integration of renewable generation affects LMPs via various financial incentives (e.g., tax credits and subsidies) that have been adopted to facilitate the faster integration of renewable generation.

⁵Note that although hydropower generation is also considered ‘conventional’ in the open literature, these resources have near-zero production costs. Furthermore, in practice, scheduling and dispatch decisions on hydropower generation are produced separately and can be driven by methods other than electricity supply priorities (e.g., flood control, irrigation, fish and wildlife conservation.). See [41] for further discussion.

These incentives allow renewable generation to submit *negative price offers*⁶, thus increasing the chances of these offers being accepted in the energy market and, sometimes, setting the LMP to negative values unacceptable for fossil-fired generators. Although these incentives improve the utilization of renewable generation, this comes at the expense of higher operating costs, excessive cycling of conventional generators, and higher gas emissions [46]. Furthermore, reference [45] demonstrates that the practice of negative offers is likely to re-enforce the replacement effect of renewable generation and force the early retirement of some fossil-fired generators due to inadequate profit opportunities. Finally, the pressure that renewable generation has on LMPs is likely to affect profit streams for emerging energy storage and demand response technologies.

In the ancillary services⁷ market, renewable generation increases the reserve requirements [29, 32, 33] and, thus, increases the cost of reserve procurement [32, 33]. However, the effect of renewable generation on reserve prices is not straightforward. While the increased reserve requirement tends to increase the market-clearing prices for this product, the conventional generators replaced by renewable generation in the energy market are likely to submit more offers in the reserve market [42], thus increasing its volatility.

In line with the open literature, this dissertation acknowledges the need for new market clearing designs that would ensure the economically sustainable integration of renewable generation and its co-existence with conventional generation technologies. This dissertation contributes to the deployment of emerging energy storage technologies by proposing a new profit-constrained approach to optimizing energy storage investments, such that their profit streams are immunized against the impacts of renewable generation resources on LMPs.

⁶Reference [45] explains the term *negative price offers*, which is counter-intuitive in terms of traditional commodity markets, where it is the ‘*inability to dispose of electricity without cost*’ and, instead, interprets it as ‘*a transfer from U.S. taxpayers to the market for taking wind power.*’

⁷The scope of this dissertation limits the ancillary services to the active power reserve.

1.2.4 *Is Energy Storage a Panacea?*

Recent advances in material science make the large-scale deployment of electrochemical energy storage⁸ in the transmission system a technically feasible option [47]. On a fundamental level, energy storage is similar to transmission lines, with the only difference being that transmission lines move energy in space while energy storage moves it in time [48]. Therefore, applications of energy storage for spatiotemporal energy arbitrage [48], peak shaving [49], frequency [50] and voltage support [51], as well as congestion management [48, 52], have been proposed. Furthermore, energy storage can compensate for the replacement effect of renewable generation and its impact on the SO's ability to control the system from the supply side by providing fast responses to dispatch signals [53]. However, electrochemical energy storage is still an emerging technology; therefore, real-life installations, beyond tens of demonstration projects, are limited due to the relatively high capital costs of these devices.

Provided that anticipated capital cost reductions and increased charging/discharging efficiency are achieved, system operators could use energy storage to facilitate the reliable integration of renewable generation. For instance, Solomon *et al.* [54] estimates that the state of California will need 186 GWh/22 GW of energy storage to enable an approximately 85% penetration of renewable generation⁹. However, the authors intentionally avoid discussing the economic implications of such large-scale energy storage deployment due to the uncertainty on the capital costs. Kintner-Meyer *et al.* [56] concludes that the Northwest Power Pool will need 10 GWh/0.7-1 GW of energy storage resources by 2019 to balance 14.4 GW of installed wind generation capacity. However, the economic analysis in [56] also reveals that the revenue streams for such a deployment of energy storage are expected to be thin.

⁸In this dissertation, energy storage is defined as a generic category of devices or physical media that store energy to perform useful processes at a later time.

⁹Note that the California Public Utilities Commission currently mandates 1.325 GW of utility-scale storage to be installed by 2024 MW [55].

Regulators and system operators acknowledge the importance of energy storage for mitigating the challenges imposed by renewable generation on power systems (surveyed in Sections 1.2.1 and 1.2.2 [57, 58]). Therefore, there has been a push to accelerate research efforts that would propose the optimal configuration of energy storage to attain the maximum benefits from these resources. However, the complexity of optimally installing energy storage resources in power systems with high penetration of renewable generation arises from the need to balance long- and short-term costs and benefits [48], as well as from the difficulties associated with taking transmission constraints into account [59]. Ignoring these factors leads to an inaccurate assessment of the value of energy storage [60]. Furthermore, energy storage is considered an energy-limited resource and its technical characteristics do not always support its participation in electricity markets on a par with other energy providers. Therefore, energy storage participation in electricity markets is likely to require special rules (e.g., the principle of energy neutrality and energy restoration mechanisms [61, 62]) to maximize their benefits.

This dissertation recognizes capital intensive investments as the primary challenge of adopting energy storage in sustainable power systems and suggests an economically sustainable approach to installing these devices in existing power systems.

1.2.5 Modelling Accuracy and Computational Complexity

Given the size of power systems, reaching optimal decisions for operation and long-term planning is computationally expensive. In addition to the notorious dimensionality curse, computational issues also arise from the non-convexity of the mathematical models representing the physical processes underlying power system operation. This non-convexity mainly stems from the physics of alternating current power flows, as well as the integer on/off and control decisions (e.g., the start-up and shutdown of conventional generators or the tap changer mechanism of power transformers). Dealing with these non-convexities typically leads to NP-hard computational problems and is bounded by

the capabilities of existing solvers.

Computational complexity has also been affected by the introduction of probabilistic methods to deal with the uncertainty and variability of renewable generation in a more cost-efficient and reliable manner. To alleviate this computational burden, modelers usually have to balance¹⁰ the accuracy of their assumptions and solution approach with the ability to produce a meaningful solution within a reasonable amount of time [64, 65]. As explained in [64], this compromise can be reached by adjusting the modeling fidelity for different studies and analyzing the sensitivity of a particular modeling approach or assumption to the goals of the study¹¹. Alternatively, the complexity of specific problems can be reduced by using specific dimensionality reduction techniques [66, 67]. However, the generality of these techniques is quite limited; therefore, they require special tuning for each application.

This dissertation fully realizes the unavoidable trade-off between the accuracy and complexity of the models and shares the common sense philosophy that ‘*all models are wrong, but some are useful*’ [68]. Therefore, for each application, this dissertation uses modeling assumptions that are relevant for a particular analysis.

1.3 Reader’s Guide

Although all of the chapters of this dissertation are closely related, each chapter is intended to be comprehensible when read separately. To facilitate navigation within the manuscript, all references in this dissertation are interactive.

The content of this dissertation is itemized below:

- Chapter 2 consists of three sections. Section 2.1 summarizes the objectives of operational

¹⁰This trade-off is unavoidable and arises in many disciplines, including some quite outside engineering. For instance, Dr. Henry A. Kissinger complains in [63] that ‘*complexity inhibits flexibility*,’ even in foreign affairs.

¹¹For example, it is customary in some studies to replace a non-convex and non-linear alternating current representation of power flows with a convex and linear direct current representation of power flows. The replacement makes it possible to take advantage of convex solvers with high computational performance at the expense of a less accurate account of the underlying physical process.

planning in power systems and compares state-of-the-art approaches to this task. Section 2.2 surveys the goals and existing methods for long-term planning and contrasts them to operational planning. Section 2.3 details the contributions of this dissertation.

- Chapters 3 and 4 present two short-term planning models that aim to address the challenges imposed by the uncertainty and variability of the renewable generation surveyed in Section 1.2.1. These Chapters evaluate the reliability and cost performance of the proposed models relative to the state-of-the-art and discusses their benefits projected on increasing penetration levels of renewable generation. The content of these chapters is based, in part, on the work reported in [29, 80, 81, 82, 83].
- Chapter 5 describes a probabilistic approach to scheduling wind power generation, to providing reserve for mitigating its own uncertainty and variability, and to reducing system-wide reserve requirements. Moreover, this Chapter shows that this approach helps deal with the controllability of conventional generation in the presence of renewables (as described in Section 1.2.2) and evaluates its cost savings. The content of this chapter is based, in part, on the work reported in [84].
- Chapter 6 departs from the short-term planning contributions of Chapters 3-5 and presents a bi-level programming model for siting and sizing energy storage in power systems with renewable generation. This model overcomes the market challenges described in Section 1.2.3 and ensures sufficient profit streams for deployed energy storage. The content of this chapter is based, in part, on the work reported in [85, 86].
- Chapter 7 summarizes the key findings of this dissertation and lays out future research directions.

Chapter 2

LITERATURE REVIEW

2.1 *Short-term Operations*

2.1.1 *Objectives*

In modern power systems with relatively large penetration levels of renewable generation (such as PV and wind resources), SOs must use short-term scheduling and dispatch procedures to account for the challenges surveyed in Section 1.2. The need for short-term planning is because the power outputs of conventional generators are subject to intertemporal mechanical and thermodynamical constraints that need to be accounted for ahead of the actual energy delivery to avoid generator damage or load shedding. For example, during the event on February 26, 2008 [87], failure to procure enough generation capacity led to the automatic tripping of several generators and involuntary load reductions in the ERCOT system. The underlying cause of this event was described as a combination of several factors, including the unforeseen reduction of wind power generation during the evening load ramp up. As penetration levels of renewable generation increase, the frequency of such unfavorable conditions is expected to grow.

In this dissertation, a combination of the following three stages is considered short-term planning¹ [92]:

- **Day-ahead stage:** This stage occurs approximately 12 hours before the beginning of the day under consideration. The SO uses the best load and renewable generation forecasts available

¹Here, a vertically integrated power system is assumed, where one entity is responsible for all physical and monetary transactions. In practice, the number of stages and their definitions may vary in different jurisdictions. Also, these stages can be affected by the market practices adopted in a particular jurisdiction. Interested readers are referred to the day-ahead scheduling manuals of real-life system operators for further details [88, 89, 90, 91].

at the time and solves the Unit Commitment (UC) problem to determine the least-cost on/off schedule and the power outputs of all conventional generators. Typically, the UC problem is solved with an hourly resolution; however, it is expected that it will shift to sub-hourly resolutions to better account for the uncertainty and variability of renewable generation [82].

- **Hour-ahead stage:** The SO uses updated load and renewable generation forecasts (which are more accurate than those that are used at the day-ahead stage) 30-90 minutes before each hourly or sub-hourly operating interval to adjust the on/off schedule and the power output of all conventional generators. This stage typically uses an Optimal Power Flow (OPF) model, which solves a cost minimization problem based on a more detailed representation of the transmission and generation assets than in the UC. The time resolution used in the hour-ahead stage is usually based on the same time resolution as the day-ahead stage.
- **Real-time stage:** When the moment of actual energy delivery occurs, the SO uses generation resources procured at the day-ahead and hour-ahead stages to meet real-time demand and renewable generation conditions, which are likely to be different than those forecasted at the day-ahead and hour-ahead stages. For the purpose of real-time operations, each operating interval is divided into 5-15 minute sub-intervals, and the generation dispatch is adjusted for each sub-interval separately based on real-time signals. Within one dispatch interval, the effects of the stochastic nature of the renewable generation resources are minimal, and their outputs can be assumed fixed (i.e., the output at the beginning of the dispatch interval is likely to be equal to the output at its end).

At both the day-ahead and hour-ahead stages, the SO faces the uncertainty and variability of renewable generation and load. To alleviate the impacts of these phenomena on real-time operations, the SO must schedule the available generation resources in such a way so that they provide a certain amount of reserve to be able to adjust their outputs on request. If the expected uncertainty and

procured reserve are overestimated, the schedule might be unnecessarily expensive. On the other hand, if the uncertainty and procured reserve are underestimated, the schedule might not be feasible in real-time and may require expensive or undesirable corrective actions (e.g., starting up expensive generators or shedding load). To maintain operational reliability of the system and simultaneously avoid high generation costs, a computationally effective approach is needed. The approach selects the most cost-effective combination of controllable generators that can effectively respond to the deviations of the renewable generators and the loads from their forecasts.

The need to simultaneously account for various reliability criteria and the different costs they cause (further complicated by the presence of renewable generation) suggests applying an optimization theory to balance these factors adequately during short-term planning [93, 94, 95, 96, 97, 98]. Historically, these optimization frameworks include linear programming [93, 94], Lagrangian relaxation [95, 97], and generalized MILP [97, 98]. Since these frameworks may have different advantages and disadvantages if applied to a particular problem, it is the SO's primary responsibility to find the appropriate techniques for the problem considered.

The SO priorities used in this selection are summarized and illustrated in Figure 2.1. Above all, the SO aims to maintain reliability standards. Then, the SO aims to meet these reliability standards at the least cost. Finally, it is desirable to meet these two conflicting objectives within the time allowed for the day-ahead and hour-ahead stages, as described above. Ironically, these priorities are rarely achieved simultaneously. For instance, [98] (which compares Lagrangian relaxation and generalized MILP) emphasizes that the first approach is more computationally efficient and is scalable to large power systems, while the second approach has a better cost performance. Therefore, given the same reliability standards, the two approaches would result in different cost and computational performance.



Figure 2.1: Priorities of the system operator when using short-term planning decision-making tools.

2.1.2 Forecasting of Renewable Generation

The accuracy of renewable generation forecasts is strongly related to the operating cost savings that can be attained with the integration of renewable generation [28, 33, 69]. Furthermore, inaccurate forecasts may affect commitment and dispatch decisions [33], the cycling of conventional generation (especially ultra-flexible generators [69]), the reserve margins required [33, 32], and the spillage of renewable generation and air pollution [46]. As acknowledged in [70, 71], forecasting wind and PV generation outputs is a complex modeling task due to the constantly changing weather conditions that affect wind speed and PV irradiance [72]. As pointed out in [69], the accuracy of the forecasts becomes more critical as the penetration level of these resources increases; therefore, currently risky investments in new forecasting technologies are expected to pay off within the next few decades.

In general, two approaches are used for forecasting renewable generation:

- **Statistical approaches:** These approaches are based on processing historical wind speed/power and PV irradiance/power time series to parametrize their uncertainty using the statistical hypotheses that this uncertainty exhibits a certain behavior.
- **Numerical Weather Prediction (NWP):** This approach is based on the output of weather and climate prediction models (e.g., Rapid Refresh [73]), which are based on detailed models of the short-term evolution of atmospheric and oceanic processes using current weather observations.

2.1.2.1 Statistical Approaches

Historically, all forecasting techniques were deterministic (i.e., they produced a unique value of the random variable for each time step within a given prediction horizon). This unique forecast, known as the central forecast, is the most likely value of the random variable [74]. However, as noted in [72], deterministic approaches fail to represent the entire range of potential realizations of the random variable and are therefore not feasible for power systems with high penetration levels of renewable generation. On the other hand, probabilistic forecasting techniques are capable of predicting forecast uncertainty densities (whether by using parametric or non-parametric statistics) in addition to the deterministic forecast [75]. The differences between the deterministic and probabilistic forecasts are illustrated in Figure 2.2. As shown in [76], probabilistic techniques outperform deterministic techniques, in terms of *quality* (i.e., statistical performance) and *value* (i.e., their ability to yield savings by producing more accurate forecasts).

Recently, probabilistic forecasts have evolved into statistical scenarios [77] to leverage stochastic programming benefits for short-term decision-making tools. The main advantage of statistical scenarios over probabilistic forecasts is that they take advantage of the interdependencies between prediction errors at different time steps of the prediction horizon. These interdependencies are accounted for by considering more than one potential realization of the random variable for each time

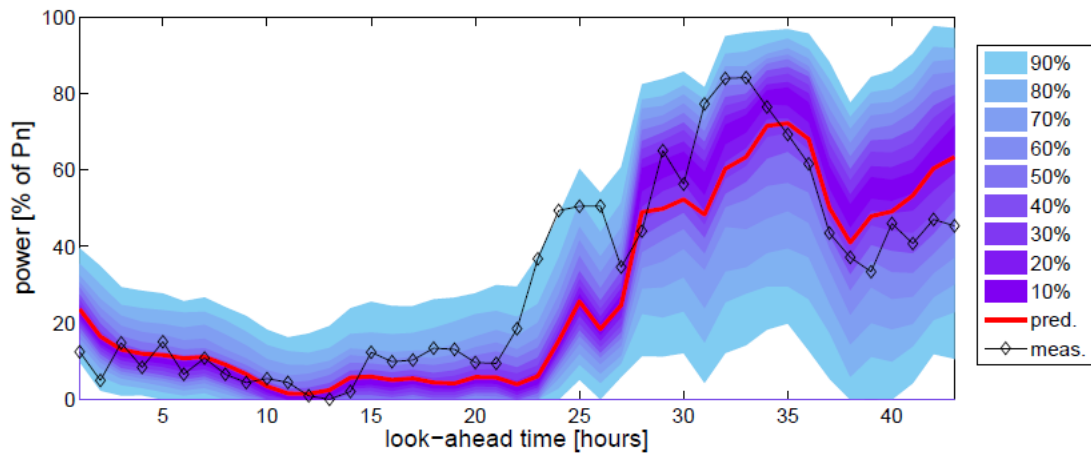


Figure 2.2: Comparison of the deterministic forecast (pred.) and probabilistic forecasts with different forecast uncertainties (in %) against actual measurements (meas.) [77].

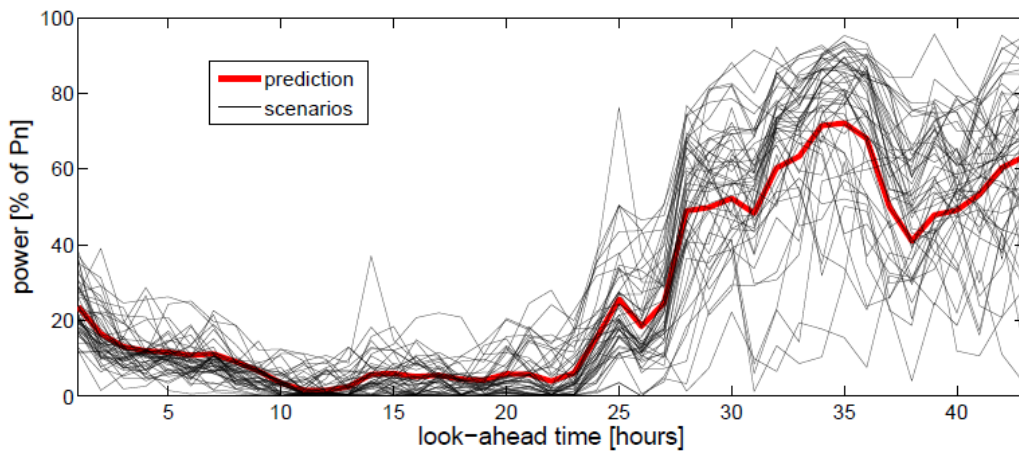


Figure 2.3: Comparison of the deterministic forecast (prediction) against statistical scenarios [77].

step, as well as the transition between different time steps. At this point, statistical scenarios are the most popular approach to forecasting renewable generation.

Statistical scenarios can be obtained from historical observations. Existing scenario generation methods are based on the algorithm proposed in [77]. This approach defines the output of renewable generation as a multivariate Gaussian random variable. The mean values of this variable at each time

step are assigned using the probabilistic forecast, and the covariance matrix is used to account for the correlation between the means of different time steps. The approach in [77] has been modified to account for spatial and spatiotemporal correlations [78].

2.1.2.2 Numerical Weather Prediction

The output of NWP models can also be used to generate scenarios. In [79], the scenarios are generated using an ensemble of six NWP models, which are fed temperature and wind measurements and can account for the temporal and spatial correlations in the scenarios that they produce. These scenarios are then re-sampled for the sake of inference analysis in short-term planning. The cost analysis shows that using scenarios in stochastic programming reduces operating costs when compared to deterministic forecasts and statistical scenarios.

2.1.3 Unit Commitment

UC is a broad class of optimization problems that are typically used in day-ahead planning to determine the binary status of generators to minimize the cost of serving forecast load subjected to operational constraints on generation resources and transmission lines, as well as the availability of renewable generation [99].

2.1.3.1 Deterministic Unit Commitment

In the Deterministic UC (DUC) formulation, the load and renewable generation at every location are modeled by a single central forecast (as shown in Figure 2.4) and the associated uncertainty is handled using ad-hoc reserve rules [29, 31, 100, 101, 102, 103]. The amount of reserve capacity under each of these rules can be fixed during the course of the day [104], vary on a multi-hourly basis [102, 20], or vary on an hourly basis [29, 31, 8, 103]. Because the DUC does not explicitly take into account more detailed information regarding the need for flexibility (such as the probability of

a particular uncertainty realization), the schedule that it produces may be too conservative or insufficient during certain hours. As the penetration of renewable resources (and hence, the uncertainty that the power system needs to withstand) increases [29], large deviations of renewable generation from the forecast values make the DUC less and less attractive [32].

To avoid using ad-hoc reserve rules, stochastic, interval, robust, and chance-constrained optimization techniques have been proposed for unit commitment. The common thread of these models is that they seek to minimize operating costs while endogenously accounting for the uncertainty of renewable generation. However, these formulations differ in their representation of this uncertainty (even for the same sources of uncertainty) and thus result in different solutions.

2.1.3.2 Stochastic Unit Commitment

In contrast to the DUC, the authors of [105] and [106] show that accounting for multiple scenarios (as illustrated in Figure 2.4) in the UC reduces operating costs. Efficient Stochastic UC (SUC) formulations [107, 108, 109, 110] have been developed on the basis of scenario generation techniques

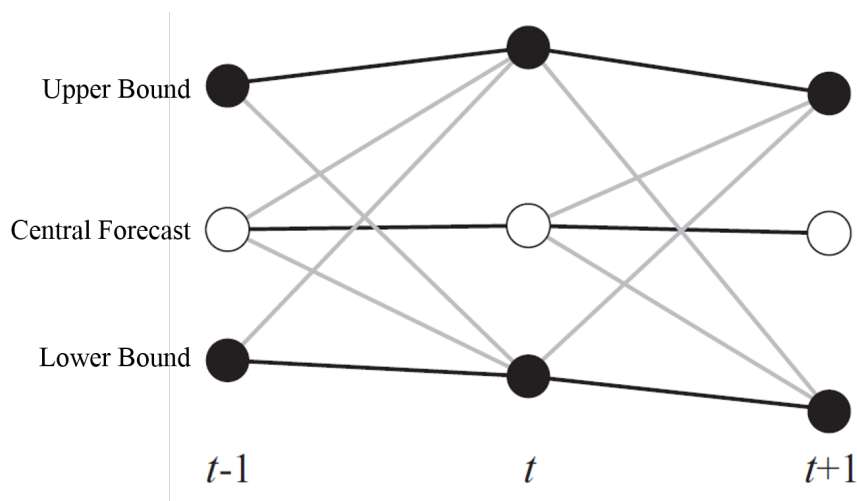


Figure 2.4: An illustration of the central forecast, upper and lower bounds, scenarios (black), and ramping requirements (gray).

[111]. Stochastic UC (SUC) techniques consider a set of load and renewable generation scenarios and their probabilities to minimize expected operating costs. In other words, SUC decisions are optimized by weighing the cost of each scenario in proportion to its likelihood.

Typically, SUC is formulated as a two-stage optimization problem [92]. First, *here-and-now* decisions are made on the binary status of generators. These decisions are common to all scenarios. Then, *wait-and-see* decisions on the dispatch of each generator committed at the first stage are made separately for each scenario. This two-stage structure aims to mirror the day- and hour-ahead decision-making stages used by system operators in their short-term planning procedures, as explained in Section 2.1.1. Since SUC produces a single schedule for all scenarios, some optimality might be sacrificed for each scenario to minimize the expected operating costs over the entire set of scenarios. Load shedding is allowed to reduce the impact of extreme scenarios with low probabilities. In this case, SUC may opt to shed load for an extreme scenario, rather than commit more potentially expensive generators, and sacrifice dispatch optimality over all scenarios. A trade-off between these decisions is sensitive to the value that a system operator places on a unit of load shedding.

SUC is computationally demanding when the problem involves a large power system or even a moderate number of scenarios. This issue can be mitigated somewhat if the set of scenarios is reduced using scenario reduction techniques [113, 114, 115, 116, 117]. These techniques aggregate similar scenarios based on a particular metric, such as their probability, hourly magnitudes, or the cost resulting from each scenario.

An unsupervised clustering method (k-means [118]) can be used to partition a given set of scenarios into a given number of clusters. As a result of this partition, scenarios with similar features are assigned to the same cluster. The centroid of each cluster represents a somewhat average pattern of all the scenarios included in a cluster. Since this centroid is an artificial scenario, the original scenario with the lowest probability distance from the centroid is used to represent the cluster. The

k-means++ method [118] (an enhancement of the k-means method) takes advantage of the initial cluster partitions. Alternatively, the original set of scenarios can be reduced by minimizing the Kantorovich distance between the scenarios in the original set and the reduced set [119]. This method is implemented in the forward scenario selection and backward scenario reduction approaches. The forward scenario selection approach [119] iteratively adds one scenario from the original set to the reduced set, until the reduced set contains the desired number of scenarios. On the other hand, the backward reduction approach [119] iteratively eliminates one scenario from the original set, until the desired number of scenarios remains and thus constitutes the reduced set. The work in [119] is improved in [120] by implementing computationally more effective forward scenario selection and backward scenario reduction approaches. Reference [121] modifies the fast forward scenario selection approach to make it compatible with the two-stage stochastic programming problems often encountered in electricity markets. Although this compatibility comes at the cost of a larger computational burden (when compared to [121]), the approach proposed in [121] remains tractable. Papavasiliou *et al.* [122] proposed an importance sampling technique to select scenarios that best represent the monetary impact of uncertainty on the operating cost. Reference [123] studies the impact of the scenario reduction techniques proposed in [118, 120, 121, 122] on the performance of the SUC model and concludes that the fast forward selection technique produces scenarios that result in the least-cost solution and require the least solving time of the SUC model.

While scenario reduction techniques aim to accelerate computing times, an insufficient number of scenarios may reduce the accuracy of the solution and increase its cost [124, 125]. However, the relationship between the number of scenarios and the cost of the SUC solution is not trivial: increasing the number of scenarios does not necessarily improve cost efficiency [124]. Similarly, reference [124] reveals that lowering the duality gap is likely to increase computing times, yet does not always provide the anticipated cost savings.

Large-scale implementations of SUC remain unfeasible for real-life power systems since it may

take up to tens of hours to obtain a reasonably accurate solution [113].

2.1.3.3 Interval Unit Commitment

The Interval UC (IUC) formulation [126] simplifies the representation of uncertainty used in SUC by considering only a central forecast and the uncertainty range around the central forecast, delimited by the upper and lower bounds on the realizations of the loads and renewable generation. The objective function of the IUC minimizes the operating cost of the central forecast and enforces feasibility of all inter-hour transitions within the bounds of uncertainty for adjacent operating hours, as shown in Figure 2.4. This approximation ensures that the IUC schedule is feasible for any scenario that remains within these bounds [127].

Although the conservatism of the IUC model can be regulated by adjusting the width of the uncertainty range, this approach is not systematic and requires fragile tuning for different operating conditions. On the other hand, the conservatism of the IUC model can be reduced using the Markovian approach [128] to reduce the number of possible states [129]. Moreover, the combined Markovian/IUC approach is less computationally demanding than the pure IUC model [129].

If the upper and lower bounds of the IUC envelope all scenarios used in the SUC, the solution of the IUC is proven to be feasible for all scenarios in the SUC [126]. However, in this case, the IUC schedule is more expensive than the SUC schedule, because it enforces inter-hour transitions with low probabilities at any cost [125]. In line with SUC, the IUC can also be implemented using Benders' decomposition [125, 126].

2.1.3.4 Robust Unit Commitment

Just like the IUC, in the Robust UC (RUC) formulation the range of uncertainty around the central forecast is defined by the upper and lower bounds, as shown in Figure 2.4. The RUC enforces the feasibility of its schedule over a given uncertainty set and minimizes dispatch costs under the

worst-case realization [130]. The worst-case realization is determined endogenously and thus simultaneously accounts for both unfavorable magnitudes and high ramp rates within the range of net loads. Although the RUC solution minimizes the cost for the worst case, the RUC solution is less cost effective for the central forecast.

The conservatism of RUC can be adjusted using the budget of uncertainty. In [130], the budget of uncertainty is defined as the number of buses that are allowed to deviate from a given central wind forecast in the worst-case scenario. The value of the budget of uncertainty must be specified before solving the RUC model. Until RUC is solved, it is unknown which buses will be chosen by the RUC model to deviate from the central wind forecast. Furthermore, the cost performance of RUC can be improved by using dynamic uncertainty sets [131], which are capable of modeling temporal and spatial correlations of wind power generation more accurately than the box uncertainty sets in [130].

Like SUC and IUC, RUC also has a two-stage structure; therefore, RUC can be implemented using Benders decomposition [130, 132, 133, 134] or the column-and-constraint generation method [135, 136]. The latter method improves the computational performance of the RUC model and reduces the number of iterations required to obtain the optimal solution while ensuring the same cost performance as Benders decomposition [135]. However, even in the simplest of Benders' decomposition implementation, RUC is tractable for large-scale power systems (e.g., ISO-NE [130]).

2.1.4 Optimal Power Flow

Since the OPF problem is solved 30-90 minutes ahead of real-time and has a lower optimization horizon than the UC problem, it can take advantage of more accurate load and renewable generation forecasts, and it usually invokes a lower computational burden due to lower dimensions. In turn, the advantage of reduced computational complexity makes it possible to increase the modeling fidelity of the OPF problem and account for phenomena that would make most UC problems

computationally infeasible. Specifically, OPF problems depart from UC problems in the following aspects:

- **Resolution:** The OPF problem is solved with a 5-15 minute resolution and captures the sub-hourly variability of renewable generation. If SUC is modeled with these resolutions, it would become infeasible even for a relatively small benchmark system [82]. Although both RUC and IUC are computationally feasible with such resolutions, their solving times increase 4x when compared to hourly-based analogs.
- **Power flow model:** The OPF problem can be solved with AC power flow constraints, thus improving UC solutions by accounting for reactive power flows and bus voltages. Modeling AC power flows requires solving a non-convex and nonlinear optimization problem, which nevertheless can be solved for the global optimum solution. For example, the method in [137] includes the necessary and sufficient conditions for this optimality, derived from the dual problem of an equivalent form of the OPF problem.
- **Corrective actions:** Given AC power flow constraints, the OPF problem can also optimize decisions on FACTS devices and tap ratios of power transformers (which are omitted in UC problems) and can be used for mitigating the impact of contingencies.
- **Contingency states:** Real-time measurements obtained from condition-based monitoring of transmission and generation assets can be fed to the OPF problem to model a credible set of contingency states. This contingency information can be used to immunize OPF decisions by using more advanced corrective actions.
- **Analytical representation of uncertainty:** Unlike UC models that approximate the uncertainty of renewable generation using a set of scenarios (SUC) or an interval (RUC and

IUC), the OPF problem can use chance-constrained programming² to reformulate analytically chance constraints based on the normal distribution as deterministic second-order cone constraints. The resulting quadratic problem can be solved using cutting planes, as is explained in [139]. The inaccuracy of the normal distribution in representing the uncertainty of wind power generation can be alleviated by introducing uncertainty sets on the mean and standard deviation values of the distribution [30, 140].

2.1.5 Energy Storage Technologies

Unlike conventional and renewable generation, energy storage does not have its own physical means to generate electric power from other sources of primary energy; therefore, this resource is considered *energy limited* [62]. On the other hand, the operation of energy storage does not include highly inertial thermodynamics and mechanical processes (as is conventional generators), which allows for adjusting its power output almost instantaneously [141], thus making energy storage very useful for fast corrective actions.

The US DOE [142] and ESA [143] identify the following ES technologies:

- **Pumped Hydropower ES (PHES):** A typical PHES consists of an upper and lower water reservoir that can be used for generating power (turbining mode) by discharging water from the upper to the lower reservoir and for consuming power (pumping mode) by elevating water from the lower to the upper reservoir. This technology has been used for several decades and, as of now, is the only large-scale energy storage technology. The advantage of this technology is that it has a relatively large expected lifetime (40-60 years) and that its energy and power capacity do not deteriorate over time [144]. Additionally, the PHES can be used for storing energy over multiple hours and even over multiple days. However, the use of this technology

²Note that existing UC formulations [138] based on chance-constrained programming use scenario sampling, not analytical reformulation, for representing uncertainty.

is limited due to the landscape and environmental constraints on its placement; the cycling efficiency can be as low as 65% [144].

- **Solid State Battery ES (SSBES):** This technology uses solid electrodes and electrolytes to convert chemical energy into electrical energy. The array of chemistries that are used for this conversion includes lithium-ion, nickel-cadmium, and sodium sulfur materials. Unlike PHES, SSBES has no landscape limits and, essentially, can be installed at every substation. Furthermore, the direction of the conversion process can be controlled instantly, which ensures a rapid response. Recent advances in material science have enabled cycling efficiencies as high as 95% [47, 145] and lifespans of up to 15 years [145]. However, the lifespan of SSBES also depends on the depth-of-discharge at each cycle, which drives the degradation of SBESS. Therefore, modeling battery degradation in short-term planning tools, such as UC and OPF, is pivotal for sustainable integration of the SBESS in existing power systems.
- **Flow Battery ES (FBES):** Just like in the SSBES, FBES converts chemical energy into electrical energy. This conversion is based on the controllable and reversible dissolving of two or more electrochemical elements in the electrolyte. This technology is implemented using vanadium and uranium redox, zinc-polyiodide, and lithium-iron phosphate chemical reactions. FBES have lower cycling efficiency than SSBES (of up to 85%), but longer lifetimes (of over 25 years) [145]. The main advantage of FBES is that the electrochemical elements used in energy conversion can be replaced, thus alleviating the effect of its degradation.
- **Flywheel ES (FES):** FES is a rotating mechanical device that stores kinetic energy. Unlike in PHES, SSBES, and FBES, FES are not able to discharge energy for more than a few tens of minutes and can, therefore, only be used for smoothing out the intermittent output of renewable generation or other short-term ancillary services. The advantage of FES is that it has a lifespan of 15-20 years [144, 145], which does not depend on its cycling history and

its cycling efficiency of 85-95% [145]. On the other hand, FES are prohibitively expensive [145], and high-speed rotating masses impose some safety concerns [147, 148].

- **Thermal ES (TES):** This type of ES includes a vast number of technologies: thermostatically-controlled residential and commercial loads, industrial heat pumps, and other thermally inertial processes. The efficiency of these technologies vary from one technology to another, but rarely exceeds 40-60% [149]. The advantage of these technologies is that they have a low capital cost. However, the SO's ability to fully control these resources is expected to be constrained by user preferences and the limitations of specific industrial processes. Further development of TES is also contingent upon the deployment of advanced communication infrastructure and metering.

In addition to existing technologies, there is a number of on-going studies that explore other means of reducing the capital cost of ES and improving its cycling efficiency and lifespan [150, 151]. As pointed out in [54, 152], the further development of affordable ES is critical for operating a sustainable power system.

2.2 Long-term Planning

2.2.1 Objectives

Whether voluntarily or under societal pressure, power systems constantly evolve to adapt to new socioeconomic and technical environments. One approach to facilitate this transition is to construct new (or upgrade existing) generation and transmission assets based on anticipated long-term economic development and energy consumption projections, environmental targets, and policy initiatives. Therefore, decisions-makers need tools that are capable of producing expansion decisions and simulating system performance under different external, and often uncertain, conditions. This uncertainty stems from prospective load and renewable generation profiles, the technical characteristics of

prospective generation technologies and their capital costs, policy instruments, and environmental regulations, all of which cannot be perfectly known beforehand [65, 64, 153, 154, 155].

Long-term planning in power systems is further complicated by its coupling with other cyber-physical infrastructures, for example, fuel supply (i.e., natural gas, coal, uranium) [153, 156, 157, 158] and electrified transportation systems [159]. Each of these systems represents a network constrained by its own physics and economics, which must be taken into account while making expansion decisions in power systems.

Given this complexity, long-term planning in power systems has traditionally been solved separately for generation and transmission expansion decisions. Although this assumption makes long-term problems computationally tractable and thus enables sensitivity analyses, it also leads to a suboptimal expansion plan. To further simplify the problem, expansion decisions on different time scales are also computed separately. Since the expected lifetime of some equipment may exceed some time scales, this simplification sacrifices some optimality. However, shorter time scales generally facilitate computational tractability and makes possible more accurate modeling of some phenomena and more complex objectives [65, 153]. The time scales for long-term planning problems are characterized as follows:

- **Near-Term (0-5 years):** The objective within this horizon is to ensure reliability at a minimum cost. The scope of this horizon is limited to generation expansion decisions, since obtaining permits for new transmission lines and constructing these lines is likely to take more than 5 years [65]. In this case, planning is based on the NWP mesoscale climate models to analyze renewable generation availability and to take advantage of the more or less accurate knowledge of available policy instruments and commercially available technologies [153]. Mathematically, this time scale is feasible for implementing an alternating current power flow model and modeling individual generators.
- **Mid-Term (5-15 years):** Unlike near-term planning, this time scale allows for transmission

expansion decisions. However, these studies are usually implemented with a direct current power flow model. Expansion decisions on generators can be clustered in technology-specific groups to alleviate computational burdens [64]. These models usually use statistical scenarios to account for the demand and renewable generation profiles [160, 161]. The technical characteristics and capital costs of new technologies are modeled within a certain range because they cannot be postulated exactly.

- **Long-Term (>15-20 years):** Within this time scale, it is difficult, if even possible, to narrow down possible variations of uncertain factors to a representative set. The primary objective of such models is to perform a scenario analysis and identify a rough set of expansion decisions for each scenario that could be further refined in near-term and mid-term studies when there are fewer uncertainty factors [65]. Mathematically, this planning can be based on transportation models, which do not explicitly account for Kirchhoff's laws.

As pointed out in [162], the methods for generation expansion planning vary for vertically integrated (monopolistic) and competitive power systems. Under the vertically integrated assumption, the explicit objective of expansion decisions is to minimize the overall cost of supplying electricity. On the other hand, in a competitive environment, market participants aim to maximize their profits; therefore, the decision for expansion should be made with respect to their profit expectations. Since this dissertation focuses on long-term planning in a competitive market, Section 2.2.2 surveys the key methods for generation and transmission expansion in such systems. Section 2.2.3 describes existing methods for expansion planning with energy storage.

2.2.2 *Long-term Planning in a Competitive Environment*

The primary challenge in long-term planning problems in a competitive environment is to model market interactions between different participants and the system operator. Complexity arises from

the need to account for different objectives and some assumptions that unavoidably depart from real-life practice:

- **System operator:** the objective of the system operator is to maximize system-wide social welfare, which generally accounts for both demand-side and supply-side interests in a *cumulative* (rather than *individual*) fashion, while providing equal access to common infrastructure (e.g., the transmission network). The objective of the system operator is also subject to regulation, which may vary in different jurisdictions.
- **Market participants:** the objective of market participants is to maximize their own profit while meeting the technical constraints on their own assets. In a competitive environment, market participants usually act with limited information regarding the behavior of the system operator and other participants.
- **Typical assumptions** ([64, 65, 42, 163, 164, 165]):
 - Offering and bidding data and strategies are known for all market participants.
 - Uncertainty on renewable generation and load growth during the planning horizon are given.
 - Every market participant has equal access to the transmission network.
 - Expansion decisions are derived for a target year and usually do not account for year-to-year evolution.
 - All expansion decisions are reduced to a set of most likely decisions using screening techniques.

Bi-level programming can be used to account simultaneously for the perspectives of the system operator and market participants. This technique has been used in generation, transmission, and

joint generation-transmission long-term planning [163, 164, 165, 166, 167, 168, 169, 170, 171]. The common thread of the models in [163, 164, 165, 166, 167, 168, 169, 170, 171] is their mathematical structure, displayed in Figure 2.5. The upper-level problem characterizes feasible expansion decisions and minimizes investment costs over a given time scale. In the lower-level problem, market equilibrium is achieved under forecast conditions. The lower-level problem explicitly maximizes social welfare and considers the offers and bids of market participants, their technical constraints, and forecast conditions. The exact formulation of the lower-level problem can be tailored to specific market rules adopted in a particular jurisdiction. Since upper-level and lower-level problems are solved simultaneously, the bi-level programming framework co-optimizes short-term and long-term costs and benefits while optimizing expansion decisions.

To further account for possible uncertainties on load and renewable generation profiles, the bi-level technique can be integrated with stochastic programming [165]. In this case, the lower-level problem is formulated for a set of scenarios, thus immunizing the market equilibrium (and, tangentially, expansion decisions) against possible uncertainty realizations. However, this increases

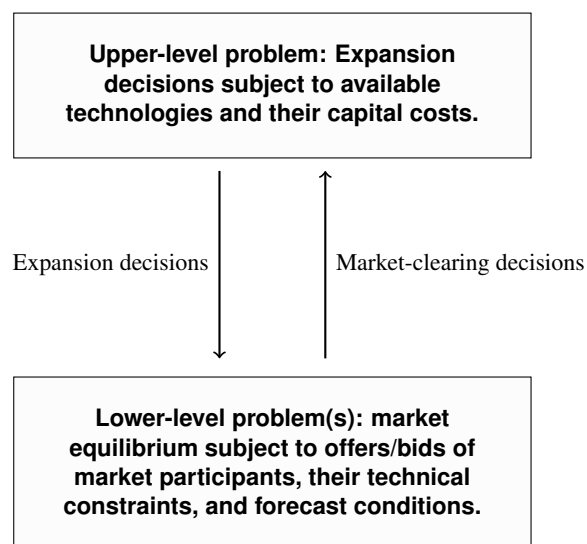


Figure 2.5: An illustration of a typical bi-level transmission and generation expansion model.

the computational complexity. Alternatively, the uncertainty in the lower-level problem can be modeled using robust optimization [163]. Since this approach involves solving a min-max problem (which is a bi-level problem itself), the lower-level problem is split into two levels, thus making the whole problem tri-level.

2.2.3 Long-term Planning with Energy Storage

Long-term planning with energy storage aims to determine the locations and design parameters of energy storage (e.g., rated power and energy capacity) that provide maximum benefits to the system or the energy storage owner. The optimal storage siting and sizing problem is similar to the transmission expansion problem; thus, all of the approaches reviewed in Section 2.2.2 can be modified for this purpose. The only difference is that transmission lines move energy in space while storage moves energy in time. Therefore, unlike in transmission expansion problems, energy storage expansion cannot isolate different operating intervals in separate subproblems and must account for the intra-day dynamics of LMPs [172].

The existing literature on energy storage expansion planning in a competitive environment distinguishes two behaviors by owners of energy storage in electricity markets:

- **Price-taker:** Under this assumption, the offers and bids of energy storage to electricity markets cannot affect market equilibrium. Therefore, energy storage cannot exercise market power in this case. This assumption is modeled in [59, 56, 173, 174, 175, 176].
- **Price-maker:** In this case, owners of energy storage can use their market power to affect market equilibrium in a way that increases their profits by taking advantage of strategic bidding, transmission congestion, and coordinated operations at different locations [177, 178, 179]. This assumption is more difficult to model than the price-taker case. To the best of the author's knowledge, reference [177] is the only available study that discusses energy storage expansion under the price-maker assumption.

Assuming that energy storage is a price-taker in a competitive environment may lead to inaccurate expansion decisions as shown in [177]. However, the simplicity of this assumption outweighs this inaccuracy in the eyes of modelers. The method in [177] is based on the iterative search within a pre-screened set of expansion decisions. At each iteration, different locations are tested for energy storage placement using historical LMP data and a short-term planning tool. This tool takes the perspective of an energy storage owner and thus models energy storage as profit-seeking, price-making, market participants. The preferable locations for energy storage deployment are then determined based on the analysis of energy storage profits at different locations. On the other hand, [177] has no information that would account for the bidding strategies of the other market participants and disregards the system operator perspective. Therefore, this method may also miscalculate the system's need for energy storage.

To the best of the author's knowledge, previous work has not addressed long-term planning with energy storage in a competitive environment with respect to both system operator and energy storage perspectives.

2.2.4 Modeling Short-term Operations in Long-term Planning

The critical feature of long-term planning models is their accurate ability to account for operational impacts that renewable generation resources will impose on existing electrical grids. These impacts are pivotal for assessing the needs of emerging, yet rather expensive, technologies (e.g., demand response, energy storage, and ultra-flexible generation). Specifically, [64] emphasizes the importance of accounting for these impacts since it '*may lead to infeasible generation mixes*' otherwise.

The complexity of modeling operational impacts is related to the granularity of the long-term planning. In real-time, the power system is operated using a 5-15 minute resolution. Such a resolution (if used in long-term planning) would explode the dimensionality of the optimization problem and lead to computational infeasibility. The value of modeling short-term operations and intra-day

dynamics in long-term planning models is shown in [35, 36], which points out that these factors mainly affect expansion decisions on flexible generation units. If these decisions are miscalculated, some assets may not recover their capital costs within a reasonable time frame.

Furthermore, the computational complexity of long-term planning models explains the following discrepancies in the modeling of the same phenomena in short-term and long-term problems that are likely to reduce the accuracy of the expansion decisions:

- **Transmission network:** As reviewed in Section 2.2.1, a few long-term planning models can tolerate an alternating current power flow model, which is a standard part of short-term planning models [153].
- **Fuel cost curves:** Short-term planning models typically use quadratic or multi-segment linearized cost curves for conventional generators, which enables fine-grade tuning of dispatch decisions. In the long-term planning model, the cost curves are usually replaced by one-block incremental costs.
- **Start-up costs:** While short-term planning can account for multi-period start-up and shut-down trajectories [185], long-term planning models usually use one-period approximations.
- **Generation flexibility:** Long-term planning studies often neglect intertemporal constraints (i.e., minimum up-time and down-time limits and dynamic ramping rates [180]), as well as the dynamic cycling costs [38, 39] of conventional generation.
- **Demand elasticity:** In short-term planning, demand can be modeled using its elasticity (i.e., its sensitivity to changes in prices). Such modeling in long-term planning problems is hardly possible, as it is impossible to accurately calculate elasticity coefficients over multi-year time scales.

2.3 Contributions

This dissertation makes the following contributions to operation and planning in sustainable power systems:

2.3.1 Short-term operation

This work analyzes the existing SUC, IUC, and RUC formulations, concludes that their cost and reliability performance can be improved, and proposes two such approaches.

The first approach, described in Chapter 3, is a modification of the IUC and SUC formulations that reduces the conservatism of the IUC solution by rigorously quantifying the ramping needs of the system and the computational burden of SUC. The case study shows that the proposed modification outperforms the RUC and IUC formulations, in terms of operating cost and the utilization of renewable generation.

The second approach, presented in Chapter 4, takes advantage of the SUC and IUC formulations applied to different intervals of the optimization horizon. This approach applies SUC to the initial operating hours of the optimization horizon (during which renewable generation scenarios are more accurate) and then switches to the IUC formulation for the remaining hours of the optimization horizon. This case study shows that optimizing for the switching time can be used to balance the cost of unhedged uncertainty from SUC against the cost of the security premium of the IUC formulation. The case study demonstrates that the proposed approach yields significant cost savings when compared to the SUC and IUC formulations, which increase with the wind penetration levels.

Furthermore, this dissertation contributes to modeling renewable generation as a reserve provider. In the probabilistic model proposed in Chapter 5, available wind power resources can be simultaneously used for energy and reserve provision. The case study validates that this model reduces operating costs by reducing system-wide reserve requirements due to the lower uncertainty on the renewable injections and reserve contributions from renewable generation.

2.3.2 *Long-term planning*

This dissertation proposes a new model based on bi-level programming to optimally site and size privately owned energy storage. The key contribution of this model is that it accounts for system-wide operating cost savings and simultaneously ensures that the energy storage owner's devices collect sufficient profits to recover their investment costs fully. The usefulness of the proposed method is illustrated using a representative case study of the ISO New England system with a prospective wind generation portfolio. The case study identifies multiple factors that affect the profitability of energy storage and study their effects on the optimal siting and sizing decisions. Among these factors, the profitability of energy storage is mostly sensitive to the capital costs of energy storage, the investment budget, the operating policy of energy storage, and their ability to influence LMPs.

2.3.3 *Impact*

Taken together, the contributions of this dissertation should provide transformative results and insights to stakeholders across power system and sustainable energy communities:

- Power system planners and operators stand to benefit from new modeling methods that improve the reliability and cost performance of previous formulations. These methods could be used in transforming power system planning toward uncertainty-aware, decision-making frameworks that reduce system-wide costs and enforce reliability criteria in a transparent and intuitive way.
- Researchers will benefit from open-source code for the proposed methods and an open-source database that can be used for benchmark simulations.
- Technology developers and manufacturers (e.g., energy storage) can learn the impacts of the design parameters required in power systems with high penetration levels.

- Policy analysts can use the policy recommendations on energy storage placement developed in this work to derive the right set of incentives for motivating transitions toward sustainable power systems.

Part II

SHORT-TERM PLANNING IN SUSTAINABLE POWER SYSTEMS

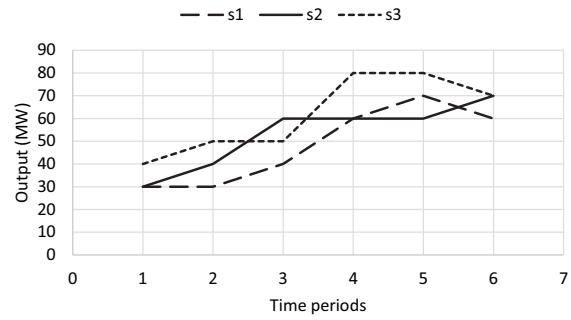
Chapter 3

IMPROVED INTERVAL UNIT COMMITMENT

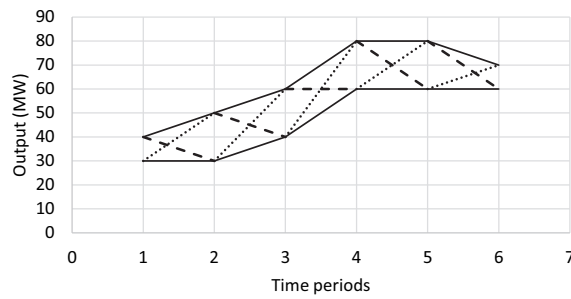
3.1 Motivation

The IUC formulation is computationally more efficient than the SUC formulation because the generation uncertainty of each wind farm is represented by only three non-probabilistic scenarios (see the black lines in Figure 2.4): the central forecast (white circles) and the lower and upper bounds (black circles). On the other hand, IUC solutions are more conservative, due to the constraints that these solutions impose on the feasibility of transitioning from the lower to the upper bound (and vice versa) between any two consecutive time periods, as illustrated by the grey lines in Figure 2.4. Such extreme transitions have very low probability and can be replaced by less severe ramp constraints. Since scenarios are accurately designed to capture the characteristics of the expected wind output, we argue that the required rampable capacity should be no more than the maximum up and down ramps observed over all stochastic scenarios. However, if ramping constraints would be completely relaxed, the day-ahead solution would be very vulnerable to wind volatility, and the overall cost of running a system would be high.

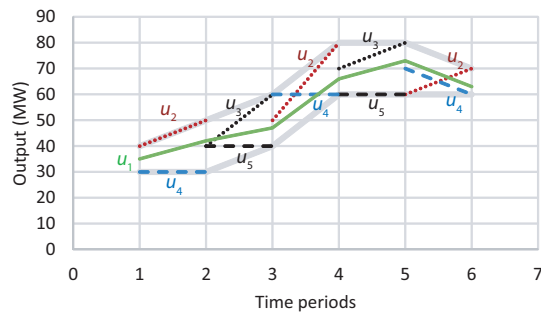
Figure 2.4 illustrates the difference between modeling wind scenarios and bounds for each wind farm in SUC, IUC, and the Improved Interval UC (IIUC). Figure 3.1a shows the scenarios used by the SUC. Bounds for both IUC and IIUC are created based on the minimum and maximum values of these scenarios at each hour. For instance, scenario s1 sets the lower bound in hours 1-4 and hour 6, while the lower bound in hour 5 is set by scenario s2. Figure 3.1b shows the IUC bounds and the up and down ramp requirements. The central forecast and its ramp constraints are omitted for clarity. Figure 3.1c shows artificial IIUC scenarios, which correspond to the ramp requirements



(a)



(b)



(c)

Figure 3.1: An illustrative example of uncertainty modeling: (a) the scenarios used in SUC; (b) the bounds (lines), up ramp requirements (dotted lines), and down ramp requirements (dashed lines) used in IUC; (c) the central forecast (green line), bounds (thick grey lines), up ramp requirements (dotted lines), and down ramp requirements (dashed lines) used in IIUC.

between consecutive hours. Each of the ramps ends at one of the bounds while the location of its *tail* at the previous hour is determined based on the highest slope over all stochastic scenarios. This way, each dotted segment in Figure 3.1c defines the up ramp requirement and upper bound, while each dashed segment defines the down ramp requirement and lower bound. For example, the up ramp requirement between hours 1 and 2 is 10 MW/h because the highest ramp of the three stochastic scenarios in Figure 3.1a is 10 MW/h (s2 and s3). Since the upper bound at hour 2 is 50 MW, the first dotted segment starts at 40 MW in hour 1 and ends at 50 MW in hour 2. Similarly, the up ramp requirement between hours 2 and 3 is 20 MW/h (set by scenario s2), and it ends at the upper bound (60 MW). The remaining up ramp requirements are 30 MW/h between hours 3 and 4 (set by s3), 10 MW/h between hours 4 and 5 (set by s1) and, again 10 MW/h, between hours 5 and 6 (set by s2). The corresponding upper bounds are 80 MW, 80 MW, and 70 MW, respectively. On the other hand, the first four down ramp requirements are equal to zero, because this is the largest down ramp observed over all three stochastic scenarios during these 5 hours. The down ramp requirement between hours 5 and 6 is -10 MW/h, as determined by scenarios s1 and s3. All dashed lines end on lower bounds determined by the stochastic scenarios from Figure 3.1a. To obtain ramp requirements and bounds for each wind farm in a given power system, the methodology explained in Figure 2.4 is applied to each wind farm individually.

A single scenario¹ cannot be used for all up ramp limits, as this would result in two operating points at each period (one at the upper bound, which is the end point of the ramp requirement between the previous hour and the current hour, and one below it, which is the tail point of the ramp limit between the current hour and the following hour). For this reason, IIUC is formulated using five scenarios: u_1 - the central forecast, where cost is minimized in the objective function; u_2 - up ramp limits between odd and even hours; u_3 - up ramp limits between even and odd hours; u_4 - down ramp limits between odd and even hours; and u_5 - down ramp limits between even and odd

¹The term *scenario* should be used with reservations, as *scenarios* in IIUC are used for modeling purposes only, and they do not consider probability.

hours.

Because the ramp constraints are less demanding, the IIUC produces less conservative generator schedules than the IUC.

3.2 Contributions

This Chapter proposes a new IIUC model, which makes the following contributions:

1. It proposes a new IIUC formulation that aims to improve day-ahead reliability unit commitment procedures and combines aspects of SUC and IUC. This model takes advantage of the cost-efficient SUC model and the computational simplicity of the IUC model.
2. It demonstrates the effectiveness of the IIUC based on extensive tests with various wind penetration levels, wind profiles, and controllable generator characteristics.
3. It also provides a systematic and rigorous comparative assessment of the cost and reliability performance of the IIUC, IUC, RUC, and SUC formulations. To the best of the authors' knowledge, such a comparison has not been performed for these UC approaches on the same set of data.

3.3 Formulation

To ensure a fair comparison among the IIUC, IUC, RUC, and SUC formulations (in terms of both cost and computing time), all constraints have been implemented in the same way except where these formulations differ. The formulation of IIUC is presented first. Other techniques are then defined in terms of how they differ from IIUC. All of the notation used in this section is defined in Appendix A.

3.3.1 Formulation of the IIUC

The objective function of IIUC aims to minimize the operating cost of the central forecast scenario u_1 and includes the no-load costs, start-up costs, and running costs for all generators:

$$\min_{\substack{q_{t,i,j}, x_{t,i}, y_{t,i}, z_{t,i}, \\ c_{t,w,u}, g_{t,i,u}, g_{t,i,b,u}^{\text{seg}}, su_{t,i}, \theta_{t,s,u}}} \sum_{t \in \Omega^T} \sum_{i \in \Omega^I} \left[su_{t,i} + A_i \cdot x_{t,i} + \sum_{b \in \Omega^B} K_{i,b} \cdot g_{t,i,b,u_1} \right] \quad (3.1)$$

The choice of this objective function is motivated by the IUC model [109]. Since the objective function (3.1) minimizes the operating cost of the central forecast, the actual materialization of uncertainty (which is expected to differ from the central forecast) will require real-time re-dispatch, which may cause additional expenses when compared to the central forecast [117]. As is shown in the case study in [117] (which performs on the 118-bus IEEE RTS), these expenses are of the same order as those resulting from the application of a SUC optimization.

This optimization is subject to the following constraints:

3.3.1.1 Binary variables logic

The commitment and start-up/shut down decisions on generators are related as follows:

$$y_{t,i} - z_{t,i} = x_{t,i} - x_{t-1,i}, \quad \forall t \in \Omega^T, i \in \Omega^I \quad (3.2)$$

$$y_{t,i} + z_{t,i} \leq 1, \quad \forall t \in \Omega^T, i \in \Omega^I \quad (3.3)$$

Constraint (3.2) determines if the generator, i , is started up or shut down at time, t , based on the change of its 0/1 status between hours $t - 1$ and t . Constraint (3.3) ensures that the generator, i , cannot be started up and shut down during the same time period.

3.3.1.2 Minimum up and down times

The minimum up and down times on generators are enforced as follows:

$$x_{t,i} = X_{e,i}^0, \quad \forall t \in [0, \bar{L}_i + \underline{L}_i], i \in \Omega^I \quad (3.4)$$

$$\sum_{r=t-UT_i+1}^t y_{r,i} \leq x_{t,i}, \quad \forall t \in [\bar{L}_i, T], i \in \Omega^I \quad (3.5)$$

$$\sum_{r=t-DT_i+1}^t z_{r,i} \leq 1 - x_{t,i}, \quad \forall t \in [\underline{L}_i, T], i \in \Omega^I \quad (3.6)$$

Constraint (3.4) sets the on/off status for the first $\bar{L}_i + \underline{L}_i$ hours based on the initial status of the generators. For example, if a generator must stay on for three hours, \bar{L}_i will be 3 and \underline{L}_i will be 0. If no minimum up or down time constraints are active at the beginning of the scheduling horizon, both \bar{L}_i and \underline{L}_i will be 0. Constraints (3.5) and (3.6) enforce minimum up and down time for the remaining time intervals as explained in [181].

3.3.1.3 Stepwise generator start-up cost

The start-up cost is computed using the stepwise linear approximation as described below:

$$q_{t,i,j} \leq \sum_{r=\underline{T}_{i,j}}^{\bar{T}_{i,j}} z_{t-r,i}, \quad \forall t \in \Omega^T, i \in \Omega^I, j \in \Omega^J \quad (3.7)$$

$$\sum_{j \in \Omega^J} q_{t,i,j} = y_{t,i}, \quad \forall t \in \Omega^T, i \in \Omega^I \quad (3.8)$$

$$su_{t,i} = \sum_{j \in \Omega^J} SUC_{i,j} \cdot q_{t,i,j}, \quad \forall t \in \Omega^T, i \in \Omega^I \quad (3.9)$$

The start-up cost of each generator depends on the number of hours that the generator has been off. Constraint (3.7) identifies the appropriate segment of the start-up cost curve to be used based on the number of hours the generator has been off. Constraint (3.8) ensures that exactly one element,

j , of $q_{t,i,j}$ is assigned the value of 1 if $y_{t,i} = 1$. The actual start-up cost is set by constraint (3.9).

3.3.1.4 Generator constraints

The following technical constraints are imposed on generators:

$$g_{t,i,u} = \sum_{b \in \Omega^B} g_{t,i,b,u}^{\text{seg}}, \quad \forall t \in \Omega^T, i \in \Omega^I, u \in \Omega^U \quad (3.10)$$

$$\underline{G}_i \cdot x_{t,i} \leq g_{t,i,u} \leq \overline{G}_i \cdot x_{t,i}, \quad \forall t \in \Omega^T, i \in \Omega^I, u \in \Omega^U \quad (3.11)$$

$$-RD_i \leq g_{t,i,u_1} - g_{t-1,i,u_1} \leq RU_i, \quad \forall t \in \Omega^T, i \in \Omega^I \quad (3.12)$$

$$g_{t,i,u_2} - g_{t-1,i,u_2} \leq RU_i, \quad (3.13)$$

$$\forall t \in \Omega^T \mid t \equiv 0 \pmod{2}, i \in \Omega^I$$

$$g_{t,i,u_3} - g_{t-1,i,u_3} \leq RU_i, \quad (3.14)$$

$$\forall t \in \Omega^T \mid t \equiv 1 \pmod{2}, i \in \Omega^I$$

$$-RD_i \leq g_{t,i,u_4} - g_{t-1,i,u_4}, \quad (3.15)$$

$$\forall t \in \Omega^T \mid t \equiv 0 \pmod{2}, i \in \Omega^I$$

$$-RD_i \leq g_{t,i,u_5} - g_{t-1,i,u_5}, \quad (3.16)$$

$$\forall t \in \Omega^T \mid t \equiv 1 \pmod{2}, i \in \Omega^I$$

Equation (3.10) defines the power output of each generator as the sum of the output on each segment of its cost curve. Constraint (3.11) enforces the minimum and maximum generator output limits. Constraint (3.12) enforces the up and down ramp limits for the central forecast scenario, u_1 . Constraint (3.13) enforces the up ramp limits for scenario u_2 (i.e., only between odd and even hours), while constraint (3.14) enforces these up ramp limits for scenario u_3 (i.e., only between even and odd hours). This is implemented using the modulo function, which returns 0 for even time

periods (the remainder when dividing an even number by 2 is 0) and 1 for odd time periods (the remainder when dividing an odd number by 2 is 1). Similarly, constraints (3.15) and (3.16) enforce the down ramp limits for scenarios u_4 (between odd and even hours) and u_5 (between even and odd hours).

3.3.1.5 Transmission constraints

Using the dc power flow approximation, the following constraints are imposed by the transmission network:

$$\sum_{i \in \Omega^{SI}} g_{t,i,u} + \sum_{w \in \Omega^{SW}} (W_{t,w,u} - c_{t,w,u}) - \sum_{\{s,m\} \in \Omega^L} B_{sm} (\theta_{t,s,u} - \theta_{t,m,u}) = D_{t,s}, \quad (3.17)$$

$$\forall t \in \Omega^T, s \in \Omega^S, u \in \Omega^U$$

$$0 \leq c_{t,w,u} \leq W_{t,w,u}, \forall t \in \Omega^T, w \in \Omega^W, u \in \Omega^U \quad (3.18)$$

$$-\bar{F}_{sm} \leq B_{sm} (\theta_{t,m,u} - \theta_{t,s,u}) \leq \bar{F}_{sm}, \quad (3.19)$$

$$\forall t \in \Omega^T, \{s, m\} \in \Omega^L, u \in \Omega^U$$

$$-\pi \leq \theta_{t,s,u} \leq \pi, \forall t \in \Omega^T, s \in \Omega^S \setminus s_{\text{ref}}, u \in \Omega^U \quad (3.20)$$

$$\theta_{t,s_{\text{ref}}} = 0, \forall t \in \Omega^T \quad (3.21)$$

Equation (3.17) enforces the nodal power balance. Equation (3.18) limits the amount of wind spillage at each wind farm. If the line flow limits imposed by (3.19) cannot be met for a given value of the available wind power at wind farm w , the available wind power will be curtailed by $c_{t,w,u}$. Equation (3.20) limits the voltage angles, while (3.21) sets the voltage angle to zero at the reference bus. To ensure the feasibility of the IIUC model, equation (3.17) can be relaxed for all scenarios, but the central forecast using slack variables penalized in the objective function can be selected (as explained in [81]) and complies with practices of real-life system operators [130, 182].

Furthermore, if these slack variables turn out non-zero, these cases should be carefully examined to avoid load shedding in real time.

3.3.2 Formulation of the IUC

The IUC is modeled using three scenarios: u_1 is the central forecast (as in the IIUC), u_2 is the upper bound, and u_3 is the lower bound. Additional constraints are used to enforce the feasibility of the transitions between the bounds (the grey lines in Figure 2.4).

The objective function and all constraints are modeled as in the IIUC formulation, except for the ramp constraints (3.12)-(3.16), which are replaced by the following constraints, as in [126]:

$$-RD_i \leq g_{t,i,u_1} - g_{t-1,i,u_1} \leq RU_i, \quad \forall t \in \Omega^T, i \in \Omega^I \quad (3.22)$$

$$g_{t-1,i,u_1} - g_{t,i,u_3} \leq RD_i, \quad \forall t \in \Omega^T, i \in \Omega^I \quad (3.23)$$

$$-g_{t-1,i,u_1} + g_{t,i,u_2} \leq RU_i, \quad \forall t \in \Omega^T, i \in \Omega^I \quad (3.24)$$

$$g_{t-1,i,u_2} - g_{t,i,u_3} \leq RD_i, \quad \forall t \in \Omega^T, i \in \Omega^I \quad (3.25)$$

$$-g_{t-1,i,u_3} + g_{t,i,u_2} \leq RU_i, \quad \forall t \in \Omega^T, i \in \Omega^I \quad (3.26)$$

Constraint (3.22) enforces both the up and down ramp limits on the central forecast scenario, u_1 . Constraints (3.23) and (3.24) enforce transitions from the central forecast scenario to the lower (u_3) and upper (u_2) bound scenarios, respectively. Transition requirements between the upper and lower bounds are enforced by constraints (3.25) and (3.26). Therefore, inequalities (3.22)-(3.26) model all possible transitions in a given uncertainty range, as illustrated in Figure 2.4. However, constraints (3.23) and (3.24) can be removed from the original IUC model in [126], since they hold automatically due to constraints (3.25) and (3.26).

3.3.3 Formulation of the SUC

The objective function of SUC weighs the cost of each scenario in proportion to its likelihood:

$$\min_{\substack{q_{t,i}, x_{t,i}, y_{t,i}, z_{t,i}, \\ su_{t,i}, g_{t,i,u}, g_{t,i,b,u}^{\text{seg}}, ct_{w,u}, \theta_{t,s,u}}} \left[\sum_{t \in \Omega^T} \sum_{i \in \Omega^I} A_i \cdot x_{t,i} + su_{t,i} + \sum_{u \in \Omega^U} \pi_u \sum_{b \in \Omega^B} K_{i,b} \cdot g_{t,i,b,u} \right] \quad (3.27)$$

The constraints (with the exception of the ramp constraints) are the same as in the IIUC formulation. However, the set of SUC scenarios contains actual scenarios, instead of the central scenario and artificial scenarios, such as IIUC and IUC. Ramp constraints (3.12)-(3.16) are replaced by constraint (3.28), which enforces ramp limits for each scenario individually:

$$-RD_i \leq g_{t,i,u} - g_{t-1,i,u} \leq RU_i, \quad \forall t \in \Omega^T, i \in \Omega^I \quad (3.28)$$

3.3.4 Formulation of the RUC

The objective function of the RUC is formulated as in [130]:

$$\min_{\substack{q_{t,i}, x_{t,i}, y_{t,i}, z_{t,i}, \\ su_{t,i}, g_{t,i}, g_{t,i,b}^{\text{seg}}, ct_{w,u}, \theta_{t,s}}} \left[\sum_{t \in \Omega^T} \sum_{i \in \Omega^I} su_{t,i} + A_i \cdot x_{t,i} + \max_{r \in \Omega^R} \sum_{b \in \Omega^B} K_{i,b} \cdot g_{t,i,b}(r) \right] \quad (3.29)$$

The first two terms of this objective function represent the start-up cost and the no-load cost of the committed generators. The third term represents the worst-case dispatch cost. Reference [130] recasts the worst-case dispatch term in (3.29) to make it solvable by existing numerical algorithms:

$$\min_{q_{t,i}, x_{t,i}, y_{t,i}, z_{t,i}, su_{t,i}} \left[\sum_{t \in \Omega^T} \sum_{i \in \Omega^I} su_{t,i} + A_i \cdot x_{t,i} + \max_{r \in \Omega^R} \min_{g_{t,i,b}, g_{t,i,b}^{\text{seg}}, ct_{w,u}, \theta_{t,s} \in \Omega^X} \sum_{b \in \Omega^B} K_{i,b} \cdot g_{t,i,b} \right] \quad (3.30)$$

The worst-case dispatch term in equation (3.30) can be interpreted as the minimum economic

dispatch cost for a fixed commitment \mathbf{x} of all generators maximized over the uncertainty set Ω^R [130]. Constraints on the start-up cost and binary logic decisions are modeled as in (3.2)-(3.9), and the constraints on the generation dispatch and transmission limits are modeled as in (3.10)-(3.21), with one scenario representing the worst case for a given Ω^R . The RUC model is solved using the decomposition approach proposed in [130] and uses the same upper and lower bounds as the IUC and IIUC formulations. To control the conservatism of the RUC model, the budget of uncertainty is defined as $\Gamma \in \{0, 1, 2, \dots, \text{card}(\Omega^W)\}$, where Γ is the number of wind farms that are allowed to deviate from their central forecast. $\Gamma = 0$ means that no wind farm deviates from its central forecast (i.e., in this case, the RUC model reduces to the deterministic UC model that considers only the central forecast). On the other hand, $\Gamma = \text{card}(\Omega^W)$ stands for the most conservative case, where all wind farms can attain any value within the given uncertainty range. In this work, the uncertainty set is modeled as described in [130]; however, a concept called “dynamic uncertainty sets” can be used to model temporal and spatial correlations of wind power generation more accurately [131].

3.4 Test Results

3.4.1 Description of the Test Cases

All four UC formulations were tested using IEEE RTS-96 [183], modified to accommodate for 19 wind farms. This test system is illustrated in Figure B.1 in Appendix B. To create additional congestion, the original line flow limits were reduced by 20%. Figure 3.2 shows the first day of the annual load data and two wind profiles that aggregate wind generation at all wind farms. These wind profiles are calculated as the sum of the central forecasts of all wind farms; therefore, the shape of the central forecast at a particular wind farm may deviate from this aggregated profile. The first aggregated wind profile in Figure 3.2 roughly coincides with the load profile and is, thus, favorable; the second peaks during a period of low load and is, thus, unfavorable. Wind energy penetration levels ranging from 10 to 50% (in 10% increments) were considered. All of the data used for these

test cases, as well as the GAMS codes for the IIUC, IUC, RUC and SUC formulations, are available in [184]. Since there is no systematic approach to choosing the best Γ for the RUC model, subsection 3.4.3 assumes that $\Gamma = \text{card}(\Omega^W)$ (i.e., the optimal solution is hedged against the whole range of uncertainty at every wind farm in set Ω^W). Subsection 3.4.4 compares the proposed IIUC model to the RUC model with different values of Γ .

Two sets of generator data were used to study the influence of generation characteristics. The first set of generator data is described in [185] and is denoted as G1 in the remainder of this chapter. The second set, denoted G2, uses the minimum output limits, minimum up/down times, and ramp limits from [186]. Generator dataset G1 has higher ramping capabilities than G2, but also higher minimum generator outputs and longer minimum up/down times. Generator types, capacities, and locations are the same for both generator datasets. The total nameplate capacity of all conventional generators in G1 and G2 datasets is 10,215 MW, while the peak load during the day is 7,540 MW.

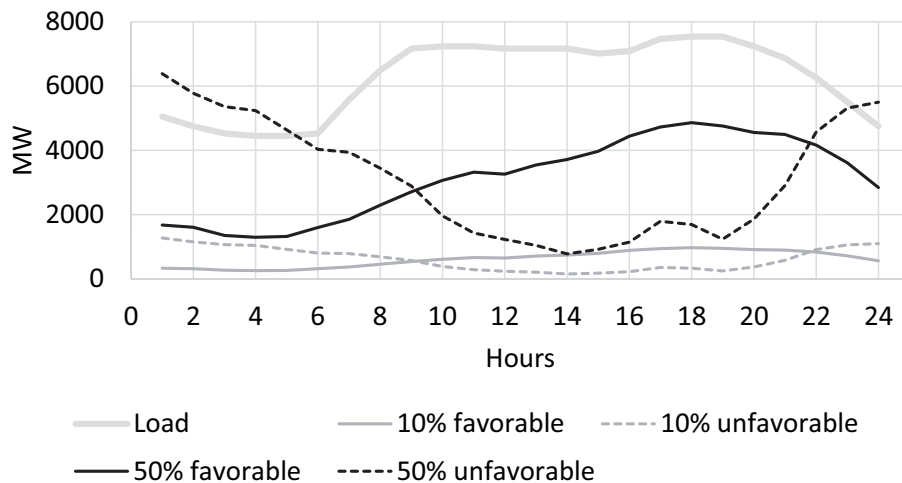


Figure 3.2: Aggregated load and wind profiles used for the test cases.

3.4.2 Wind Data

An approach combining multiple statistical methods [187] was used to obtain an ensemble of 1000 wind generation scenarios for each wind farm. Note the ensemble of scenarios obtained from different scenario generation algorithms leads to lower forecasting errors than when using a single scenario generation algorithm [188]. Each of the following statistical algorithms was used to produce 250 scenarios: regularized linear regression [189], support vector regression [190], multi-layer perceptron [191], and random forest [192]. These algorithms use historical wind power and speed data to generate wind power scenarios in a non-parametric manner, which avoids making the assumption that wind forecast errors follow a known distribution (e.g., Normal, Cauchy, skew-Laplace). These algorithms also ensure better fitting of the historical data to nonlinear wind turbine power curves [193]. Information regarding the geographical location of the wind farms is used to characterize the spatial correlations between them. The central forecast, W_{t,w,u_1} , for each wind farm is then calculated as the average of the 1000 scenarios in the ensemble. Because the central forecast for each wind farm is generated using the same statistical algorithms and the same estimation parameters, it naturally reflects the temporal correlations. Thus, no Gaussian copula is needed. This approach to modeling wind generation scenarios and the central forecast is based on processing empirical (historical) observations; thus, this approach avoids making any assumptions on the distribution of wind generation. Since the tractability of the SUC deteriorates as the number of scenarios increases [83], the original ensemble of 1000 scenarios for each wind farm was reduced to 10 scenarios using the fast forward selection algorithm [194]. As shown in [117, 83, 81], the choice of 10 scenarios for each wind farm represents a suitable trade-off between the computational complexity of SUC and its cost performance. The choice of the fast forward selection algorithm is justified by its better cost and computational performance when compared to other scenario reduction techniques [83]. Instead of modeling a set of scenarios for each wind farm, the IIUC, IUC, and RUC formulations enforce the range of uncertainty for each wind farm, which hedges the optimal solution against deviations

within a predetermined region covered by these scenarios. The lower and upper bounds of this range for the IIUC, IUC and RUC models were set for each time step at the 5th and 95th percentile of the empirical probability distribution of the original ensemble of 1000 scenarios. Reference [83] proves via MC simulations that using the original ensemble of 1000 scenarios for deriving these bounds, instead of the reduced 10 scenario set enforced in SUC, results in a more cost-effective schedule.

The NREL Western Wind dataset [195] provides the wind data. Wind farm locations were mapped to IEEE RTS-96, respecting the lengths of the lines.

3.4.3 Assessing Cost and Reliability Performance using Monte Carlo Simulations

The day-ahead schedules produced by each formulation were tested using MC simulations against realizations of wind uncertainty. These realizations are different from the ensemble of scenarios used for day-ahead decision-making to account for the imperfection of wind prediction tools and were generated for each wind farm as the sum of its central forecast (calculated as explained in subsection 3.4.2) and the historical error of the central forecast for this location. Therefore, the simulated realization of wind uncertainty, $W_{t,w}^{MC}$, can be formally defined as $W_{t,w}^{MC} = W_{t,w,u_1} + \epsilon_{t,w}$, where W_{t,w,u_1} is the central forecast and $\epsilon_{t,w}$ is its historical error. In line with [33], $\epsilon_{t,w}$ was sampled from a multivariate normal distribution, $\epsilon_{t,w} \sim N(\mu^w, \Sigma^w)$, where μ^w is the vector of historical forecasting error means for each operating hour, and Σ^w is the covariance matrix obtained from historical data (as explained in [33]). Note that other distributions can be used to sample the error of the wind power central forecast (e.g., the Cauchy distribution [196] and the Skew-Laplace distribution [197]). In this work, the selection of the normal distribution is based on the Kolmogorov-Smirnov goodness-of-fit test, which indicates that the normal distribution may fit this forecast error better than other distributions if ramp rates are taken into account [29]. The number of realizations required for each day-ahead schedule is calculated using the variance reduction method to achieve an error of lower than 1% with a confidence of 95% [198]. This method assumes that

the minimum number of realizations will vary for each day-ahead schedule depending on its cost distribution. In this work, the minimum number of realizations for each day-ahead schedule ranges from 1877 to 2188 trials.

Since the main goal of this work is to address wind uncertainty, the load was considered deterministic. Also, the load uncertainty is much lower than the wind uncertainty [70].

To assess the realistic performance of day-ahead schedules against the simulated realizations of uncertainty, an MC simulation is performed for each realization of uncertainty. To meet each of these realizations, re-dispatch and re-commitment decisions are modeled to reflect the intra-day actions of the system operators. Re-dispatch decisions allow changes to the power output of the committed generators if the constraints on the minimum and maximum generation output, the up and down ramp rates, and the power flow limits are met. The re-commitment decisions assume that adjustments to the day-ahead binary decisions can be performed on the day if the intertemporal constraints (3.2)-(3.6) are not violated. Since this work focuses on the reliability UC process in the context of a vertically integrated utility, real-time re-dispatch and re-commitment decisions are priced at the marginal start-up and fuel cost of the generators. However, if the re-dispatch and re-commitment decisions are insufficient, avoiding infeasibility may require load shedding, which is penalized in the objective function, at \$10/kWh. Interested readers are encouraged to see [81] for further reading on the impacts of the load curtailment penalty on the day-ahead schedule.

Figure 3.3 shows the cumulative probability distribution functions (CDF) of the expected operating cost as calculated using the MC simulations for various test cases and the four UC formulations. In all cases, regardless of the generator characteristics and wind penetration, the SUC formulation is the most cost-effective, IIUC is the second most effective followed by RUC, and IUC is the least cost-effective. The IIUC has a significant advantage over RUC for an unfavorable wind profile as can be seen in parts (B) and (D) of Figure 3.3. The poor performance of IUC is more notable for favorable wind profiles in parts (A) and (C) of Figure 3.3.

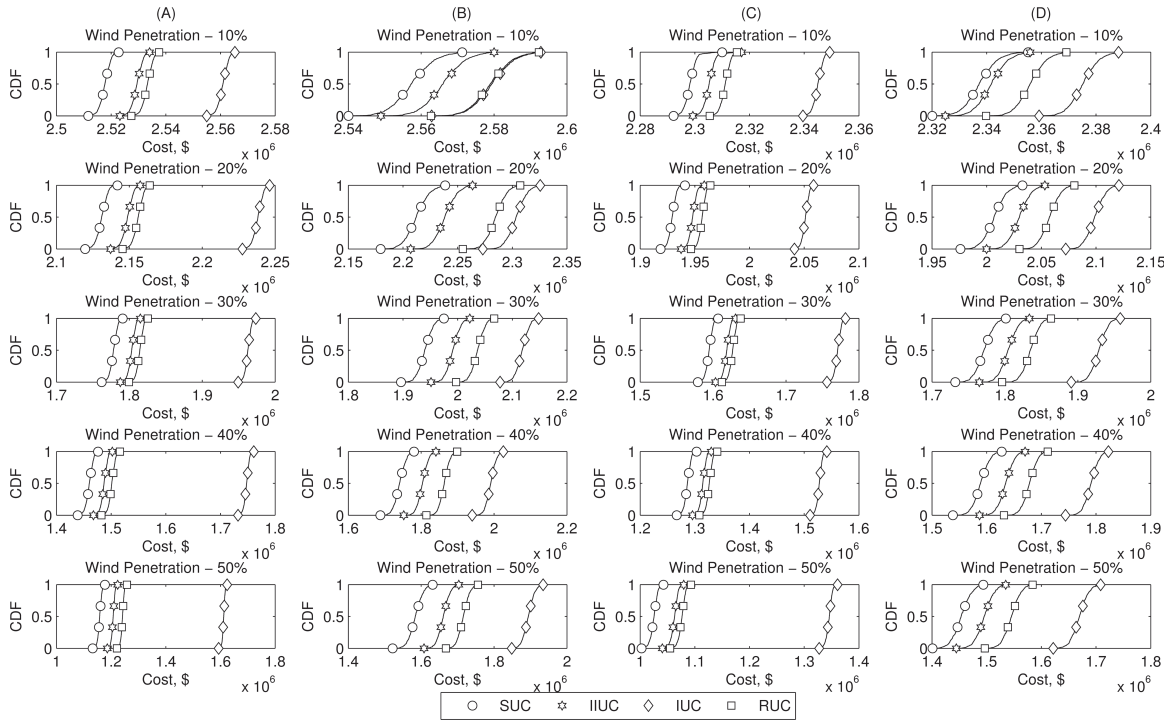


Figure 3.3: Comparison of expected operating costs of the day-ahead schedules obtained with the SUC, IIUC, IUC and RUC ($\Gamma = \text{card}(\Omega^W)$) for different wind penetration levels - (A) generator dataset G1, favorable wind profile; (B) generator dataset G1, unfavorable wind profile; (C) generator dataset G2, favorable wind profile; and (D) generator dataset G2, unfavorable wind profile.

Table 3.1 compares the cost performance of the SUC, IIUC, RUC, and IUC models in terms of expected cost (EC) and the standard deviation (SD) of the cost distribution obtained using MC simulations. The EC is the mean value of the CDF (shown in Figure 3.3), while the SD presents the expected deviation from this value, in percentages. For each case, the SD is also calculated in percentage of its corresponding EC.

The EC of each UC model decreases as wind penetration increases. Test system G2 consistently results in a lower value of EC due to its less stringent minimum up and down time constraints on generators than in test system G1. This difference increases with the wind penetration level. Figure 3.4 compares the cost of the IIUC, IUC, and RUC models with the cost of the SUC model. For the 10% wind penetration case, the IIUC solution costs less than 0.5% more than the SUC. On the

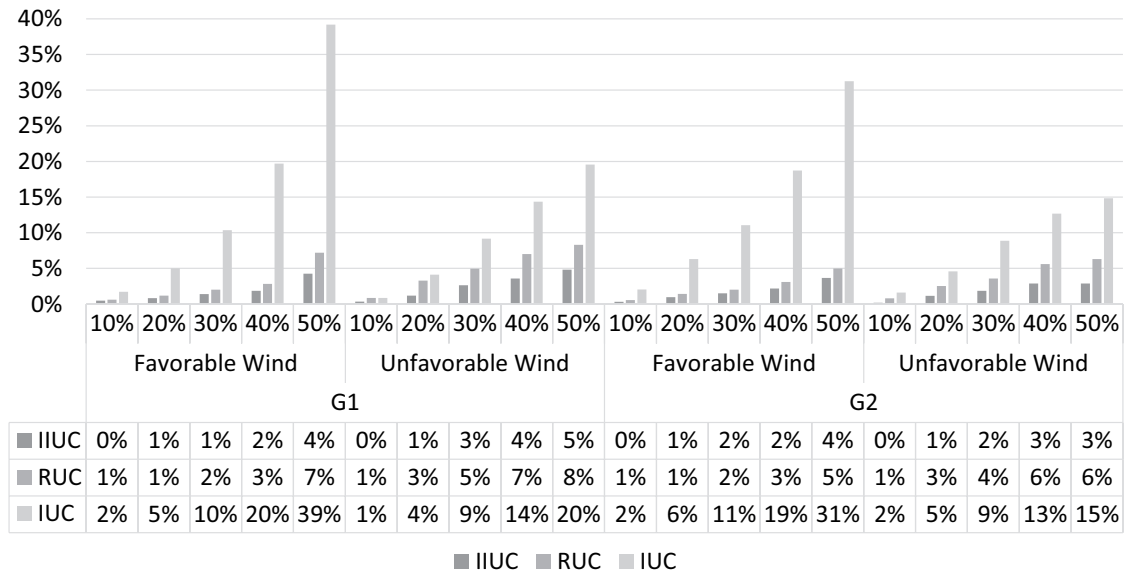


Figure 3.4: Increase in the expected costs of the schedules produced by IIUC, RUC ($\Gamma = \text{card}(\Omega^W)$), and IUC when compared to SUC for different wind penetration levels.

other hand, the RUC and IUC models cost up to 0.8% and 2.0% more, respectively. For a 20% wind penetration case, the expected cost with the IIUC, RUC and IUC models are up to 0.8%, 1.2%, and 5.0% higher, respectively. These differences in cost grow further as the wind penetration increases. Using IUC may result in up to 39% higher operating costs than SUC. The worst IIUC and RUC cost increases are much lower, at 4.8% and 8.3%, respectively. This comparison of the cost-performance of various UC models supports the usefulness of the proposed IIUC model, which reduces the unnecessary conservatism of the RUC and IUC models by modeling realistic ramping scenarios.

The SD can be used to characterize the adaptability of the day-ahead schedule to the true realization of uncertainty. Thus, if the SD is high, the day-ahead schedule may require expensive corrective actions for some realizations of wind. On the other hand, the absolute and relative values of the SD tend to increase with wind penetration, which indicates that all of the considered UC models become more sensitive to deviations from the central forecast under high wind penetration levels. The SD also depends on the temporal correlation between wind generation and load. If this

correlation is favorable, all UC models under any wind penetration level have a lower SD than under the unfavorable correlation. As shown in Table 3.1, the day-ahead schedule obtained using the SUC model results in the largest SD among all UC models for any wind profile, wind penetration level, and test system. On the other hand, the IUC approach systematically results in the lowest SD among all UC models considered. We conclude that conservative formulations (e.g., IUC and RUC) are more adaptive to the extreme realizations of uncertainty than the IIUC and SUC models.

Table 3.1.
COMPARISON OF THE COST PERFORMANCE (EC - EXPECTED COST; SD - STANDARD DEVIATION)

	10%		20%		30%		40%		50%		
	EC, ·10 ⁶ \$	SD, ·10 ³ \$ (%)	EC ·10 ⁶ \$	SD, ·10 ³ \$ (%)	EC, ·10 ⁶ \$	SD, ·10 ³ \$ (%)	EC, ·10 ⁶ \$	SD, ·10 ³ \$ (%)	EC, ·10 ⁶ \$	SD, ·10 ³ \$ (%)	
Favorable	SUC	2.518	1.928 (0.08%)	2.131	3.721 (0.17%)	1.778	5.070 (0.29%)	1.460	6.651 (0.46%)	1.158	7.345 (0.63%)
	IIUC	2.529	1.919 (0.08%)	2.149	3.609 (0.17%)	1.803	4.837 (0.27%)	1.487	5.902 (0.40%)	1.207	6.350 (0.53%)
	RUC*	2.533	1.846 (0.07%)	2.156	3.391 (0.16%)	1.814	4.631 (0.26%)	1.501	5.770 (0.38%)	1.241	6.002 (0.48%)
	IUC	2.561	1.846 (0.07%)	2.238	3.356 (0.15%)	1.963	4.224 (0.22%)	1.758	6.937 (0.40%)	1.612	4.838 (0.30%)
Unfavorable	SUC	2.557	5.429 (0.21%)	2.212	10.340 (0.47%)	1.940	12.997 (0.67%)	1.741	15.540 (0.89%)	1.584	18.253 (1.15%)
	IIUC	2.566	5.324 (0.21%)	2.239	9.611 (0.43%)	1.991	12.166 (0.61%)	1.804	14.334 (0.79%)	1.661	15.958 (0.96%)
	RUC*	2.579	5.128 (0.20%)	2.285	8.663 (0.38%)	2.037	11.719 (0.58%)	1.863	13.564 (0.73%)	1.716	15.324 (0.89%)
	IUC	2.580	5.188 (0.20%)	2.304	8.594 (0.37%)	2.118	11.397 (0.54%)	1.991	13.540 (0.68%)	1.894	15.213 (0.80%)
Favorable	SUC	2.298	5.678 (0.10%)	1.929	9.742 (0.18%)	1.595	11.951 (0.30%)	1.286	14.411 (0.47%)	1.025	16.232 (0.64%)
	IIUC	2.305	5.359 (0.10%)	1.948	9.285 (0.18%)	1.619	11.610 (0.29%)	1.315	13.680 (0.43%)	1.063	15.529 (0.59%)
	RUC*	2.311	5.073 (0.08%)	1.957	8.607 (0.16%)	1.627	10.932 (0.28%)	1.326	12.931 (0.42%)	1.076	14.854 (0.57%)
	IUC	2.345	5.071 (0.07%)	2.051	8.418 (0.15%)	1.771	10.756 (0.25%)	1.527	12.757 (0.33%)	1.345	14.587 (0.41%)
Unfavorable	SUC	2.338	2.307 (0.24%)	2.007	3.555 (0.49%)	1.772	4.768 (0.67%)	1.589	5.989 (0.91%)	1.438	6.511 (1.12%)
	IIUC	2.342	2.299 (0.23%)	2.030	3.520 (0.46%)	1.805	4.721 (0.64%)	1.635	5.697 (0.84%)	1.496	6.268 (1.04%)
	RUC*	2.356	1.785 (0.22%)	2.058	3.154 (0.42%)	1.835	4.578 (0.60%)	1.678	5.539 (0.77%)	1.545	6.170 (0.96%)
	IUC	2.375	1.757 (0.21%)	2.099	3.107 (0.40%)	1.929	4.468 (0.56%)	1.791	5.052 (0.71%)	1.670	5.560 (0.87%)

* - RUC is solved with $\Gamma = \text{card}(\Omega^W)$

Table 3.2.
COMPARISON OF ENERGY IMBALANCES(EWS - EXPECTED WIND SPILLAGE; EENS - EXPECTED ENERGY NOT SERVED)

	10%		20%		30%		40%		50%		
	EWS, MWh	EENS, MWh (freq.)									
Favorable G1	SUC	0	0.009 (1)	0	0.008 (6)	0	0.005 (6)	20	0 (0)	62	0 (0)
	IIUC	0	0.001 (2)	0	0 (0)	0	0 (0)	0	0 (0)	59	0 (0)
	RUC*	0	0 (0)	0	0 (0)	0	0 (0)	8	0 (0)	383	0 (0)
	IUC	0	0 (0)	0	0 (0)	0	0 (0)	3	0 (0)	3,294	0 (0)
Unfavorable G1	SUC	0	0.007 (6)	16	0.004 (2)	1,124	0 (0)	5,044	0 (0)	12,161	0 (0)
	IIUC	0	0 (0)	20	0 (0)	1,134	0 (0)	5,215	0 (0)	12,736	0 (0)
	RUC*	0	0 (0)	98	0 (0)	1,717	0 (0)	6,845	0 (0)	14,427	0 (0)
	IUC	0	0 (0)	16	0 (0)	2,457	0 (0)	10,166	0 (0)	19,735	0 (0)
Favorable G2	SUC	0	0.045 (22)	0	0.038 (21)	0	0.012 (9)	9	0.009 (8)	211	0.008 (6)
	IIUC	0	0.043 (17)	0	0.034 (14)	0	0.011 (8)	1	0.007 (6)	151	0 (0)
	RUC*	0	0 (0)	0	0 (0)	0	0 (0)	2	0 (0)	271	0 (0)
	IUC	0	0 (0)	0	0 (0)	0	0 (0)	3	0 (0)	444	0 (0)
Unfavorable G2	SUC	0	0.035 (17)	31	0.033 (20)	1,965	0.021 (10)	6,432	0.021 (18)	13,462	0.010 (10)
	IIUC	0	0 (0)	40	0 (0)	1,973	0 (0)	6,527	0 (0)	13,846	0 (0)
	RUC*	0	0 (0)	118	0 (0)	2,366	0 (0)	7,396	0 (0)	15,080	0 (0)
	IUC	0	0 (0)	67	0 (0)	2,883	0 (0)	9,650	0 (0)	18,099	0 (0)

* - RUC is solved with $\Gamma = \text{card}(\Omega^w)$

Table 3.2 shows the Expected Wind Spillage (EWS) and Expected Energy Not Served (EENS) observed at each simulation. These outcomes are also quantified by the frequency of their occurrence. This frequency (denoted as freq. in Table 3.2) is defined as the number of samples in MC simulations where the load is shed during at least one operating hour.

EWS is much lower for favorable wind scenarios than unfavorable wind scenarios. For the favorable wind profile, no wind spillage is observed for all UC techniques for up to 30% wind energy penetration. However, starting at 40% wind energy penetration, some wind energy is spilled with almost all techniques. The proposed IIUC model results in the least EWS among all UC models for the favorable wind profile under 40% and 50% wind penetration levels. This outcome indicates that the proposed IIUC model outperforms other UC models in terms of the total usage of available wind generation and, thus, facilitates cost-effective scheduling and dispatch under high wind penetration levels. On the other hand, the day-ahead schedule obtained using the IUC model leads to an unnecessarily high EWS of 3,294 MWh for the G1 generator dataset at 50% wind penetration and for the favorable wind profile. This excessive wind spillage is mainly caused by the day-ahead IUC schedule being very protected against load shedding. In this case, the IUC model commits a large number of generators to be able to serve all loads under a low production of wind farms so that wind spillage is necessary to meet their minimum output constraints enforced by equation (3.11). When comparing the wind spillage that occurred under the day-ahead IUC and IIUC models, it can be seen that the approach to model ramping scenarios (as proposed in the IIUC model) is more realistic than the overly conservative ramp requirements in the IUC model. For the unfavorable wind profile, the SUC model consistently results in the lowest EWS observed, while wind spillage under the day-ahead IIUC schedule almost always results in the second least wind spillage, especially for higher wind penetrations. The RUC and IUC models result in a substantially larger wind spillage when compared to the SUC and IIUC models. This observation illustrates the claim that the conservatism of the UC approaches that model the range of uncertainty must be controlled by modeling realistic

ramp requirements.

Since the IUC and RUC with $\Gamma = \text{card}(\Omega^W)$ models are conservative, they result in no load shedding (EENS=0 MWh) regardless of the chosen test case parameters, wind penetration, and wind profile (Table 3.2). On the other hand, the SUC solution is drawn from a set of 10 scenarios, which may not protect it against some extreme outcomes and, thus, may lead to some load shedding under almost all wind penetration levels. As can be observed in Table 3.2, the EENS of the SUC model decreases as the wind penetration increases. For higher wind penetrations, more fast-starting generators remain uncommitted on the day ahead and can, thus, be synchronized in real time to avoid shedding load. Furthermore, load shedding under the SUC solution for the favorable wind profile and wind penetration of up to 20% case tends to be larger than that of the unfavorable wind profile. We also observe that there is no systematic relation between the magnitude of the EENS and the frequency of load shedding (i.e., EENS can be higher for a lower frequency and vice-versa). Additionally, the SUC solution avoids load shedding for high wind penetrations and the favorable wind profile. However, in these cases, load shedding is also dependent on the flexibility of the generation mix. Test system G1 incurs less load shedding than test system G2. Although in some simulations the IIUC model results in load shedding, the EENS in these cases is lower than that of the SUC schedule. The load shedding statistics for the IIUC and SUC shows that the modeling of ramping scenarios in the IIUC model tends to reduce the EENS and its frequency when compared to SUC. When comparing the results of Tables 3.1 and 3.2, it can be seen that the UC models with higher EC and lower SD tend to result in lower EENS. This observation is consistent with [81], which explains the sensitivity of the UC models to the load shedding penalty.

3.4.4 Comparison of the IIUC model and the RUC model with different budgets of uncertainty

While the budget of uncertainty, Γ , can be used to regulate the conservatism of the RUC model, there is no systematic approach for choosing the most cost-effective Γ before solving the optimization

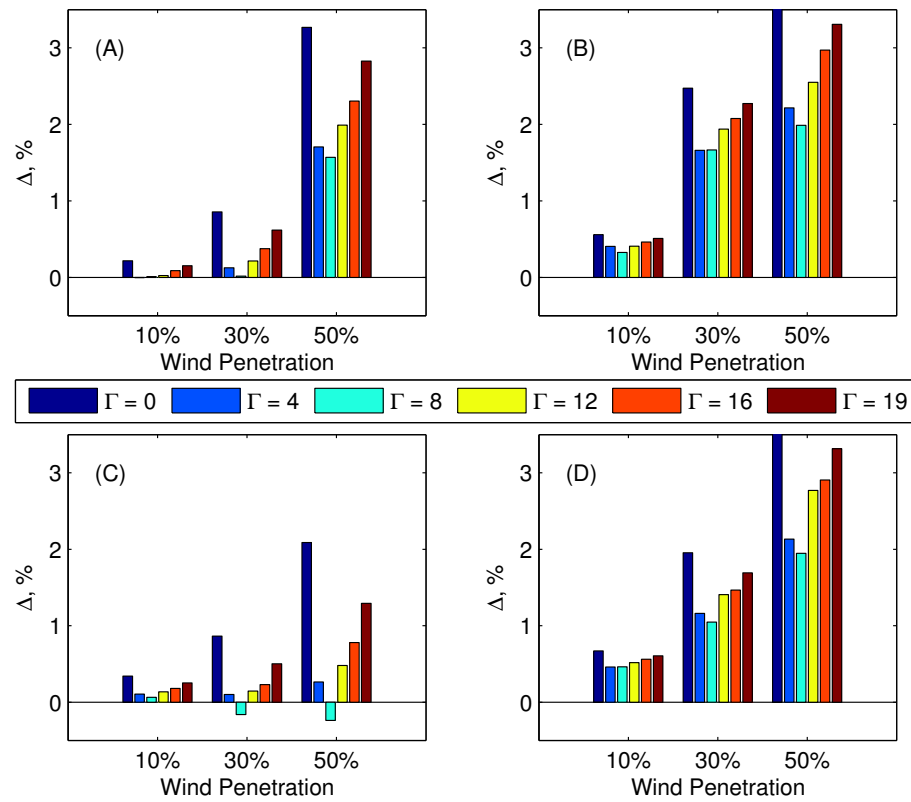


Figure 3.5: Difference in the expected costs of the schedules produced by the IIUC and RUC with different budgets of uncertainty Γ - (A) generator dataset G1, favorable wind profile; (B) generator dataset G1, unfavorable wind profile; (C) generator dataset G2, favorable wind profile; and (D) generator dataset G2, unfavorable wind profile.

problem. Figure 3.5 compares the differences between the expected cost of the IIUC and RUC with different values of Γ . This difference is calculated as $\Delta = (EC_{\Gamma}^{\text{RUC}} - EC^{\text{IIUC}})/EC^{\text{IIUC}} \cdot 100\%$, where EC_{Γ}^{RUC} is the expected cost of the RUC model for a given budget of uncertainty, Γ , and EC^{IIUC} is the expected cost of the IIUC model. EC_{Γ}^{RUC} decreases as Γ increases and reaches its minimum for $\Gamma = 8$. Increasing Γ beyond 8 results in more conservative schedules, and EC_{Γ}^{RUC} increases. When compared to the IIUC model, the RUC model consistently results in a more expensive solution, except for cases with 30% and 50% wind penetration in test system G2 with a favorable wind profile. It can also be seen in Figure 3.5 that Δ (i.e., the cost savings achieved with the proposed IIUC model) increases with wind penetration for each case considered.

Table 3.3 summarizes the cost and reliability performance of the least-cost RUC schedule, ($\Gamma = 8$). The least-cost RUC model tends to trade-off the EC, SD, EWS, and EENS performance of the IIUC model and the RUC model with $\Gamma = 19$. In most of the cases, the least-cost RUC model remains more expensive and conservative than the IIUC model. On the other hand, there are two cases (also shown in Figure 3.2) where the least-cost RUC model outperforms the IIUC model in terms of the EC (these cases are shown in bold in Table 3.3). However, a lower EC (when compared to IIUC) also leads to a larger SD, which indicates that reducing the value of the budget of uncertainty also decreases the ability of the RUC model to deal with uncertainty. Furthermore, in the case of the generator dataset G2, favorable wind profile, and 30% wind penetration, the least-cost RUC solution results in larger and more frequent load shedding than the IIUC model. These observations suggest that the value of the budget of uncertainty should be carefully tuned to ensure that a potential reduction in the EC does not worsen the reliability performance of the RUC model.

3.4.5 Computation Efficiency

All of the simulations were carried out using CPLEX 12.1, run under the GAMS 23.7 environment, on an Intel i7 1.8 GHz processor with 4 GB of memory. To improve numerical stability and avoid

convergence issues [203, 202, 201, 200, 199], as well as the effects of these issues on the cost performance of different UC formulations, this dissertation does not implement advanced solution techniques like those discussed in [199]. Therefore, the results of this case study should be inter-

Table 3.3.
COST AND RELIABILITY PERFORMANCE OF THE RUC MODEL FOR $\Gamma = 8$. (EC - EXPECTED COST; SD - STANDARD DEVIATION OF THE COST; EWS - EXPECTED WIND SPILLAGE; EENS - EXPECTED ENERGY NOT SERVED)

		10%	30%	50%	
G1	Favorable	EC, $\cdot 10^6\$$	2.530	1.805	1.226
		SD, $\cdot 10^3\$$ (%)	1.851 (0.07%)	4.706 (0.26%)	6.097 (0.49%)
		EWS, MWh	0	0	2,114
		EENS, MWh (freq.)	0.001 (2)	0 (0)	0 (0)
	Unfavorable	EC, $\cdot 10^6\$$	2.574	2.025	1.694
		SD, $\cdot 10^3\$$ (%)	5.201 (0.20%)	11.803 (0.58%)	15.612 (0.92%)
		EWS, MWh	0	1,810	16,107
		EENS, MWh (freq.)	0 (0)	0 (0)	0 (0)
G2	Favorable	EC, $\cdot 10^6\$$	2.307	1.616	1.060
		SD, $\cdot 10^3\$$ (%)	5.340 (0.23%)	11.710 (0.72%)	15.618 (1.47%)
		EWS, MWh	0	0	191
		EENS, MWh (freq.)	0.040 (14)	0.013 (9)	0 (0)
	Unfavorable	EC, $\cdot 10^6\$$	2.353	1.824	1.525
		SD, $\cdot 10^3\$$ (%)	1.911 (0.08%)	4.403 (0.24%)	6.300 (0.41%)
		SD, $\cdot 10^3\$$ (%)	1.911	4.403	6.300
		EWS, MWh	0	2,104	14,882
EENS, MWh (freq.)	0 (0)	0 (0)	0 (0)		

Bold denotes the cases where the RUC model is with $\Gamma = 8$ outperforms the IIUC model in terms of the expected cost.

preted as providing an upper bound on computing performance. Figure 3.6 shows the wall-clock times (in seconds) required to reach a 1% optimality gap. Overall, RUC is by far the most efficient method. For the G1 generator dataset, IIUC and IUC perform similarly, while for the G2 dataset, IIUC outperforms IUC in 80% of the cases. SUC is the most computationally demanding method, except for the 30-50% wind penetration levels applied to the G1 dataset and favorable wind.

3.5 Conclusions

The numerical results presented in this chapter show that SUC is still the most cost-effective way of dealing with wind uncertainty. However, despite the small number of scenarios (10) considered, its computational burden is generally very high. The proposed IIUC is the second best option in terms of cost-effectiveness (the average operating cost is increased by 2.0%), but a much better option in terms of computing time (the average computing time is reduced by 53%). The operating cost of the RUC schedules is, on average, 3.5% higher than that of the SUC schedules, but the computing times are reduced by 93%, on average. The IUC is the least attractive method, because the average

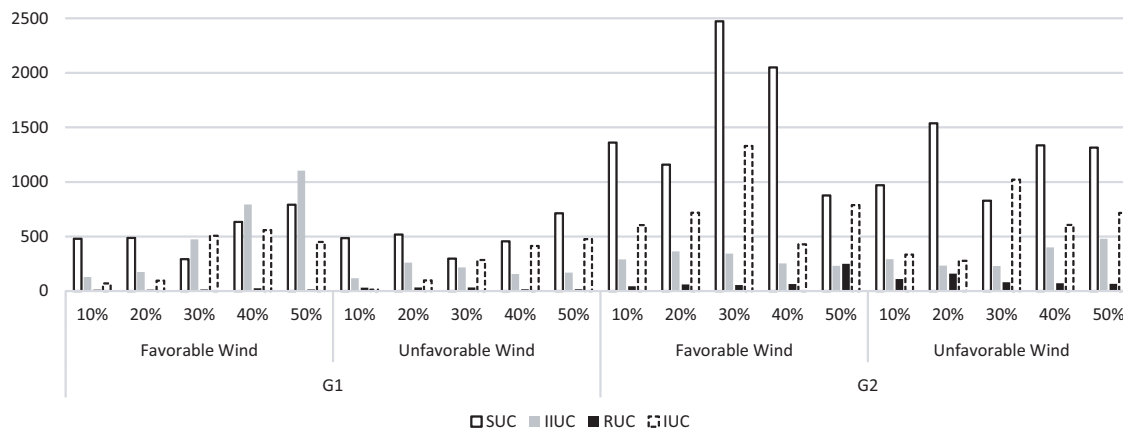


Figure 3.6: Wall-clock times (in seconds) required to reach a 1% optimality gap for different wind penetration levels.

expected operating cost is 11.8% higher than that of the SUC model, and the computing time is reduced by only 41% when compared to the SUC model.

Chapter 4

HYBRID STOCHASTIC/INTERVAL UNIT COMMITMENT**4.1 Motivation**

Since the scenarios used in SUC are, by their nature, uncertain, the SO must assume that the actual values will deviate from the anticipated values. These deviations start at the first operating hour of the following day, and their expected magnitude increases during the course of the day (as is schematically shown in Figure 4.1). In the process of minimizing expected day-ahead operating costs over a set of scenarios, SUC might decide that shedding some load or spilling some energy from renewable sources for some of the most extreme scenarios is cheaper than modifying the schedule in such a way that it can serve net load in all scenarios. In other words (and as illustrated in Figure 4.1), the SUC solution carries a certain amount of unhedged uncertainty. Typically, this unhedged uncertainty increases over time. It can be quantified in terms of Expected Energy Not Served (*EENS*, sometimes referred to as load curtailment) and expected renewable energy spilled

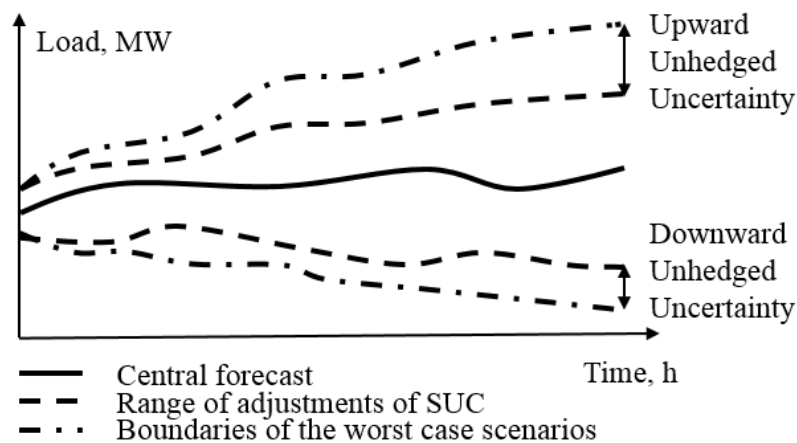


Figure 4.1: Schematic representation of the unhedged uncertainty associated with the SUC solution.

(also referred to as renewable curtailment). In turn, these quantities can be translated into a cost using the Value of Lost Load ($VoLL$, also known as the cost of load curtailment), which represents the value that an SO puts on 1 MWh of energy not served and the Value of Wind Spillage ($VoWS$, also known as the cost of wind curtailment), which represents the marginal value of 1 MWh of wind spilled. The $VoLL$ mainly depends on the type of curtailed load, but can typically be determined based on customer surveys in a particular power system [204]. The $VoWS$ is subject to jurisdictional variations and generally depends on tax credits and monetary incentives [45] or the loss of the opportunity cost [205] of wind producers. Although the $VoWS$ is currently used in many power systems [206], its high value may result in an inefficient dispatch of conventional generators because it could lead to unnecessary cycling [45, 207].

On the other hand, the IUC formulation ensures that any scenario within a predefined range of uncertainty can be handled without having to resort to load shedding, regardless of the low probability associated with these scenarios. Therefore, the solution produced by the IUC has zero unhedged uncertainty. However, improved operational reliability requires more committed capacity, resulting in higher day-ahead costs than SUC. The Hybrid Unit Commitment (HUC) strives to minimize day-ahead costs by optimally balancing the security cost of IUC against the cost of the unhedged uncertainty of SUC. It achieves this by taking advantage of the lower day-ahead cost of the SUC solution during the early hours of the optimization horizon (i.e., when the cost of the unhedged uncertainty is low), and then switching to an IUC solution (i.e., when this cost rises). As shown

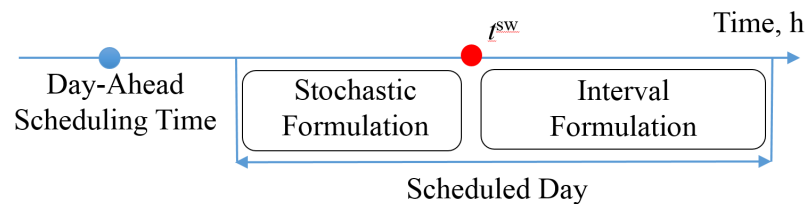


Figure 4.2: Schematic representation of the Hybrid Unit Commitment (HUC).

in Figure 4.2, the SUC formulation is applied to the first $(t^{\text{sw}} - 1)$ hours of the optimization horizon. During these operating hours, the HUC formulation uses the same objective function, input scenarios, and constraints as SUC. In this case, the HUC schedule obtained for hour $t \in [1, t^{\text{sw}} - 1]$ ought to acquire some of the features of the SUC model, such as its relatively low expected cost and its real-time performance against actual realizations of uncertainty. The remaining operating hours, $t \in [t^{\text{sw}}, \text{card}(\Omega^T)]$, are solved using the IUC formulation (i.e., during those hours that HUC mirrors the objective function), the uncertainty model, and the constraints of the IUC formulation. Consequently, this part of the HUC schedule aims to inherit the conservatism of the IUC model to be protected against the relatively large uncertainty levels at the end of the optimization horizon. Thus, the switching time t^{sw} should be chosen in such a way that the resulting HUC schedule combines the benefits of both the SUC and IUC models.

To ensure consistency between the SUC and IUC decisions, coupling constraints are enforced. These constraints account for intertemporal limits on controllable generation, such as ramping limits and minimum up- and down-times. Switching to IUC from SUC at the end of the optimization horizon is also justified by a reduction in the forecast accuracy for individual scenarios when compared to the range of uncertainty. As reported in [208] and [209], the mean and standard deviation of the wind forecasting error for an individual scenario increases significantly for a prediction horizon of 6 hours or more. The range of uncertainty in the IUC formulation can be adjusted in such a way that its bounds cover individual scenarios with a given level of confidence. When compared to SUC, a larger range between bounds in IUC does not require a larger number of scenarios and, therefore, does not increase the size of the optimization problem to be solved.

4.2 Formulation of the HUC

This Chapter operates with all of the notation used in Chapter 3 and defines several new terms as described in Appendix A.

The objective function of the HUC is given as follows:

$$\begin{aligned}
& \min_{\substack{q_{t,i,j}, x_{t,i}, y_{t,i}, z_{t,i}, \\ c_{t,w,u}, g_{t,i,u}, g_{t,i,b,u}^{\text{seg}}, su_{t,i}, \\ \theta_{t,s,u} ENS_{t,s,u}}} \sum_{t \in \Omega^T} \sum_{i \in \Omega^I} (su_{t,i} + A_{t,i} \cdot x_{t,i}) + \\
& \sum_{i \in \Omega^I} \sum_{b \in \Omega^B} \left(\sum_{t \in T^{\text{SUC}}} \sum_{u \in \Omega^U} \pi_u \cdot K_{i,b} \cdot g_{t,i,b,u} + \sum_{t \in \Omega^T} K_{i,b} \cdot g_{t,i,b,u_1} \right) + \\
& \sum_{t \in \Omega^T} \sum_{s \in \Omega^S} \sum_{u \in \Omega^U} (\pi_u \cdot ENS_{t,s,u} \cdot VoLL + \pi_u \cdot c_{t,s,u} \cdot VoWS_{t,s}) + \\
& \sum_{t \in \Omega^T} \sum_{s \in \Omega^S} (c_{t,s,u_1} \cdot VoWS_{t,s}) \tag{4.1}
\end{aligned}$$

The first term of this objective function accounts for the start-up costs of the generator, i , at hour, t , as calculated in constraint, (3.9). The second term represents the expected dispatch cost and consists of two parts: the SUC day-ahead cost for the first card ($\Omega^{T^{\text{SUC}}}$) hours and the IUC day-ahead cost for the remaining card ($\Omega^{T^{\text{IUC}}}$) hours. The SUC cost calculates the sum of the dispatch cost for each scenario weighed by the probability of this scenario. The IUC cost involves only the cost of the dispatch for the central forecast (u_1). The third term in (4.1) represents the cost of the energy not served ($ENS_{t,s,u}$) and wind spilled ($c_{t,s,u}$) for each scenario over the period of time covered by the SUC formulation. These quantities are weighed by the probability of each scenario, π_u . Energy not served is monetized using the value of loss load, $VoLL$, while involuntary wind spillage is penalized at the value of wind spillage, $VoWS_{t,s}$. The value of $VoLL$ is assumed to be uniform for each bus and operating hour, while the value of $VoWS_{t,s}$ varies for different locations and times. The fourth term represents the cost of wind spilled over the period of time covered by the IUC formulation. Note that the IUC solution does not permit any load shedding, since this approach does not account for the likelihood of an individual scenario.

4.2.0.1 Constraints on Binary Decision Variables

Both the SUC and IUC parts of the HUC formulation are subject to the constraints on the binary variables logic, minimum up and down times, and stepwise generator start-up costs, which are modeled as:

$$\text{Equation (3.2) – (3.9), } \forall t \in \Omega^T \quad (4.2)$$

4.2.0.2 Constraints on the SUC part

$$\sum_{i \in \Omega^{SI}} g_{t,i,u} + \sum_{w \in \Omega^{SW}} (W_{t,w,u} - c_{t,w,u}) - \sum_{\{s,m\} \in \Omega^L} B_{sm} (\theta_{t,s,u} - \theta_{t,m,u}) = D_{t,s} - ENS_{t,s,u},$$

$$\forall t \in \Omega^{T^{SUC}}, s \in \Omega^S, u \in \Omega^U \quad (4.3)$$

$$\text{Equation (3.10) – (3.11), (3.18) – (3.21), (3.28), } \forall t \in \Omega^{T^{SUC}} \quad (4.4)$$

Constraint (4.3) differs from constraint (3.17) in its right-hand side. Note that it includes the term for modeling load curtailment, $ENS_{t,s,u}$. This term relaxes constraint (4.3) when the cost of providing security outweighs the benefits of avoiding load curtailment. This relaxation is sensitive to the value of $VoLL$. The constraints in (4.4) are identical to the SUC formulation in Section (3.3.2).

4.2.0.3 Constraints on the IUC part

$$\text{Equation (3.10) – (3.11), (3.17) – (3.26), } \forall t \in \Omega^{T^{IUC}} \quad (4.5)$$

Constraints in (4.5) are modeled exactly as in Section (3.3.3). As compared to constraint (4.3),

the power balance is not relaxed in the IUC formulation. Therefore, its central forecast and bounds must be served at any cost, which may result in mathematical infeasibilities. To avoid this problem, slack variables can be introduced in the power balance and power flow constraints. These slack variables must be penalized in the objective function by a sufficiently large price. Each non-zero slack variable must then be carefully examined when the optimal schedule is obtained.

4.2.0.4 Coupling Constraints between SUC and IUC

$$g_{t^{\text{sw}},i,u_1} - g_{t^{\text{sw}}-1,i,u} \leq RU_i, \quad \forall i \in \Omega^I, u \in \Omega^U \quad (4.6)$$

$$g_{t^{\text{sw}}-1,i,u} - g_{t^{\text{sw}},i,u_1} \leq RD_i, \quad \forall i \in \Omega^I, u \in \Omega^U \quad (4.7)$$

Constraints (4.6) and (4.7) model the transition from the SUC part to the IUC part. These constraints ensure that the difference between the dispatch decisions made at hour $(t^{\text{sw}} - 1)$ by SUC and at hour t^{sw} by IUC meet the limitations on the ramp rates of the committed generators.

The operating cost of HUC (C^{HUC}) is a function of the switching time, t^{sw} . If the switching time is zero, HUC is equivalent to IUC, and $C^{\text{HUC}} = C^{\text{IUC}}$. If the switching takes place at early periods, the cost of HUC will be close to the cost of IUC because the SUC formulation will be applied only for a few periods and the resulting schedule will be obtained based mostly on IUC. As the switching time increases, C^{HUC} decreases at the expense of exposing the system to low probability events. If switching occurs later, the ramping and intertemporal generator constraints of the SUC solution limit the number of generators available to improve the robustness of the schedule. Thus, IUC may not be as cost-effective as it would have been if applied to the whole optimization horizon. Finally, if no switching takes place in the solution process, HUC is equivalent to SUC, and $C^{\text{HUC}} = C^{\text{SUC}}$.

Hedging the system against all possible realizations of uncertainty can be achieved with an early t^{sw} . However, this results in a high operating cost. Therefore, HUC needs to strike a balance between its running cost (RC) and the economic savings achieved by allowing some unhedged uncertainty.

The running cost accounts for the cost of commitment decisions and dispatch:

$$\begin{aligned}
RC(t^{\text{sw}}) &= \sum_{t \in \Omega^T} \sum_{i \in \Omega^I} (su_{t,i} + A_{t,i} \cdot x_{t,i}) \\
&+ \sum_{i \in \Omega^I} \sum_{b \in \Omega^B} \left(\sum_{t \in T^{\text{SUC}}} \sum_{u \in \Omega^U} \pi_u \cdot K_{i,b} \cdot g_{t,i,b,u} + \sum_{t \in \Omega^{T^{\text{TUC}}}} K_{i,b} \cdot g_{t,i,b,u_1} \right) \quad (4.8)
\end{aligned}$$

Thus, the running cost increases as the switching time decreases, since more hours are solved using the conservative IUC formulation. As the switching increases, there are more periods during which SUC dominates the solution, increasing the allowed unhedged uncertainty. The cost of unhedged uncertainty, CoU , is then given by:

$$\begin{aligned}
CoU(t^{\text{sw}}) &= \sum_{t \in \Omega^{T^{\text{SUC}}}} \sum_{s \in \Omega^S} \sum_{u \in \Omega^U} (\pi_u \cdot ENS_{t,s,u} \cdot VoLL + \pi_u \cdot c_{t,s,u} \cdot VoWS_{t,s}) \\
&+ \sum_{t \in \Omega^{T^{\text{IUC}}}} \sum_{s \in \Omega^S} (\cdot c_{t,s,u_1} \cdot VoWS_{t,s}) \quad (4.9)
\end{aligned}$$

where $ENS_{t,s,u}$ and $c_{t,s}$ are the energy not served and the wind spilled at time, t , for scenario, u . The cost in Equation (4.9) accounts for the unhedged uncertainty predicted on the day ahead. Although an actual realization may exceed the most extreme scenario considered in day-ahead planning, such an event cannot be anticipated in the day ahead and cannot, therefore, be considered in the decision-making process. On the other hand, this realization can be handled by real-time adjustments.

Since the value of the optimal switching time depends on the relative proportion between the running cost and the cost of unhedged uncertainty, it can be affected by the variations on the right-hand-side of Equations (4.8) and (4.9). For example, if the generation fleet has limited flexibility, then the transition between the proposed schedules might be impossible due to the intertemporal constraints on the generators. Also, high start-up and fuel costs can make switching prohibitively

expensive. If the range of scenarios in the SUC is relatively narrow, the unhedged uncertainty might be too insufficient to switch to a more expensive IUC solution. Similarly, if the $VoLL$ or $VoWS_{t,s}$ are relatively low, this may result in no switching, because providing the additional robustness of the IUC would not be economically justified. Therefore, by accurately estimating the $VoLL$ and $VoWS_{t,s}$, as well as improving the forecasting accuracy, an SO can change the switching time. The next subsection describes two approaches to optimizing t^{sw} .

4.2.1 Optimal Switching Time

As explained in Section (4.2), the switching time minimizes the objective function of HUC via balancing its running cost and cost of unhedged uncertainty. The operating cost of HUC, C^{HUC} , is a function of the switching time. As the switching time increases, the running cost decreases (as shown in equation (4.8)), while the cost of unhedged uncertainty increases (as shown in equation (4.9)). Therefore, the operating cost of HUC, C^{HUC} , which sums the running cost and the cost of unhedged uncertainty, is guaranteed to have a minimum. Since the commitment or de-commitment of a generator abruptly changes the value of the cost of unhedged uncertainty and the running cost, C^{HUC} can have local minimums, which makes it almost unimodal¹. Therefore, traditional derivative-based methods to calculate its minimum are not applicable due to the risk of being trapped in a local minimum. The domain of the switching time is limited to a finite number of integer solutions over the interval $[1, \text{card}(\Omega^T)]$. Therefore, the minimum of $C^{HUC}(t^{sw})$ can be obtained by solving the HUC formulation at most $\text{card}(\Omega^T)$ times. This can be done using a parallel implementation or a single processor implementation, as discussed below.

4.2.1.1 Parallel Computing Implementation

Parallel computing makes it possible to carry out multiple simulations at the same time. In this im-

¹A function, f , is almost (noisy) unimodal in $[a, b]$ if and only if, for some $x \in [a, b]$, $f' < 0$ almost everywhere on $[a, x]$ and $f' > 0$ almost everywhere on $[x, b]$ [210]. Examples of almost unimodal functions can be found in [210, 211].

plementation, each parallel simulation solves the HUC problem for a particular value of the switching time and produces its cost, $C^{\text{HUC}}(t^{\text{sw}})$. Therefore, the HUC formulation is solved $\text{card}(\Omega^T)$ times. When all parallel simulations are completed, the optimal switching time is determined as the minimum of $C^{\text{HUC}}(t^{\text{sw}})$. The computation time τ of the parallel implementation is then determined as the maximum computation time of all parallel simulations. In line with this definition, the computing time of the parallel implementation is given as $\tau = \max \left[\tau^{t^{\text{sw}}=1}, \tau^{t^{\text{sw}}=2}, \dots, \tau^{t^{\text{sw}}=\text{card}(\Omega^T)} \right]$.

4.2.1.2 Single Processor Implementation

Since a single processor cannot carry out multiple simulations at the same time, the single processor implementation solves HUC problems in series (i.e., this implementation requires solving the HUC formulation $\text{card}(\Omega^T)$ times, consecutively). To reduce the required number of iterations, a search method can be used. A three-point grid search algorithm (a derivative-free search method) has been shown to converge and estimate the optimum of the almost unimodal functions precisely [211]. As proven in [211], this method has linear convergence and has already been applied in power system applications dealing with uncertainty [212]. This algorithm operates as follows. First, an interval $[T^{\text{LB}}, T^{\text{UB}}]$ containing t^{sw} is chosen. Second, three equally spaced points within the search intervals, $[t^{\text{sw}1}, t^{\text{sw}2}, t^{\text{sw}3}]$, are chosen, and HUC (as formulated in (4.1)-(4.7)) is solved for each of them. Third, the two neighbors (possibly including one of the bounds of the interval) of the points among these three that would give the lowest values of C^{HUC} are chosen as the bounds of the next search interval. This procedure is repeated, until the optimal t^{sw} is found with enough accuracy. Since the domain of the switching time is finite, the optimal switching time can be found in a finite number of iterations. The search range of the switching time reduces by $(1/4)^n$ after n iterations [211]. Although the three-point grid search algorithm reduces the number of solution candidates, its computation time consists of the sum of the computation times of all iterations. Therefore, the computation time of the single processor implementation would be larger than the computation time

of the parallel computer implementation.

4.3 Case Study

4.3.1 Description of the Test Cases and Data

The proposed HUC, as well as the DUC, SUC, and IUC formulations, have been tested on a modified version of the 24-bus IEEE RTS. Details of this system can be found in [185]. The cost curves of the generating units in this system are approximated by three-segment piece-wise linear functions with equally spaced elbow points. Generators U12 and U20 can be synchronized or shutdown within a single operating hour. The wind and load data are based on ERCOT data [213]. Wind penetration is assumed to provide 10% of the electricity consumed daily system-wide. A set of 1000 wind scenarios are generated, as described in [122]. A forward selection scenario reduction technique reduces this set to 10 scenarios used by SUC. The 5- and 95- percentiles of the original set are used to define the lower and upper bounds for IUC. These bounds envelope all of the scenarios in SUC. In the reference case $VoLL = \$5/\text{kWh}$ for all operating hours, the $VoWS$ is calculated based on the lost opportunity of wind producers for each operating hour. This lost opportunity cost of wind producers is calculated as the difference between two cases: when wind curtailment is not enforced and when wind curtailment is enforced (as explained in [205]).

The HUC formulation is described in (4.1)–(4.7), and the switching time is optimized as described in Section 4.2.1. The SUC formulation includes constraints (4.3)–(4.4), and the IUC formulation includes constraints in (4.5). The DUC formulation is identical to IUC, but without bounds and without the constraints (3.23)–(3.26). Table 4.3.1 compares the DUC, SUC, IUC, and HUC formulations in terms of the number of variables and constraints. All formulations have the same number of binary variables: $x_{t,i}$, $y_{t,i}$, $z_{t,i} - 768$ each, $q_{t,i,j} - 6,144$. The number of continuous variables and constraints differ for each formulation: DUC and SUC have, respectively, the smallest and the largest number of continuous variables and constraints. Since the optimal switching hour

is unknown until HUC is solved, the number of continuous variables is characterized by a range of SUC and IUC formulations, as is shown in Table 4.3.1. The number of constraints in HUC is also characterized by this range plus the number of coupling constraints, (4.6) and (4.7).

Table 4.1: Summary of Different UC formulations

Number of	DUC	SUC	IUC	HUC
binary variables	8,448	8,448	8,448	8,448
continuous variables	15,148	73,900	35,308	35,308–73,900
constraints	22,019	128,291	63,299	63,939–128,931

Simulations for this case study have been performed on an Intel[®] Core i7 2.80 GHz processor, with 4 GB of RAM, under the 64-bit Windows[®] 7 operating system. The CPLEX 12.1 optimization engine and GAMS 24.0.2 environment have been used to implement all UC formulations. The minimum relative MIP gap has been set to 10^{-3} .

4.3.2 Day-Ahead Cost of the DUC, SUC, and IUC

Table 4.2 shows the day-ahead cost (*DAC*), the security cost (*SC*), and the cost of unhedged uncertainty (*CoU*) for the DUC, SUC, and IUC formulations for different *VoLLs*. The day-ahead cost is defined as the value of the objective function for a particular UC approach. The security cost is calculated as the difference between the day-ahead cost of a particular UC approach and the the day-ahead cost of the DUC formulation without reserve requirements. Since DUC accounts for a single central forecast scenario, this formulation results in the least expensive day-ahead and security costs for any *VoLL*. The SUC formulation models uncertainty via a set of scenarios, and it, therefore, results in larger day-ahead and security costs. Since DUC does not tolerate any load shedding, its cost of unhedged uncertainty is incurred by the cost of wind spillage. The IUC results in the most conservative day-ahead schedule, which results in the largest day-ahead and security costs among

all UC formulations. Since IUC does not enable load shedding, its cost of unhedged uncertainty only includes the cost of wind spillage, and it is, thus, less than that of the SUC.

Table 4.2: Day-ahead Costs for Different UC Approaches (in 10^3 , \$)

	VoLL=\$1/kWh			VoLL=\$5/kWh			VoLL=\$10/kWh		
	DAC	SC	CoU	DAC	SC	CoU	DAC	SC	CoU
DUC	897	29	2	897	29	2	897	29	2
SUC	899	31	13	908	40	9	912	44	7
IUC	1022	154	4	1022	154	4	1022	154	4
HUC	908	41	8.3	958	99	34	973	105	67

4.3.3 Day-Ahead Cost of the HUC

Table 4.2 presents the day-ahead results of HUC for different $VoLLs$. Figure 4.3 shows how the day-ahead cost (DAC), the running cost (RC), and the cost of the unhedged uncertainty (CoU) of HUC vary as a function of t^{sw} and compares it to the day-ahead cost of SUC and IUC for $VoLL = \$5/kWh$. The cost of unhedged uncertainty of HUC increases as the switching time increases because more operating hours are solved using the SUC formulation; thus, more unhedged uncertainty is allowed in the resulting schedule. The running cost is also a function of the switching time, but it is not monotonic in [1, 24] as the cost of the unhedged uncertainty. As illustrated in Figure 4.3, the day-ahead cost decreases almost everywhere over the interval [1, 16] and increases over the interval [16, 24]. Note that this function increases from hour 6 to hour 7, which makes it almost unimodal in [1, 24].

If switching occurs early in the optimization horizon, the solution would be conservative, so an increment in the switching time causes a reduction in the objective function. However, switching later requires the enforcement of the IUC boundaries that are subject to the commitment decisions made previously on the day. This constrains the cycling of the base load generators and requires

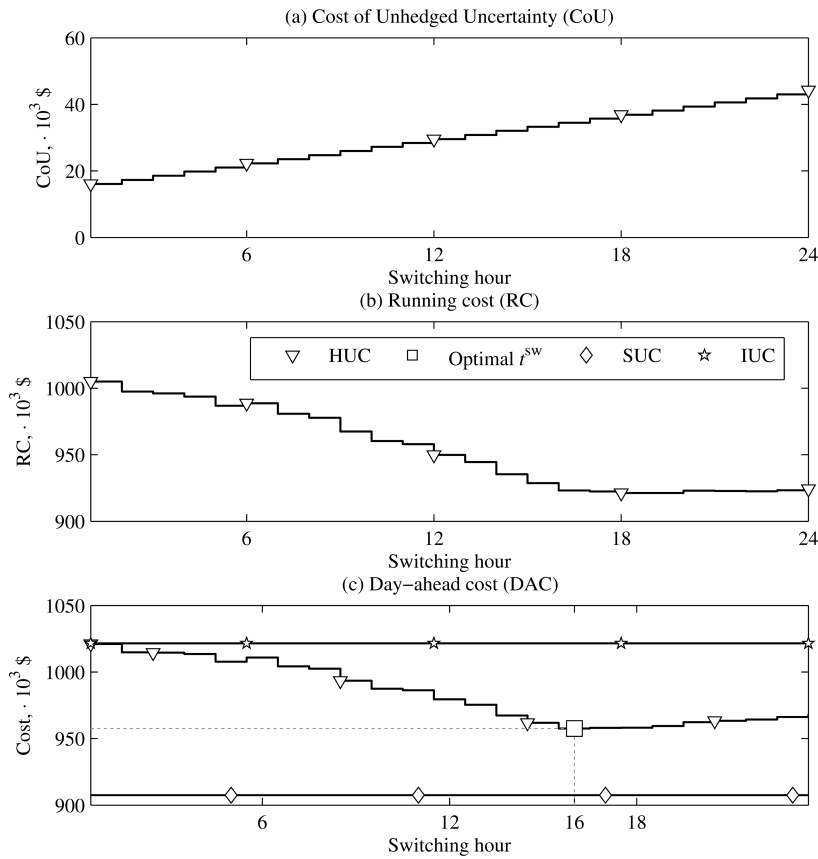


Figure 4.3: (a) Cost of unhedged uncertainty; (b) running cost of the HUC formulation; and (c) comparison of the total day-ahead costs of the IUC, SUC, and HUC formulations. The optimal switching time is highlighted with a square.

committing expensive flexible generation, which causes a slight increase in running costs at the end of the optimization horizon. Therefore, both the cost of unhedged uncertainty and running costs (and thus, the day-ahead cost of the HUC) increase at the end of the optimization horizon, which makes late switching less cost-efficient. Figure 4.4 illustrates the difference for the optimal generation pool committed by the HUC formulation with different *VoLLs*. As the *VoLL* increases, the HUC formulation tends to commit more generators of the types U20, U50, and U76, while the number of commitment of other generators (which are less flexible) remains unchanged.

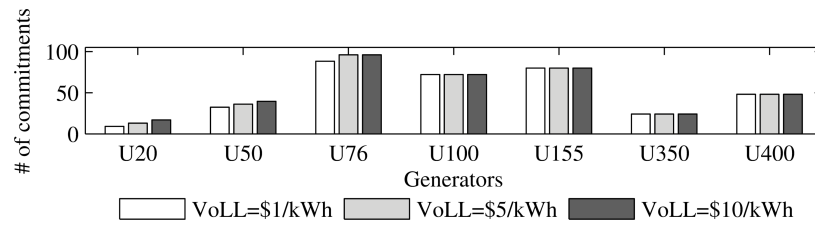


Figure 4.4: Comparison of the cumulative number of commitments by the HUC throughout the optimization horizon for different VoLLs.

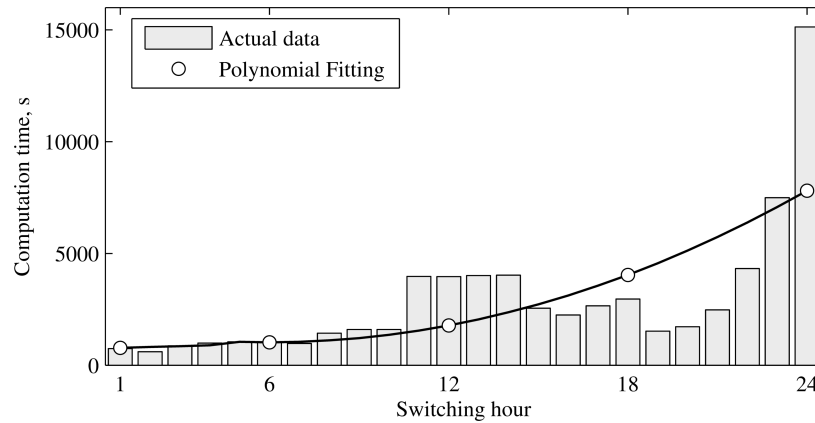


Figure 4.5: Computation time of the HUC formulation with different switching times.

4.3.4 Optimizing the Switching Time

The switching time optimization has been performed as described in Section 4.3.3 for the the parallel computing implementation and the single processor implementation. The domain of the switching time in the reference case is the integer numbers in $[1, 24]$, $VoLL = \$5/kWh$, and the optimal switching hour is 16. Figure 4.5 shows the computation time of the HUC formulation for different switching times and its trend, approximated with a polynomial function. As the switching time increases, the computation time increases as well, due to an increased number of constraints and continuous variables, as is shown in Table 4.3.1.

4.3.4.1 *Parallel computing implementation*

In the parallel implementation, the HUC formulation is solved for all 24 values of the switching time simultaneously. The overall time of the parallel implementation is equal to the longest computation time of all parallel simulations (as is explained in Section 4.2.1). In the reference case $\tau = 15,135$ s (4h:12m:15s), which is also equal to the computation time of the SUC formulation. The computation time of the HUC formulation is longer than the computation time of the IUC formulation - 332 s (6m:32s).

4.3.4.2 *Single processor implementation*

In the single processor implementation case, four iterations of the three-point grid search method are required to obtain the optimal switching time. The range between the upper and lower bounds of the day-ahead cost decreases at each iteration (Figure 4.6a) and so does the range between the upper and lower bounds of the switching time (Figure 4.6b). Figure 4.6c shows the computation time for each iteration, which are added together in Figure 4.6d. The first iteration is the longest because it involves solving the SUC formulation for the whole optimization horizon and, thus, involves more continuous variables and constraints than any other iteration. As the number of iterations increases, the duration of each iteration decreases because the upper bound of the switching time reduces and more operating hours are solved by IUC. The overall computation time for the reference case in the single processor implementation is 32,647 s (9h:4m:7s).

4.3.4.3 *Impact of the VoLL*

Since the switching time determines a number of hours solved by SUC and IUC, it depends on the $VoLL$ chosen. Figure 4.7 shows how the switching time varies as a function of the $VoLL$. Scheduling the generating fleet with a higher $VoLL$ results in an earlier switching time; therefore, more hours are solved by IUC, which makes the schedule more robust and, thus, avoids having to

resort to load curtailment. As the V_{oLL} changes, the commitment status of the generators, the cost of uncertainty, and the security cost may change as well. These changes are discrete due to the indivisible nature of the binary commitment decisions on the generating units, as is explained in [212]. Hence, there might also be some fluctuations in the switching time for an incremental change in the V_{oLL} . The inset of Figure 4.7 shows that the switching time has a local extremum for $V_{oLL} = \$30/\text{kWh}$.

4.3.4.4 Impact of the domain of the switching time

As Figure 4.3 illustrates, if switching occurs at the end of the optimization horizon, a longer computation time is required because of the larger number of hours solved using the SUC formulation. If the initial domain of the switching time is reduced in a way that avoids these computationally intensive calculations, HUC can be solved faster. This, however, may result in a sub-optimal solu-

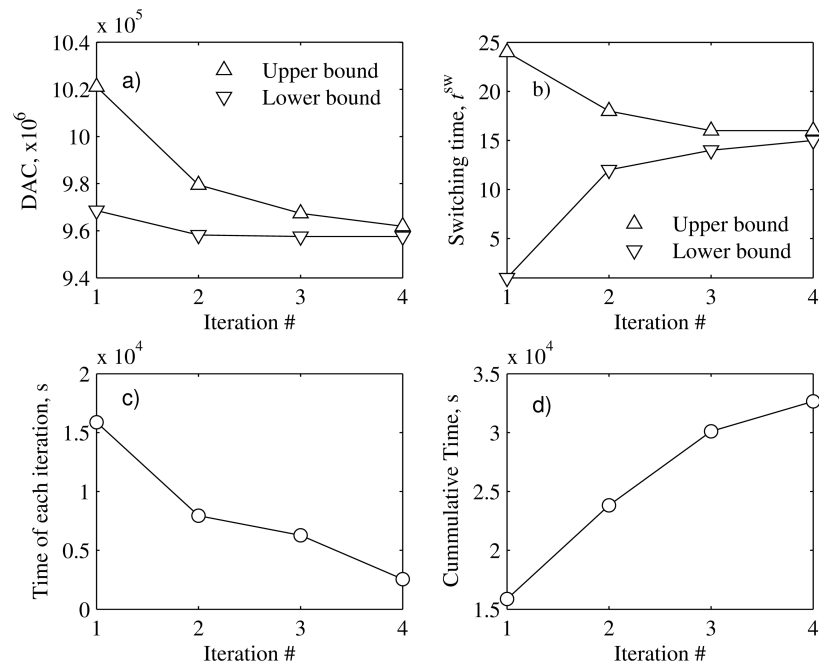


Figure 4.6: Convergence of the day-ahead cost (DAC) and the switching time of the HUC formulation in the single processor implementation

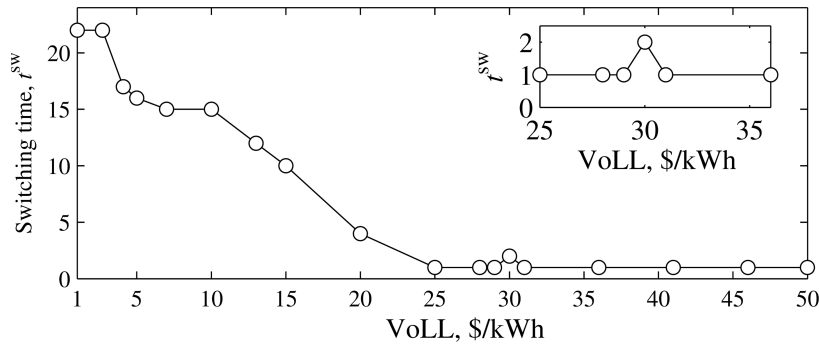


Figure 4.7: The optimal switching time as a function of the VoLL.

tion because the truncated operating hours may contain the optimal switching time, especially if the $VoLL$ is relatively high or low, as illustrated in Figure 4.7. To demonstrate the computing performance of the HUC formulation with a reduced interval of possible switching times, the interval of switching times is limited to the hours between the beginning of the morning ramp and the peak net load. This rule-of-thumb was validated on a set of representative net load profiles for six days. This set includes four representative days for each calendar season and two days with the maximum and minimum daily net load.

In this case study, reducing the switching time by one hour will eliminate 1,608 continuous variables and 2,708 constraints from the HUC formulation. If the domain of the switching time is reduced to the interval between hour 8 (beginning of the morning ramp) and hour 19 (the interval of the switching times), the parallel computing implementation is solved in 4,027 s (1h:7m:7s), and the single processor implementation is solved in three iterations, which require 13,203 s (3h:40m:3s). Therefore, both implementations are solved faster than the SUC formulation.

4.3.4.5 Impact of the switching time on committed capacity

Figure 4.8 compares the hourly committed capacity (CC) for the day-ahead schedules obtained with SUC, IUC, and HUC with an optimal switching time for $VoLL = \$5/\text{kWh}$. Until switching at hour

16, HUC has a pattern similar to the committed capacity of SUC. After the switching occurs, HUC reaches the same committed capacity as the IUC approach at hour 19. In between, HUC achieves the robustness of IUC using a smaller amount of committed capacity, but with more flexible (and therefore, more expensive) units than the IUC. During the remainder of the optimization horizon, the hourly committed capacity of the HUC schedule repeats the trend of the hourly committed capacity of the IUC schedule. Figure 4.9 shows the difference between the committed generation pool under different UC approaches. The same number of inflexible and relative cheap generators, such as U100, U350, and U400, are committed using any of the approaches. This figure also shows that HUC has the largest number of commitments of flexible generators (U20 and U50), so it can enforce its robustness after switching occurs. Since IUC needs to provide robustness during the course of the whole optimization horizon, it commits the largest number of inflexible generators, U155.

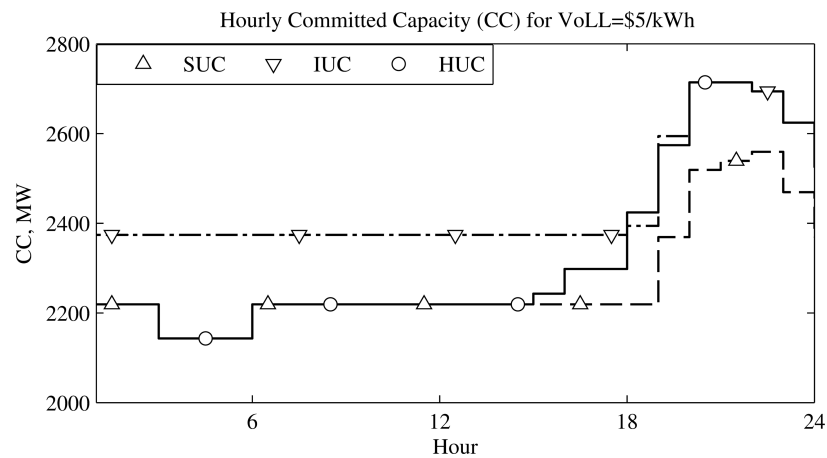


Figure 4.8: Comparison of the hourly committed capacity for the day-ahead schedules of IUC (dash-dot), SUC (dash-dash), and HUC (solid) formulations.

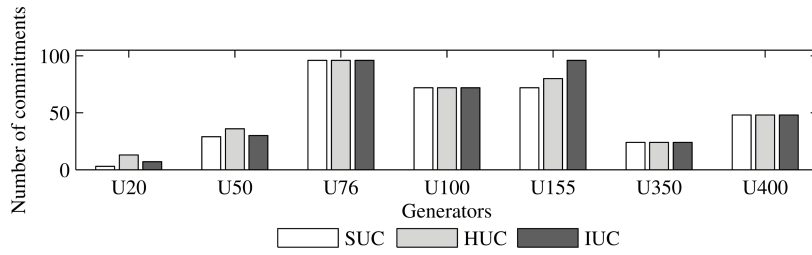


Figure 4.9: Comparison of the cumulative number of commitments by different UC approaches throughout the optimization horizon.

4.3.5 Results of Monte Carlo Simulations

The statistical behavior of the schedules obtained with each of the UC approaches was tested using MC simulations. At each trial of the MC simulation, the day-ahead schedule produced by each method is dispatched to meet the actual net load. Real-time commitments of additional generators are allowed if the day-ahead intertemporal constraints on the generators are not violated. At each MC trial, the corresponding value of the actual operating cost (AOC) is calculated. This AOC includes the generation dispatch and start-up costs based on the day-ahead schedule, as well as the cost of additional commitments required in real time and the penalties for wind spillage and load shedding. The number of MC trials required is set at $\min[1000, N_{MC}]$, where N_{MC} is the number of MC trials required to ensure (with a 95% confidence level) that the estimate of the AOC has an error of less than 1% [198]. A normal distribution and a skew-Laplace distribution are assumed for load forecast errors [33] and wind power forecast errors [197], respectively.

Figure 4.10 shows the cumulative probability distributions (CDFs) of the AOC , as calculated using MC simulations. Table 4.3 gives the expected AOC (EC), the maximum AOC (AOC^{max}), the minimum AOC (AOC^{min}), the expected cost of the corrective actions ($EC(\Delta)$), the standard deviation of the AOC distribution (SD), and the expected values of $EENS$ and EWS .

These MC simulations demonstrate that the HUC schedule results in the lowest AOC for any $VoLL$ when compared to the SUC and IUC schedules. For $VoLL = \$1/\text{kWh}$, SUC and HUC

result in a positive expected cost of corrective actions, since these schedules were not optimized to accommodate for large deviations from the forecast and underestimate the influence of uncertainty. The cost of corrective dispatch for the HUC schedule is less expensive than for the SUC schedule, which demonstrates that the HUC formulation models uncertainty more accurately than SUC. The IUC results in an unnecessarily robust schedule when compared to the HUC and SUC formulations and has a negative expected cost of corrective dispatch, which indicates that the IUC formulation is likely to overestimate uncertainty. As $VoLL$ increases, the schedules obtained with all UC formulations become more robust, and its cost of corrective dispatch decreases. If $VoLL = \$5/\text{kWh}$ or $VoLL = \$10/\text{kWh}$, the SUC does not schedule sufficient resources to meet the deviations and results in a positive expected cost of corrective actions. On the other hand, the HUC schedule for $VoLL = \$5/\text{kWh}$ and $VoLL = \$10/\text{kWh}$ results in a negative expected cost of corrective actions. Although the HUC formulation overestimates uncertainty, the absolute value of the expected cost of

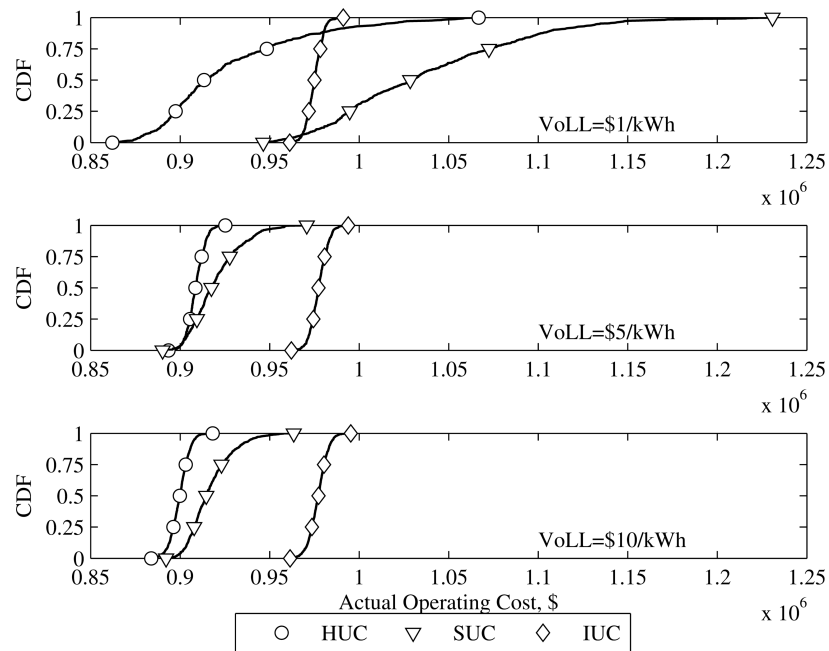


Figure 4.10: Cumulative distribution function (CDF) of the actual operating cost (AOC) obtained with MC simulations for different $VoLLs$.

Table 4.3: Statistics of MC Simulations for different $VoLL$

VoLL	Variable	HUC	SUC	IUC
\$1/kWh	$AOC^{\min}, \cdot 10^3\$$	863.1	939.4	961.2
	$EC, \cdot 10^3\$$	926.9	1037.0	975.0
	$AOC^{\max}, \cdot 10^3\$$	1079.5	1216.7	991.3
	$EC(\Delta), \cdot 10^3\$$	18.9	138	-47
	$SD, \cdot 10^3\$$	42	53	0.45
	$EENS, MWh$	36.1	62.3	0
	EWS, MWh	33.4	26.1	29.3
\$5/kWh	$AOC^{\min}, \cdot 10^3\$$	892.7	889.5	961.3
	$EC, \cdot 10^3\$$	908.7	919.6	977.4
	$AOC^{\max}, \cdot 10^3\$$	922.8	969.6	995.1
	$EC(\Delta), \cdot 10^3\$$	-49.3	11.6	-44.6
	$SD, \cdot 10^3\$$	0.47	1.4	0.46
	$EENS, MWh$	0.019	0.34	0
	EWS, MWh	21.7	18.5	24.3
\$10/kWh	AOC^{\min}	883.2	891.5	960.8
	$EC, \cdot 10^3\$$	899.7	916.7	977.1
	$AOC^{\max}, \cdot 10^3\$$	916.6	964.9	993.6
	$EC(\Delta), \cdot 10^3\$$	-73.3	2.6	-44.9
	$SD, \cdot 10^3\$$	0.50	1.2	0.47
	$EENS, MWh$	0.006	0.021	0
	EWS, MWh	22.8	14.3	24.6

corrective dispatch, in this case, is lower than for the IUC formulation. The low standard deviation of the AOC distribution, in the case of the HUC, demonstrates its adaptability to extreme cases. In particular, for $VoLL = \$5/\text{kWh}$ and $VoLL = \$10/\text{kWh}$, the upper tail of the CDF of the HUC is shorter than the tails for the IUC and SUC (lower AOC^{\max}). Large $VoLLs$ amplify this effect because they justify an increase in the robustness of the schedule to deal with extreme cases. Because the IUC schedule is insensitive to the $VoLL$, its standard deviation remains nearly constant, and it achieves the lowest $EENS$ for all cases. On the other hand, as the $VoLL$ increases, the $EENS$ of the HUC decreases because more periods are solved with the IUC constraints. While SUC is also sensitive to the $VoLL$, its schedules do not balance security costs against the $EENS$ costs as well

Table 4.4: Statistics of MC Simulations for different wind penetration

Wind Penetration	Variable	HUC	SUC	IUC
10 %	$EC, \cdot 10^3\$$	908.7	919.6	977.4
	$EENS, MWh$	0.019	0.34	0
	EWS, MWh	33.4	18.5	24.3
20 %	$EC, \cdot 10^3\$$	712.4	727.8	800.1
	$EENS, MWh$	0.023	0.59	0
	EWS, MWh	99.6	108.1	214.3
30 %	$EC, \cdot 10^3\$$	654.1	679.7	709.4
	$EENS, MWh$	0.024	0.59	<0.001
	EWS, MWh	151.4	152.0	331.2

as the HUC. Unlike load shedding, the expected wind spillage remains approximately the same for all UC formulations because the penalty for spillage is significantly smaller than $VoLL$.

Table 4.4 compares UC formulations under different wind penetration levels for $VoLL = \$5/kWh$. The HUC results in the lowest expected cost for all wind penetration levels. The HUC formulation is attractive to the SO, because it achieves savings from 1.2% to 3.9% for 10% and 30% wind penetration, respectively, when compared to SUC. Furthermore, HUC results in lower wind spillage than any other UC formulation for 20% and 30% wind penetration levels and also results in less load shedding than SUC. The IUC formulation consistently overestimates uncertainty and results in substantial wind spillage at higher levels of wind penetration, which lead to an unnecessarily expensive operating cost. However, this formulation results in no load shedding for any wind penetration level.

4.4 Conclusion

This Chapter describes a UC formulation that balances the robustness of IIUC and the low expected cost of SUC. Instead of enforcing a uniformly high level of robustness (like IUC) or tolerating a certain amount of infeasibility (like SUC), this hybrid approach optimally decides when a more

expensive schedule is justified. A detailed MC simulation demonstrates that it always achieves the lowest expected actual operating cost. The schedules produced by this hybrid formulation depend on the $VOLL$ (i.e., the value that customers attach to the short-term continuity of supply). As this value increases, the hybrid formulation schedules more resources to reduce the uncertainty that SUC leaves unhedged.

The importance of this hybrid approach to sustainable power systems is manifold:

- This approaches yield a lower operating cost than SUC, thus effectively arbitrage day-ahead uncertainty between earlier and later periods of the planning horizon.
- Furthermore, cost savings achieved under the HUC model increases with the wind penetration levels, thus underscoring the importance of this uncertainty arbitrage in such systems.
- Unlike SUC, the computational burden of HUC can be alleviated by considering reasonable domains for the switching times.

Chapter 5

WIND GENERATION AS A RESERVE PROVIDER

5.1 Motivation

As shown in Chapters 3 and 4, the accommodation of high volumes of renewable generation requires the provision of additional amounts of flexibility (i.e., spare generation capacity) from conventional generation to coping with uncertainty and the variability of renewables. However, as explained in Section 1.2.3, the integration of renewable generation replaces the conventional generators that are most feasible for providing this flexibility. Furthermore, to provide additional spare capacity, conventional generators are operated in a less than economically optimal manner [18]. As the penetration level of WG grows, so too does the uncertainty of the net load and flexibility requirements [29, 31]. The cost of operating a power system is sensitive to the amount of flexibility required [212], which is driven by the reserve policy chosen [214]. Even a marginal increment in reserve requirements may result in a sizable increase in operating costs because it may require the synchronization of additional generators, which may then force other generators to operate at less than optimal efficiency [32].

On the other hand, some renewable generation could be scheduled at a derated level to reduce the amount of associated uncertainty and the cost of additional reserve requirements [206]. The resulting headroom in renewable generation could then be used to provide an upward reserve. Existing wind turbine control systems have the technical ability to follow secondary and tertiary dispatch commands [215]. If a portion of the reserve requirements is contributed by wind generation, a lower cost of dispatch of conventional generators can be attained. On the other hand, wind generators must be compensated for the loss of opportunity that they would suffer by providing reserve rather

than energy [205]. This loss of opportunity is typically larger for wind generation than for conventional generation because the wind generation has a lower, nearly zero, operating cost. However, the authors of [206] show that the reserve provision by wind generation is justified in power systems with large wind penetration levels. As shown in [216], wind generation could increase its profit by participating in both the energy and reserve markets as opposed to trading only in the energy market.

This Chapter studies how wind generation can be operated by a controllable resource, thus simultaneously contributing to the reserve requirements and reducing the associated uncertainty.

5.2 Contributions

This Chapter uses MILP to formulate a day-ahead DUC model that minimizes operating costs by derating wind production and, consequently, reducing the reserve requirements. Note that unlike the models in Chapters 4 and 3, this model uses only one (deterministic) forecast and a probability distribution of this distribution's uncertainty. While this approach does not fit the formal definitions of the SUC, IUC, and RUC models, it accounts for the stochastic nature of wind power generation in a probabilistic fashion. The contributions of this approach are as follows:

1. It achieves a lower operating cost through the provision of reserve from wind generation and through a reduction in reserve requirements.
2. Unlike traditional DUC models with different reserve policies, this approach accounts for the non-linearity of wind power generation.
3. The case study demonstrates that the proposed approach is more cost effective under higher wind penetration levels than traditional DUC models with “ 3.5σ ”¹ and “ $(3 + 5)\%$ ”² reserve

¹The “ 3.5σ ” policy sets the hourly reserve requirement in proportion to the standard deviation of the net load forecast, “ σ ”. See reference [32] for further details.

²The “ $(3 + 5)\%$ ” sets the hourly reserve requirement to the sum of 3% of the hourly load forecast and 5% of the hourly wind forecast. When compared to the “ 3.5σ ” policy, this policy treats hourly load and wind forecasts separately. See reference [103] for further details.

policies.

5.3 Formulation

This chapter uses the same notation as Chapters (3) and (4) and as described in Appendix A. However, the additional notation that is not used in Chapters (3) and (4) are defined when they are used for the first time.

The objective function of DUC is given as follows:

$$\min_{\substack{q_{t,i,j}, x_{t,i}, y_{t,i}, z_{t,i}, c_{t,w,u_1}, \\ g_{t,i,u_1}, g_{t,i,b,u_1}^{\text{seg}}, su_{t,i}, r_{t,i,u_1}^{\text{up}}, \theta_{t,s,u_1}}} \left[\sum_{t \in \Omega^T} \sum_{i \in \Omega^I} \left(su_{t,i} + A_i \cdot x_{t,i} + \sum_{b \in \Omega^B} K_{i,b} \cdot g_{t,i,b,u_1} + C_{t,i}^{\text{LOC}} \right) + \sum_{t \in \Omega^T} \sum_{w \in \Omega^W} C_{t,w}^{\text{wind}} \right] \quad (5.1)$$

The first three terms of the objective function (5.1) represents the start-up, mo-load, and fuel costs, which are identical to the terms in (3.1). The fourth term in (5.1) represents the lost opportunity cost of the generators that is compensated if the procurement of the upward reserve results in an out-of-merit-order dispatch of the generator i :

$$C_{t,i}^{\text{LOC}} = r_{t,i,u_1}^{\text{up}} \cdot \lambda_{t,i}^{\text{LOC}}, \quad (5.2)$$

where $\lambda_{t,i}^{\text{LOC}}$ is the marginal cost of the lost opportunity calculated for each generator, i , at every operating hour, t , as explained in [205]. The fifth term of the objective function (5.1), $C_{t,s}^{\text{wind}}$, accounts for the lost opportunity cost of wind power generation due to either wind spillage or scheduled wind

deration³. Therefore, $C_{t,w}^{\text{wind}}$, can be computed as:

$$C_{t,w}^{\text{wind}} = \lambda_{t,w}^{\text{LOC}} \cdot (\alpha_{t,w}) \cdot W_{t,w,u_1}, \quad (5.3)$$

where $\lambda_{t,w}^{\text{LOC}}$ the marginal cost of the lost opportunity calculated for each generator w and $\alpha_{t,w} \in [0, 1]$ is a decision variable that determines the portion of the foretasted wind production, W_{t,w,u_1} , to derated.

5.3.0.1 Constraints on Binary Decision Variables

The binary decisions variables, $q_{t,i,j}$, $x_{t,i}$, $y_{t,i}$, and $z_{t,i}$, are constrained by the binary variables logic, the minimum up and down time limits, and the stepwise start-up cost constraints as follows:

$$\text{Equation (3.2) – (3.9), } \forall t \in \Omega^T, i \in \Omega^I, j \in \Omega^J. \quad (5.4)$$

5.3.0.2 Dispatch Constraints on Conventional Generators

The dispatch constraints on conventional generators include the minimum and maximum power output and the ramp up and down limits, which are enforced as follows:

$$\text{Equation (3.10) – (3.12), } \forall t \in \Omega^T, i \in \Omega^I, u = u_1. \quad (5.5)$$

³Note that, technically, there is a difference between the term wind deration (which refers to wind power generation that is reduced to provide reserve) and the term wind spillage (which is used for wind curtailments resulting from the enforcement of security criteria, e.g., binding transmission generation constraints.)

5.3.0.3 Transmission Constraints

Flow limits on transmission lines are modeled using a linear dc power flow as follows:

$$\text{Equation (3.18) – (3.21), } \forall t \in T, s \in S, l \in L, u = u_1 \quad (5.6)$$

$$\sum_{i \in \Omega^I} g_{t,i,u_1} + \sum_{w \in \Omega^S} (W_{t,w,u_1}^{\text{net}} - c_{t,w,u_1}) - \sum_{\{s,m\} \in \Omega^L} B_{sm} (\theta_{t,s,u_1} - \theta_{t,m,u_1}) = D_{t,s},$$

$$\forall t \in \Omega^T, s \in \Omega^S. \quad (5.7)$$

From the formulation in Section 3.3, the network constraints of the proposed DUC depart in the nodal power balance constraint, see (5.7). As compared to constraint (5.7) in Section 3.3, constraint (5.7) includes the net nodal injection of the wind power generation, W_{t,w,u_1}^{net} . This decision variable accounts for wind power deration.

5.3.0.4 Wind Power Deration Constraints

The net wind power injection at wind farm, w , W_{t,w,u_1}^{net} , is defined as:

$$W_{t,w,u_1}^{\text{net}} = (1 - \alpha_{t,w}) \cdot W_{t,w,u_1}, \quad t \in \Omega^T, w \in \Omega^W, \quad (5.8)$$

where W_{t,w,u_1} is the forecasted (available) wind production and $\alpha_{t,w}$ is the wind production deration rate. This deration rate is a decision variable in the range $[0, 1]$. If $\alpha_{t,w}$ is zero, the forecasted wind production is not derated and all of the forecasted power is scheduled as power production (i.e., $W_{t,w,u_1}^{\text{net}} = W_{t,w,u_1}$). On the other hand, if $0 < \alpha_{t,w} \leq 1$, only a portion of the forecasted wind is scheduled as power production ($0 < W_{t,w,u_1}^{\text{net}} \leq W_{t,w,u_1}$) while the rest constitutes a headroom that can be used for reserve. If $\alpha_{t,w} = 1$, the forecasted wind power is not used for power production, but used entirely for reserve and $W_{t,w,u_1}^{\text{net}} = 0$.

Figure 5.1 illustrates wind deration using the cumulative distribution function (CDF) of the net

wind power injection. This CDF is modeled for each operating hour based on fitting wind forecast error to the Skew-Laplace distribution as explained in [197]. As the wind deration increases (i.e., as $\alpha_{t,w}$ approaches 1), the probability that an actual realization of wind production exceeds the value of the derated state increases. The difference between wind power production in the derated state and the wind forecast (illustrated as the grey area in Figure 5.1) represents the maximum headroom that can be used for reserve provision.

The expected amount of the upward reserve that wind power generation can provide is calculated as follows:

$$r_{t,w}^{\text{w,up}} \leq \int_{W_{t,w,u_1}^{\text{net}}}^{W_{t,w,u_1}^{\text{net}}} \Pr(W_{t,w,u_1}^{\text{net}}) dW_{t,w,u_1}^{\text{net}}, \forall t \in \Omega^T, w \in \Omega^W, \quad (5.9)$$

where $\Pr(\cdot)$ is the cumulative probability function, as illustrated in Figure 5.1. Since this probability is no greater than 1, the amount of reserve that can be obtained from derating the wind production is lower than the amount of derated wind power:

$$r_{t,w}^{\text{w,up}} \leq W_{t,w,u_1} - W_{t,w,u_1}^{\text{net}}, \forall t \in \Omega^T, w \in \Omega^W. \quad (5.10)$$

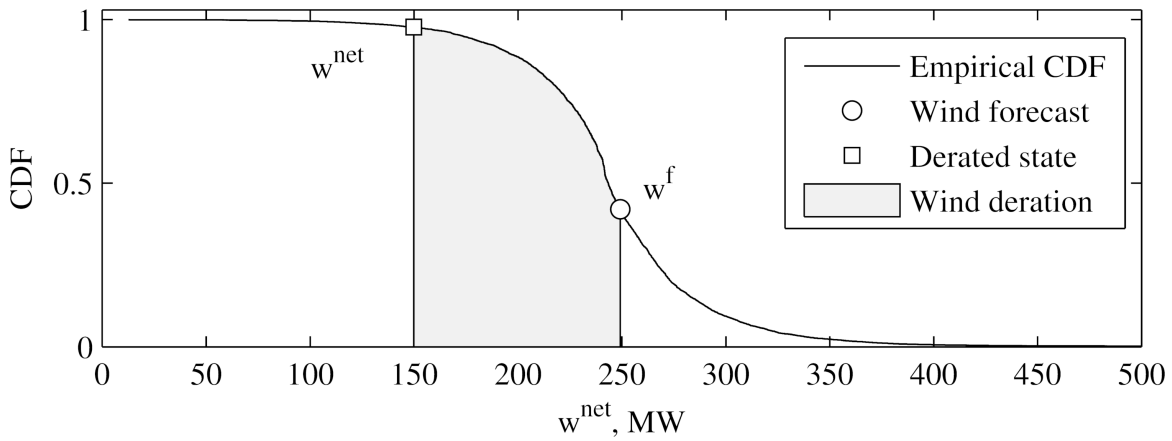


Figure 5.1: Empirical cumulative distribution function (CDF) of the net wind power injection. The central forecast is marked with a circle and the derated state is marked with a square.

This reserve procurement is remunerated in (5.1) through $C_{t,w}^{\text{wind}}$. The amount of this compensation is based on the full amount of wind deration, i.e., $W_{t,w,u_1} - W_{t,w,u_1}^{\text{net}}$, since this quantity represents an actual loss of opportunity cost of wind power generation.

Constraints (5.9) are non-linear, not only because of the non-linear nature of the CDF, but also because of the product of this function with the continuous variable W_{t,w,u_1}^{net} . This CDF can be linearized by dividing it across its vertical axis in a number of segments (as proposed in [32] and [218] and illustrated in Figure 5.2). The accuracy of this approximation depends on the number of segments and can be adjusted for each particular application. A larger number of segments would increase the accuracy of the model, but would also result in longer computing times. Each segment, j , is defined by two parameters: its probability, $\pi_{t,w,j}$, and the range of the net wind power injection, $\Delta w_{t,w,j}^{\text{net}}$. A binary variable, $v_{t,w,j}$, is assigned to each segment, j . Constraints (5.9) can then be reformulated in a linear manner as follows:

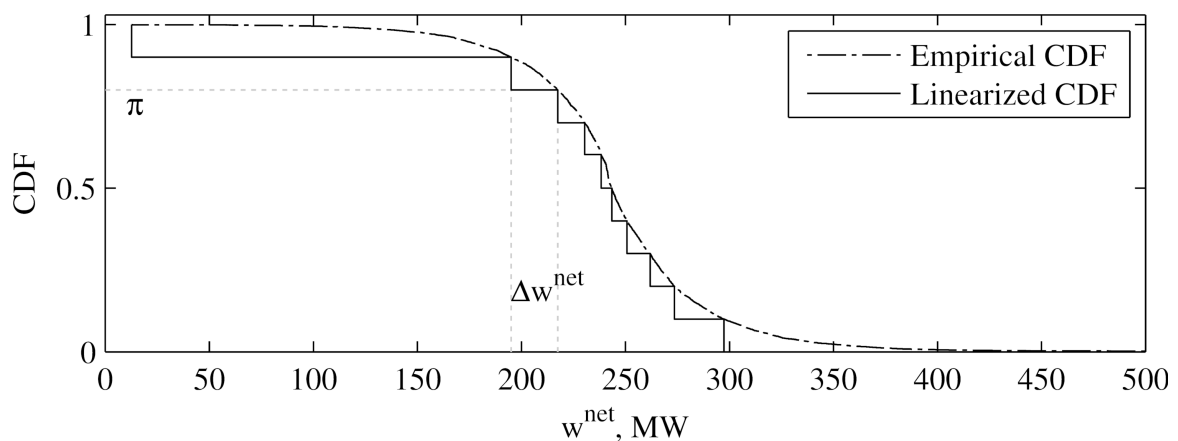


Figure 5.2: Empirical and linearised CDF of the net wind power injection. Data: BPA.

$$r_{t,w}^{\text{w,up}} \leq \sum_j \pi_{t,w,j} \cdot \Delta W_{t,w,j}^{\text{net}} \cdot v_{t,b,j}, \forall t \in \Omega^T, w \in \Omega^W \quad (5.11)$$

$$W_{t,w,u_1}^{\text{net}} \leq W_{t,w,u_1} - \sum_j \Delta w_{t,w,j} \cdot v_{t,w,j}, \forall t \in \Omega^T, w \in \Omega^W \quad (5.12)$$

Constraints (5.11) calculate the expected amount of reserve provided by wind power generation by integrating the intervals that have non-zero binary variables $v_{t,w,j}$. Constraints (5.12) ensure that the net wind power injection, W_{t,w,u_1}^{net} , is less than the difference between the wind forecast, W_{t,w,u_1} , and the derated wind power, $\sum_j (\Delta w_{t,w,j} \cdot v_{t,w,j})$.

Wind integration policies that restrict the amount of deferred wind can be enforced as follows:

$$W_{t,w,u_1} - W_{t,w,u_1}^{\text{net}} \leq \Phi_{t,w}, \forall t \in \Omega^T, w \in \Omega^W \quad (5.13)$$

Constraint (5.13) limits the total amount of wind deration using parameter $\Phi_{t,w}$, which can be determined by a particular wind integration policy. If $\Phi_{t,w} = 0$, no wind deration can be scheduled (i.e., wind power generation provides no reserve). Alternatively, if the $\Phi_{t,w}$ is large, economic benefits can be attained if wind power generation is used as a reserve provider.

5.3.0.5 Reserve Constraints

Conventional generator i provides $r_{i,t}^{\text{up}}$ of upward reserve at time t :

$$r_{i,t}^{\text{up}} \leq \min \left\{ \Delta r_{i,t}^{\text{up}}, \bar{G}_i \cdot x_{t,i} - g_{t,i,u_1} \right\}, \forall t \in \Omega^T, i \in \Omega^I, \quad (5.14)$$

where $\Delta r_{i,t}^{\text{up}}$ is the available upward rampable capacity of that generator. Unlike reserve provided by wind power generation, the ability to deploy reserve provided by conventional generators is subject to less uncertainty, e.g., failure to synchronize an offline generator providing non-spinning reserve

[217]. This uncertainty is outside the scope of this dissertation, since equation (5.14) assumes that only synchronized controllable generators ($u_{t,i} = 1$) can participate in the provision of reserve.

The constraint on the total upward reserve requirement can then be expressed as follows:

$$\sum_{i \in \Omega^I} r_{t,i}^{\text{up}} + \sum_{w \in \Omega^W} r_{t,w}^{\text{w, up}} \geq \sum_{w \in \Omega^W} R^{\text{req}}(W_{t,w,u_1}^{\text{net}}) + \sum_{s \in \Omega^S} R^{\text{req}}(D_{t,s}), \forall t \in \Omega^T. \quad (5.15)$$

The first term on the left-hand side of (5.15) represents the amount of reserve provided by all conventional generators. The second term represents the expected amount of reserve provided by WG. The right-hand side of (5.15) is the sum of the reserve requirements induced by wind power generation, $R^{\text{req}}(W_{t,w,u_1}^{\text{net}})$, and by the load, $R^{\text{req}}(D_{t,s})$.

If the “3.5 σ ”-rule is adopted, the hourly amount of reserve required due to wind power generation can be calculated as follows:

$$R^{\text{req}}(W_{t,w,u_1}^{\text{net}}) = 3.5 \cdot (1 - \alpha_{t,w}) \cdot \sigma(W_{t,w,u_1}), \forall t \in \Omega^T, w \in \Omega^W, \quad (5.16)$$

where $\sigma(W_{t,w,u_1})$ is the standard deviation of the wind power forecast error distribution. On the other hand, if the “(3 + 5)%”-rule is used, the reserve requirement due to wind power generation is given by:

$$R^{\text{req}}(W_{t,w,u_1}^{\text{net}}) = 0.05 \cdot (1 - \alpha_{t,w}) \cdot (W_{t,w,u_1}), \forall t \in \Omega^T, w \in \Omega^W \quad (5.17)$$

Both the “3.5 σ ”-rule and “(3 + 5)%”-rule decrease reserve requirements linearly as the wind deration increases. For both reserve policies, the deration of wind production has a twofold impact on the reserve requirements. First, a lesser amount of reserve is provided by the conventional generators, as is shown in (5.15). Second, as (5.16) and (5.17) show, the reserve requirements decrease as wind deration increases due to the reduced uncertainty. Downward reserve requirements are enforced in a similar way, as in (5.15)–(5.17), and controllable generators are the only provider of this

reserve.

5.4 Case Study

5.4.1 Description of the Test Cases and Data

The proposed case study uses a modified version of the 24-bus IEEE RTS, as described in [185]. The proposed UC model in Section 5.3 is tested for different wind penetration levels and for wind forecast profiles that are positively and negatively correlated with the load. Figure 5.3 illustrates these wind profiles normalized based on the nameplate capacity. The wind penetration level is defined as the percentage of energy produced by wind power generation system-wide. The loss of opportunity cost is compensated for controllable generators that provide reserve, as explained in [205]. Similarly, wind spillage and wind deration are compensated based on the marginal cost of energy in the unconstrained dispatch. Load shedding is monetized through the Value of Loss Load ($VoLL$), which is set at $\$5000/MWh$. To compare the proposed UC formulation with other methodologies, this case study considers three cases. In Case I, wind power generation is not derated, and it, therefore, does not provide reserve. In this case, constraints (5.8) and (5.12) are enforced with $\alpha_{t,s} = 0$. Case II implements conditions reported in [206] (i.e., wind deration is enabled, but is not considered when setting the reserve requirements). Therefore, constraints (5.8) are enforced with $0 \leq \alpha_{t,s} \leq 1$, but constraints (5.12) are enforced with $\alpha_{t,s} = 0$. In Case III, wind deration

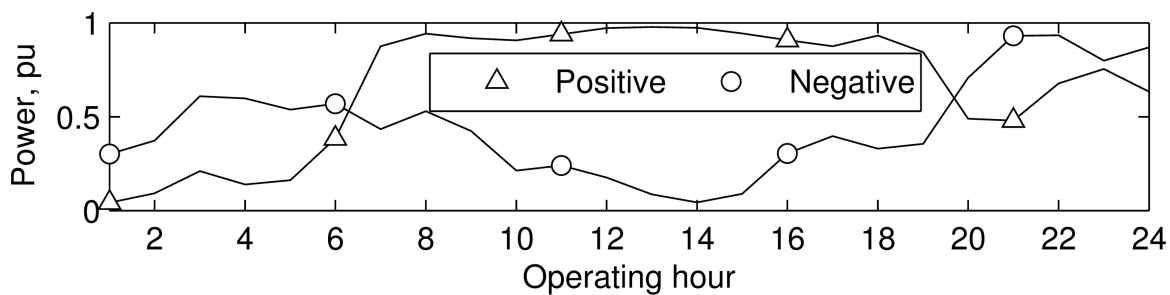


Figure 5.3: Normalized central wind power forecast profiles with positive and negative correlations with load.

is enabled and taken into account in the reserve requirements (i.e., constraints (5.8) and (5.12) are enforced with $0 \leq \alpha_{t,s} \leq 1$). Cases I and II are enforced with no limits on the amount of wind that could be derated (i.e., constraint (5.13) is unbounded).

5.4.2 *Day-Ahead Cost*

Tables 5.1 and 5.2 show the DAC (which is calculated using the objective function (5.1)) for different reserve policies and wind penetration (WP) levels. If the wind penetration is under 10%, all three cases for both wind profiles result in the same schedule and day-ahead operating cost. As the wind penetration increases, the proposed formulation (Case III) results in a cheaper schedule when compared to the operating costs obtained with Cases I and II. Case III enables wind deration at the 20% wind penetration level, while Cases I and II apply wind deration at the 30% wind penetration level. Therefore, the methodology proposed in this dissertation produces a cheaper solution than that obtained with the method proposed in [206]. Regardless of the reserve policy chosen, the day-ahead cost in Cases I and II achieves a minimum for a 40% wind penetration level. Further wind integration increases operating costs. On the other hand, the cost of Case III strictly decreases as the wind penetration increases. Thus, the proposed approach would allow for larger penetrations of wind power generation than traditional approaches and approaches that do not account for wind deration in the reserve requirements [206].

5.4.3 *Wind Utilization*

This subsection discusses the utilization of available wind power generation and its allocation between energy production, reserve provision, and wind spillage. Figures 5.4 and 5.5 illustrate the wind utilization in the different schedules obtained for both wind profiles. The amount of wind deration increases as the wind penetration grows. A higher wind penetration also results in wind spillage, which is due to the constraints on the transmission lines connected to the wind generation

Table 5.1: Day-Ahead Cost (DAC) for the “ 3.5σ ”-rule (in 10^3 , \$)

WP, %	Positive correlation			Negative correlation		
	Case I	Case II	Case III	Case I	Case II	Case III
0%	1032.0	1032.0	1032.0	1032.0	1032.0	1032.0
10%	816.2	816.2	816.2	894.5	894.5	894.5
20%	639.3	639.3	639.3	791.4	791.4	790.9
30%	502.2	502.0	502.0	743.8	730.5	729.3
40%	471.7	456.8	445.7	710.4	698.4	689.7
50%	493.9	471.1	428.8	718.9	663.4	638.5

Table 5.2: Day-Ahead Cost (DAC) for the “ $(3 + 5)\%$ ”-rule (in 10^3 , \$)

WP, %	Positive correlation			Negative correlation		
	Case I	Case II	Case III	Case I	Case II	Case III
0%	1057.1	1057.1	1057.1	1057.1	1057.1	1057.1
10%	830.7	830.7	830.7	917.9	917.9	917.9
20%	653.8	653.8	653.8	811.5	811.5	811.4
30%	516.1	513.2	511.6	755.4	714.0	669.5
40%	469.2	451.8	448.1	748.3	702.3	655.1
50%	488.1	462.1	426.6	719.9	699.3	648.4

location. For the negative correlation between load and wind, wind spillage occurs even for relatively low wind penetration. This spillage is driven not only by transmission constraints, but also by the minimum down time constraints of the generators. Thereby the SO curtails wind to avoid shutting down the base load generators U350 and U400. Figures 5.6 and 5.7 show the itemized contributions to the reserve requirements for both wind profiles. The reserve requirements decrease when wind deration is applied. This typically happens during peak wind production periods (i.e., during daytime hours for correlated profiles and during nighttime hours for negatively correlated profiles). Figures 5.6 and 5.7 also illustrate that wind deration leads to 100% reserve procurement from wind power generation during some operating hours if the wind penetration is high.

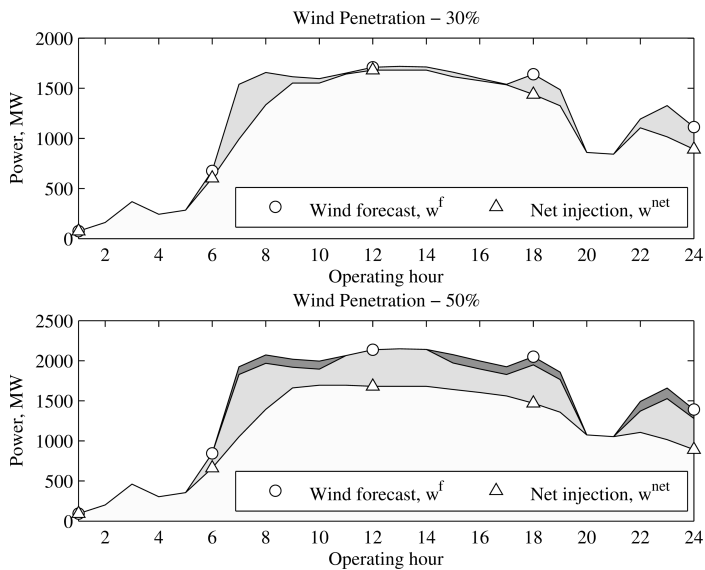


Figure 5.4: Wind usage for the positively correlated wind and load profiles with the “(3 + 5) %” reserve policy. The dark gray area denotes wind spillage, the light grey area represents wind deration, and the white area stands for the energy produced by WG.

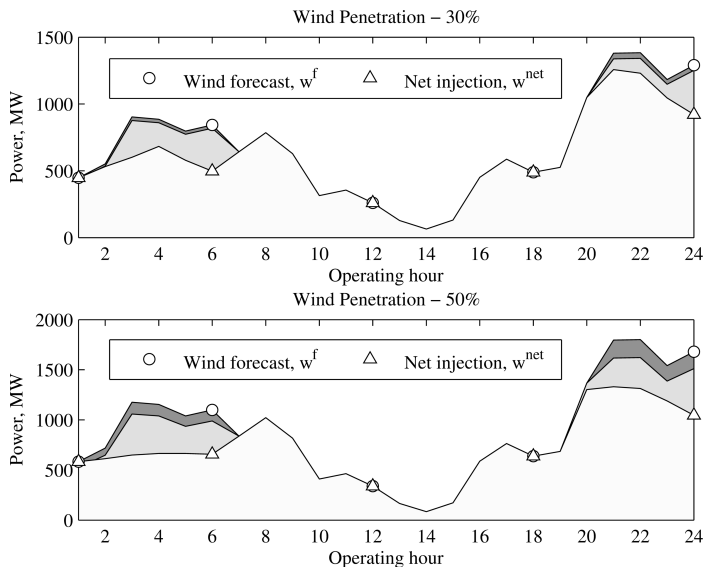


Figure 5.5: Wind usage for the negatively correlated wind and load profiles with the “(3 + 5) %” reserve policy. The dark gray area denotes wind spillage, the light grey area represents wind deration, and the white area stands for the energy produced by WG.

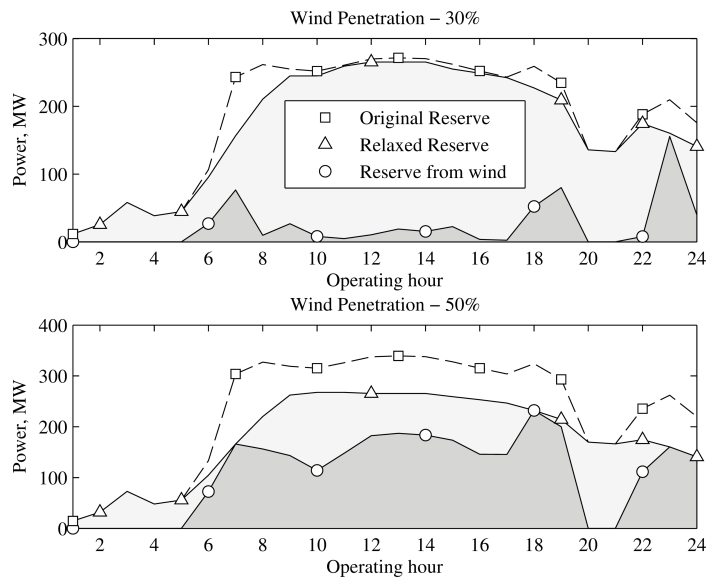


Figure 5.6: Fulfillment of the reserve requirements for the positively correlated wind and load profiles under the “(3 + 5) %” reserve policy. The light grey area is the portion provided by conventional generators. The dark grey area is the portion provided by wind. The white area represents the reduction in the reserve requirement achieved with the proposed methodology.

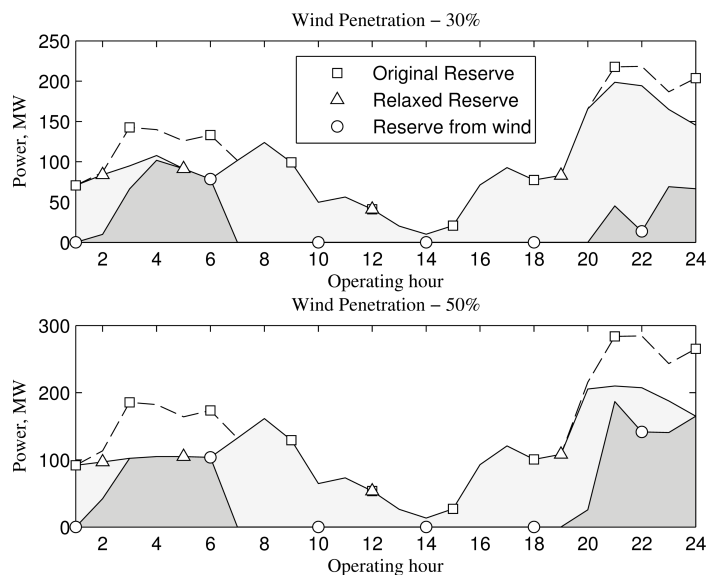


Figure 5.7: Fulfillment of the reserve requirements for the negatively correlated wind and load profiles under the “(3 + 5) %” reserve policy. The light grey area is the portion provided by conventional generators. The dark grey area is the portion provided by wind. The white area represents the reduction in the reserve requirement achieved with the proposed methodology.

5.4.4 Validation using Monte Carlo simulations

Since the actual wind energy production differs from its forecast, the day-ahead schedules must be compared using MC simulations that reflect the uncertainty on WG. For each trial of these MC simulations, the day-ahead schedules are dispatched in pseudo-real time to follow randomly generated wind and load profiles.

Additional commitments are allowed at this stage if the day-ahead constraints (3.2)–(3.6) are not violated. Tables 5.3 and 5.4 show the numerical results for the expected operating cost calculated using these MC simulations. Figure 5.8 illustrates these results. These operating costs includes the day-ahead and real-time start-up cost, the running cost, the cost of lost opportunity, the penalty cost of wind spillage, and the social cost of load shedding. As wind penetration grows, Case I consistently produces the most expensive solution. Case III results in the least expensive solution for both reserve procurement rules and wind power generation profiles. The difference in the expected costs of Case II and III is driven by the reduction in the reserve requirements due to decreased wind uncertainty, as shown in equation (5.15).

Table 5.3: Expected operating cost for the “ 3.5σ ”-rule (in 10^3 , \$)

WP, %	Positive correlation			Negative correlation		
	Case I	Case II	Case III	Case I	Case II	Case III
0%	1041.3	1041.3	1041.3	1041.3	1041.3	1041.3
10%	829.2	829.0	829.0	917.2	917.2	917.2
20%	671.0	664.3	660.3	830.9	825.6	815.8
30%	524.2	516.0	508.7	761.7	751.1	744.1
40%	483.6	477.3	450.1	724.2	706.3	693.4
50%	501.0	473.9	436.2	723.7	682.5	641.3

Table 5.4: Expected operating cost for the “(3 + 5) %”-rule (in 10^3 , \$)

WP, %	Positive correlation			Negative correlation		
	Case I	Case II	Case III	Case I	Case II	Case III
0%	1059.3	1059.3	1059.3	1059.3	1059.3	1059.3
10%	844.2	844.2	844.2	936.0	936.0	936.0
20%	684.8	671.4	671.4	840.1	831.6	827.4
30%	529.1	527.9	526.8	767.4	733.4	704.6
40%	478.9	464.7	456.0	759.1	709.4	661.6
50%	499.1	477.8	439.4	764.3	734.6	654.3

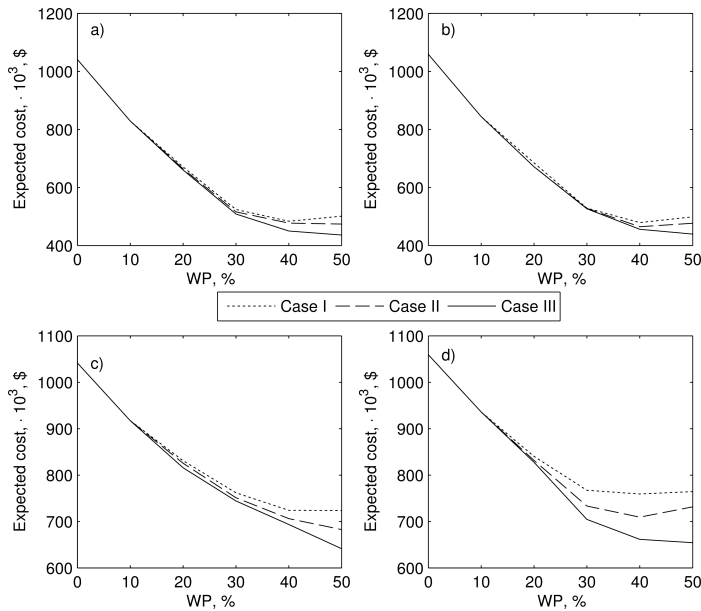


Figure 5.8: Expected Cost (EC) of the MC simulations for the (a) positively correlated wind profile and “ 3.5σ ”-rule, (b) positively correlated wind profile and “(3 + 5) %”-rule, (c) negatively correlated wind profile and “ 3.5σ ”-rule, and (d) negatively correlated wind profile and “(3 + 5) %”-rule.

5.5 Conclusion

This Chapter proposes a day-ahead DUC that schedules wind generation to participate in both energy and reserve procurement. The performance of this model has been tested on the 24-bus IEEE RTS using MC simulations for different wind penetration levels and different correlations of wind

energy production and load. According to these simulations, the main conclusions are as follows:

1. The proposed DUC model achieves lower operating costs by derating wind power generation to reduce the uncertainty on wind power generation simultaneously and, thus, the reserve requirements. Conventional generators are, therefore, dispatched more efficiently because their contribution to the reserve requirements is reduced.
2. Cost savings achieved using the proposed method increases with wind penetration, even though wind power generation receives its full lost opportunity cost for reducing its production. For high wind penetration levels, the proposed method avoids intra-day cycling of inflexible generators.
3. The wind deration also reduces wind spillage due to transmission constraints and, thus, increases the capacity factor of wind power generation. Therefore, the proposed method facilitates further integration of wind power generation in existing power systems in a cost-efficient, reliable, and sustainable manner.

Part III

LONG-TERM PLANNING IN SUSTAINABLE POWER SYSTEMS

Chapter 6

PROFIT-CONSTRAINED ENERGY STORAGE SITING AND SIZING

6.1 Motivation

Energy storage is a pivotal technology for dealing with the challenges caused by the integration of renewable energy sources. It is expected that decreases in the capital costs of storage will eventually spur the deployment of large amounts of ES. These devices will provide transmission services, such as spatiotemporal energy arbitrage, i.e., storing surplus energy from intermittent renewable sources for later use by loads while reducing the congestion in the transmission network. Hence, the ability of ES to provide spatiotemporal arbitrage is subject to its location in the network and the available power and energy capacities. Therefore, it is important for optimal ES operations to optimize both its location and its size. This joint optimization is necessary because, unlike pumped-hydro plants that can only be installed in a limited number of locations, electrochemical ES can be distributed more widely in the transmission network [48, 54, 57].

The complexity of joint siting and sizing of ES arises from the need to balance long- and short-term costs and benefits [48], as well as from the difficulties associated with taking transmission constraints into account [59]. In [60], the value of ES siting and sizing is itemized for different storage technologies and grid services. Based on their numerical studies, the authors of [60] conclude that ignoring the levelizing of short- and long-term benefits of ES and transmission constraints leads to an inaccurate assessment of the value of ES. To overcome this complexity, Dvijotham *et al.* [219] and Pandžić *et al.* [48] use sampling-based approaches that site and size ES to provide spatiotemporal energy arbitrage for each day of the year separately. To aggregate daily decisions in the preferable ES locations and sizes, Dvijotham *et al.* [219] analyze the daily frequency of the

siting and sizing using a heuristic greedy algorithm. Similarly, Pandžić *et al.* [48] select the preferred locations of ES based on their daily frequency over the course of the year and compute the optimal size of ES at every bus as the average of the daily sizing decisions. Makarov *et al.* [50] limit the application of ES to providing balancing services and aggregate the Western Electricity Coordinating Council system to a one-bus model. In [50], the ES ratings for various time scales are computed by performing a Discrete Fourier Transform on the balancing power profile. Unlike in [219, 48, 60], the approach in [50] does not consider economic factors and, thus, calculates the maximum physical limit of ES deployment that could be theoretically installed.

The common thread of [48, 50, 56, 60, 219] is that ES is installed solely to minimize system-wide operating costs. However, in practice, ES is likely to be owned by independent entities that aim to maximize their profits [177]. ES devices are, therefore, likely to be scheduled differently from those in [48, 50, 60, 219], thus affecting the cost savings that the SO might achieve from their deployment. Wogrin *et al.* [59] and Castillo *et al.* [172] co-optimize system-wide operating costs and the operating costs of ES. As shown in [172], minimizing system-wide operating costs in a convex economic dispatch formulation also yields the maximum profit for ES owners in a perfectly competitive market. However, binary commitment decisions on conventional generators and their minimum up and down time constraints are neglected in [172]. This approach may, therefore, yield inaccurate ES siting and sizing decisions. Finally, the models in [172, 59] do not guarantee that the maximized ES profit will be sufficient to recover fully the investments made by ES owners.

6.2 Contributions

This dissertation proposes a computationally tractable bilevel program (BP) to optimize ES siting and sizing decisions in a meshed transmission network considering the perspective of both the SO and ES owners. The main contributions are as follows:

1. As in [48, 59, 60, 172, 219], the proposed BP jointly sites and sizes ES used for spatiotemporal

energy arbitrage to minimize system-wide operating costs and ES investment costs. Unlike in [48, 59, 60, 172, 219], the proposed BP explicitly accounts for the ES profit collected from the electricity market. Finally, unlike in [59, 172], it also accommodates for the binary nature of commitment decisions on conventional generators.

2. Additionally, the bilevel structure of the model makes it possible to compute endogenously locational marginal prices (LMPs), which can be used to relate explicitly the investment costs of ES and their expected profit, as well as to study the ability of ES to influence LMPs. Thus, the proposed BP accounts for the mutual dependency between investment decisions on ES and LMPs. The relationship between the investment costs and expected profit is then enforced by a minimum expected profit constraint, ensuring that ES profits are sufficient to recover investment costs.
3. The resulting profit-constrained BP gives rise to a nonlinear problem since the ES profit is formulated as a nonlinear expression. This work presents a duality-based approach to transforming the proposed BP into a nonlinear equivalent and a novel linearization scheme that makes it possible to reformulate it as an equivalent MILP problem.
4. The proposed approach is applied to a model of the ISO-NE system [220] with off-the-shelf software. The case study analyzes the impact of the profit constraint on the ES siting and sizing decisions, the SO operating costs and savings, and the ES profits. The sensitivity of these decisions is analyzed for different investment budgets, operating strategies, and ES capital cost scenarios. The numerical results obtained in this case study demonstrate the usefulness of this approach for regulators and SOs in assessing the economic viability of ES deployment by balancing the SO cost savings and ES owner profits.

6.3 Formulation

All of the notation used in this section is defined in Appendix A. The proposed BP consists of an upper-level (UL) and a lower-level (LL) problem, as shown in Figure 6.1. The UL problem minimizes expected system-wide operating costs over all representative days and the investment costs of the profit-constrained ES siting and sizing decisions. A separate LL problem is formulated for each representative day to compute the least-cost system-wide operating costs subject to the operational constraints and conditions for that day. As explained in [221], this BP can be solved using a duality-based solution technique that requires the convexity of the LL problems. Therefore, as in [164, 222, 223], the constraints on the binary decisions (e.g., the on/off statuses of conventional generators) are enforced in the UL problem and the corresponding binary decisions parametrize the LL problems.

Figure 6.1 shows that the ES ratings (p_s^{\max} and $eSoC_s^{\max}$) and binary decisions on the generators ($x_{e,t,i}$ and $y_{e,t,i}$) resulting from the UL problem that affect the decisions made in the LL problems. Similarly, the dispatch decisions ($g_{e,t,i}$ and $c_{e,t,s}$) and the ES charging/discharging decisions, ($ch_{e,t,s}$ and $dis_{e,t,s}$), resulting from the LL problems, affect the decisions made in the UL problem. The LL problems yield LMPs ($\lambda_{e,t,s}$), which, in turn, are used in the UL problem to compute the profit collected by the ES owners.

6.3.1 Upper-Level Problem

The UL objective function is:

$$\min_{\Xi_{\text{UL}}} \sum_{e \in E} (\omega_e \cdot OC_e^{\text{PLL}}) + IC, \quad (6.1)$$

where OC_e^{PLL} is the system-wide operating cost as defined in (6.10), and the set of UL decision variables is defined as $\Xi_{\text{UL}} = \{IC, p_s^{\max}, SoC_s^{\max}, x_{e,t,i}, y_{e,t,i}, z_{e,t,i}\}$. The first term in equation (6.1) represents the operating cost over all representative days, OC_e^{PLL} , calculated using the weighing

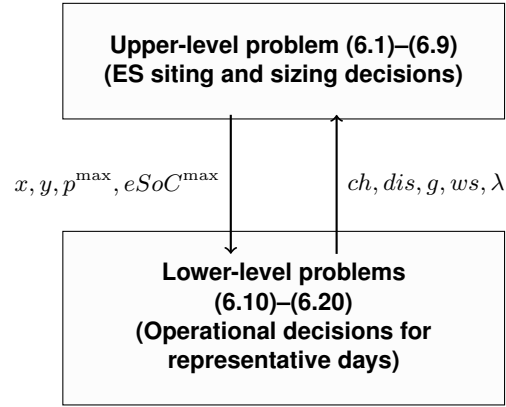


Figure 6.1: An illustration of the proposed bilevel program and the interfaces between the upper- and lower-level problems. For the sake of clarity, the indices of the decision variables have been omitted.

factor ω_e of each representative day, e . The second term in equation (6.1) represents the investment cost resulting from ES siting and sizing decisions. The UL constraints are as follows:

6.3.1.1 Investment constraints

To balance modeling accuracy and computational complexity, the investment model is assumed to be static, i.e., all investment decisions are optimized for operations during a given target year in the future [224]. Thus, the investment cost is computed as in [48] using the ES ratings (p_s^{\max} and $eSoC_s^{\max}$) and daily prorated per MWh and MW capital costs (c^{eSoC} and c^P):

$$IC = \sum_{s \in \Omega^S} (c^{eSoC} \cdot eSoC_s^{\max} + c^P \cdot p_s^{\max}), \quad (6.2)$$

$$IC \leq IC^{\max}, \quad (6.3)$$

where parameters c^{eSoC} and c^P are calculated based on the net present value approach assuming no depreciation of the installed ES. Note that depreciation can be factored in parameters c^{eSoC} and c^P (as explained in [225]) if decision-makers have a reasonable estimate of the residual worth of

installed ES. In addition, constraint (6.3) imposes a budget limit on the total investment cost.

6.3.1.2 Profit constraint

ES owners pay or get paid the LMP ($\lambda_{e,t,s}$) when they charge or discharge their units. Therefore, the expected profit of an ES owner over the representative days is related to the investment cost by the following constraint:

$$\sum_{e \in \Omega^E} \omega_e \cdot \sum_{s \in \Omega^S} \sum_{t \in \Omega^T} \lambda_{e,t,s} \cdot (dis_{e,t,s} \cdot \aleph^{\text{dis}} - ch_{e,t,s} / \aleph^{\text{ch}}) \geq \chi \cdot IC. \quad (6.4)$$

In (6.4), parameter χ can be viewed as a rate of return that the ES owner anticipates to receive from investment, IC [226]. This parameter can be set by investors according to their profitability preferences. If $\chi \geq 1$, the expected profit in the left-hand side of (6.4) is sufficient for the investor to fully recover investment costs, including energy losses due to $\aleph^{\text{dis/ch}} < 1$. Therefore, (6.4) precludes siting and sizing decisions that would result in insufficient profit opportunities¹, which is a significant improvement over the techniques described in [48, 59, 172, 60, 219].

Mathematically, $\lambda_{e,t,s}$ in (6.4) is a LL dual variable associated with constraint (6.19); therefore, the left-hand side of (6.4) contains two nonlinear products of LL dual and primal decision variables ($\lambda_{e,t,s} \cdot dis_{e,t,s}$ and $\lambda_{e,t,s} \cdot ch_{e,t,s}$). Section 6.4.4.1 presents a novel linearization scheme, which reformulates (6.4) as an equivalent linear constraint.

¹Since constraint (6.4) computes the expected profit over all representative days, it does not guarantee nonnegative profits at every representative day individually. However, such guarantees could be enforced if constraint (6.4) were modified as follows: $\sum_{s \in \Omega^S} \sum_{t \in \Omega^T} \lambda_{e,t,s} \cdot (dis_{e,t,s} \cdot \aleph^{\text{dis}} - ch_{e,t,s} / \aleph^{\text{ch}}) \geq 0, \forall e \in \Omega^E$.

6.3.1.3 Binary constraints on generators

These constraints are enforced as follows ($\forall e \in \Omega^E, i \in \Omega^I$):

$$y_{e,t,i} - z_{e,t,i} = x_{e,t,i} - x_{e,t-1,i}, \quad \forall t \in \Omega^T, \quad (6.5)$$

$$y_{e,t,i} + z_{e,t,i} \leq 1, \quad \forall t \in \Omega^T, \quad (6.6)$$

$$x_{e,t,i} = X_{e,i}^0, \quad \forall t \leq \bar{L}_{e,i} + \underline{L}_{e,i}, \quad (6.7)$$

$$\sum_{k=t-UT_i+1}^t y_{e,k,i} \leq x_{e,t,i}, \quad \forall t \in [\bar{L}_{e,i}, n_T], \quad (6.8)$$

$$\sum_{k=t-DT_i+1}^t z_{e,k,i} \leq 1 - x_{e,t,i}, \quad \forall t \in [\underline{L}_{e,i}, n_T]. \quad (6.9)$$

Constraints (6.5)–(6.6) implement the binary logic for on/off status, start-up, and shutdown decisions. Constraint (6.7) accounts for the on/off status at the beginning of each day. Constraints (6.8)–(6.9) enforce the minimum up and down times.

6.3.2 Primal Lower-Level Problem

The objective function of the primal LL (PLL) problem for each representative day e is:

$$\min_{\Xi_{\text{PLL}}} OC_e^{\text{PLL}} = \sum_{t \in \Omega^T} \sum_{i \in \Omega^I} \bar{K}_i \cdot g_{e,t,i} + \sum_{t \in \Omega^T} \sum_{s \in \Omega^S} VoWS \cdot c_{e,t,s} + \sum_{t \in \Omega^T} \sum_{i \in \Omega^I} (TSUC_i \cdot y_{e,t,i} + A_i \cdot x_{e,t,i}), \quad (6.10)$$

where $\Xi_{\text{PLL}} = \{ch_{e,t,s}, dis_{e,t,s}, eSoC_{e,t,s}, f_{e,t,l}, g_{e,t,i}, c_{e,t,s}, \theta_{e,t,s}\}$ are the PLL decision variables. The first two terms in equation (6.10) account for the incremental cost of generation and the cost of wind spillage. The last term represents the start-up and no-load cost associated with the binary decisions $y_{e,t,i}$ and $x_{e,t,i}$, which are optimized in the UL problem. The PLL constraints are defined as follows (dual variables for each constraint are given in parentheses after a colon):

6.3.2.1 Dispatch constraints

The power output of generators is limited by their minimum and maximum limits (6.11) and inter-hour ramp rates (6.12) ($\forall t \in \Omega^T, i \in \Omega^I$):

$$\underline{G}_i \cdot x_{e,t,i} \leq g_{e,t,i} \leq \overline{G}_i \cdot x_{e,t,i} : (\underline{\alpha}_{e,t,i}, \overline{\alpha}_{e,t,i}), \quad (6.11)$$

$$-RD_i \leq g_{e,t,i} - g_{e,t-1,i} \leq RU_i : (\beta_{e,t,i}^{\text{RD}}, \beta_{e,t,i}^{\text{RU}}). \quad (6.12)$$

6.3.2.2 DC network constraints

Since the proposed BP concerns storage siting and sizing in transmission networks, a meshed topology is assumed. The power flow of each transmission line is calculated in equation (6.13) and the power flow limits are enforced in equation (6.14) ($\forall t \in \Omega^T, l \in \Omega^L$):

$$f_{e,t,l} = \frac{\theta_{e,t,o(l)} - \theta_{e,t,r(l)}}{x_l} : (\xi_{e,t,l}), \quad (6.13)$$

$$-\overline{F}_l \leq f_{e,t,l} \leq \overline{F}_l : (\underline{\delta}_{e,t,l}, \overline{\delta}_{e,t,l}). \quad (6.14)$$

6.3.2.3 ES constraints

Constraint (6.15) computes the ES state-of-charge and constraints (6.16)–(6.18) enforce the maximum ES power and energy limits ($\forall t \in \Omega^T, s \in \Omega^S$) ($\forall t \in \Omega^T, s \in \Omega^S$):

$$eSoC_{e,t,s} = eSoC_{e,t-1,s} + ch_{e,t,s} \cdot \Delta\tau - dis_{e,t,s} \cdot \Delta\tau : (\epsilon_{e,t,s}), \quad (6.15)$$

$$0 \leq ch_{e,t,s} \leq p_s^{\text{max}} : (\underline{\varphi}_{e,t,s}^{\text{ch}}, \overline{\varphi}_{e,t,s}^{\text{ch}}), \quad (6.16)$$

$$0 \leq dis_{e,t,s} \leq p_s^{\text{max}} : (\underline{\varphi}_{e,t,s}^{\text{dis}}, \overline{\varphi}_{e,t,s}^{\text{dis}}), \quad (6.17)$$

$$0 \leq eSoC_{e,t,s} \leq eSoC_s^{\text{max}} : (\underline{\varphi}_{e,t,s}^{\text{eSoC}}, \overline{\varphi}_{e,t,s}^{\text{eSoC}}). \quad (6.18)$$

In equations (6.16)–(6.18), decisions on ES ratings p_s^{\max} and $eSoC_s^{\max}$ are optimized in the UL problem. As in [48], the lower bound in equation (6.18) assumes that ES is placed with zero energy charged on the top of its minimum state-of-charge requirement.

6.3.2.4 Nodal power balance

At each bus, the power balance includes the injections from conventional and wind generation, ES, and adjacent transmission lines ($\forall t \in \Omega^T, s \in \Omega^S$):

$$\begin{aligned} \sum_{i \in I_s} g_{e,t,i} - \sum_{l|o(l)=s} f_{e,t,l} + \sum_{l|r(l)=s} f_{e,t,l} + (W_{e,t,s} - c_{e,t,s}) \\ - ch_{e,t,s}/N^{\text{ch}} + dis_{e,t,s} \cdot N^{\text{dis}} = d_{e,t,s} : (\lambda_{e,t,s}), \end{aligned} \quad (6.19)$$

where the wind spillage is constrained by:

$$0 \leq c_{e,t,s} \leq W_{e,t,s} : (\gamma_{e,t,s}). \quad (6.20)$$

6.4 Solution Method

The BP (6.1)–(6.20) can be recast as a single-level equivalent using a duality-based technique that involves two steps [221, 227, 228, 229]. First, the primal-dual transformation is applied to the PLL problems because of the convexity of the LL problems (Section 6.4.1). Second, the PLL and the dual LL (DLL) objective functions are equated to enforce the strong duality theorem (Section 6.4.2). The UL and LL decisions are, thus, simultaneously optimized via the exchange of their decision variables as depicted in Figure 6.1. The nonlinear single-level equivalent of the BP is presented in Section 6.4.3. This nonlinear equivalent is then converted into the single-level MILP problem described in Section 6.4.5 using the linearization process shown in Section 6.4.4. Finally, Section 6.4.6 summarizes the computational complexity of the single-level MILP problem.

6.4.1 Dual Lower-Level Problem

Given the dual variables shown after a colon in (6.11)–(6.20), the DLL problem for each representative day e is written as follows:

6.4.1.1 Dual Lower-Level Objective Function

$$\begin{aligned}
\max_{\Xi_{\text{DLL}}} OC_e^{\text{DLL}} := & \sum_{t \in \Omega^T} \sum_{s \in \Omega^S} \left[\gamma_{e,t,s} \cdot W_{e,t,s} + eSoC_s^{\text{max}} \cdot \bar{\varphi}_{e,t,s}^{\text{eSoC}} + p_s^{\text{max}} \cdot (\bar{\varphi}_{e,t,s}^{\text{ch}} + \bar{\varphi}_{e,t,s}^{\text{dis}}) \right] \quad (6.21) \\
& + \lambda_{e,t,s} \cdot (d_{e,t,s} - W_{e,t,s}) + \sum_{t \in \Omega^T} \sum_{i \in \Omega^I} \left[x_{e,t,i} \cdot (\bar{\alpha}_{e,t,i} \cdot \bar{G}_i + \underline{\alpha}_{e,t,i} \cdot \underline{G}_i) \right] \\
& + (\beta_{e,t,i}^{\text{RU}} \cdot RU_i - \beta_{e,t,i}^{\text{RD}} \cdot RD_i) + \sum_{i \in \Omega^I} (\beta_{e,1,i}^{\text{RU}} + \beta_{e,1,i}^{\text{RD}}) \cdot G_{e,i}^0 \\
& + \sum_{t \in \Omega^T} \sum_{l \in \Omega^L} (\bar{\delta}_{e,t,l} - \underline{\delta}_{e,t,l}) \cdot \bar{F}_l,
\end{aligned}$$

where $\Xi_{\text{DLL}} = \{ \bar{\alpha}_{e,t,i}, \beta_{e,t,i}^{\text{RU}}, \bar{\delta}_{e,t,l}, \gamma_{e,t,s}, \bar{\varphi}_{e,t,s}^{\text{eSoC}}, \bar{\varphi}_{e,t,s}^{\text{ch}}, \bar{\varphi}_{e,t,s}^{\text{dis}} \leq 0; \underline{\alpha}_{e,t,i}, \beta_{e,t,i}^{\text{RD}}, \underline{\delta}_{e,t,l}, \underline{\varphi}_{e,t,s}^{\text{eSoC}}, \underline{\varphi}_{e,t,s}^{\text{ch}}, \underline{\varphi}_{e,t,s}^{\text{dis}} \geq 0; \lambda_{e,t,s}, \xi_{e,t,l}, \epsilon_{e,t,s} \}$ are the DLL decision variables.

6.4.1.2 Dual Lower-Level Constraints

$$\bar{\delta}_{e,t,l} + \underline{\delta}_{e,t,l} + \xi_{e,t,l} - \lambda_{e,t,o(l)} + \lambda_{e,t,r(l)} = 0, \quad \forall t \in \Omega^T, l \in \Omega^L, \quad (6.22)$$

$$\gamma_{e,t,s} - \lambda_{e,t,s} \leq VoWS, \quad \forall t \in \Omega^T, s \in \Omega^S, \quad (6.23)$$

$$\begin{aligned} \bar{\alpha}_{e,t,i} + \underline{\alpha}_{e,t,i} + \beta_{e,t,i}^{\text{RU}} - \beta_{e,t+1,i}^{\text{RU}} + \beta_{e,t,i}^{\text{RD}} - \beta_{e,t+1,i}^{\text{RD}} \\ + \lambda_{e,t,b(i)} = \bar{K}_i, \quad \forall t = 1 \dots n_T - 1, i \in \Omega^I, \end{aligned} \quad (6.24)$$

$$\begin{aligned} \bar{\alpha}_{e,n_T,i} + \underline{\alpha}_{e,n_T,i} + \beta_{e,n_T,i}^{\text{RU}} + \beta_{e,n_T,i}^{\text{RD}} + \lambda_{e,n_T,s(i)} = \bar{K}_i, \quad \forall i \in \Omega^I, \\ \bar{\varphi}_{e,t,s}^{\text{ch}} + \underline{\varphi}_{e,t,s}^{\text{ch}} - \epsilon_{e,t,s} \cdot \Delta\tau - \lambda_{e,t,s} / \aleph^{\text{ch}} = 0, \quad \forall t \in \Omega^T, s \in \Omega^S, \end{aligned} \quad (6.25)$$

$$\bar{\varphi}_{e,t,s}^{\text{dis}} + \underline{\varphi}_{e,t,s}^{\text{dis}} + \epsilon_{e,t,s} \cdot \Delta\tau + \lambda_{e,t,s} \cdot \aleph^{\text{dis}} = 0, \quad \forall t \in \Omega^T, s \in \Omega^S, \quad (6.26)$$

$$\bar{\varphi}_{e,t,s}^{\text{eSoC}} + \underline{\varphi}_{e,t,s}^{\text{eSoC}} + \epsilon_{e,t,s} - \epsilon_{e,t+1,s} = 0, \quad \forall t = 1 \dots n_T - 1, s \in \Omega^S, \quad (6.27)$$

$$\bar{\varphi}_{e,n_T,s}^{\text{eSoC}} + \underline{\varphi}_{e,n_T,s}^{\text{eSoC}} + \epsilon_{e,n_T,s} = 0, \quad \forall s \in \Omega^S, \quad (6.28)$$

$$- \sum_{l|o(l)=s} \frac{\xi_{e,t,l}}{x_l} + \sum_{l|r(l)=s} \frac{\xi_{e,t,l}}{x_l} = 0, \quad \forall s \in \Omega^S, t \in \Omega^T. \quad (6.29)$$

6.4.2 Strong Duality Condition

For each LL problem and, thus, each representative day, e , the strong duality condition is enforced as follows:

$$OC_e^{\text{PLL}} = OC_e^{\text{DLL}} + \sum_{t \in \Omega^T} \sum_{i \in \Omega^I} (TSUC_i \cdot y_{e,t,i} + A_i \cdot x_{e,t,i}). \quad (6.30)$$

Note that the last term in the right-hand side of (6.30) offsets the start-up and no-load costs optimized in the UL problem.

6.4.3 Nonlinear Single-Level Equivalent

As explained in [221], each LL problem can be replaced by its primal feasibility constraints (6.11)–(6.20), its dual feasibility constraints (6.22)–(6.29), and the strong duality condition (6.30). Therefore, the BP (6.1)–(6.20) can be recast as a single-level equivalent given by (6.1)–(6.9) and {(6.11)–

(6.20), (6.22)–(6.30), $\forall e \in \Omega^E$ }. This equivalent is nonlinear because of the following nonlinearities that appear in the problem:

- (i) products of continuous DLL ($\lambda_{e,t,s}$) and continuous PLL ($dis_{e,t,s}, ch_{e,t,s}$) decision variables in the ES profit constraint (6.4),
- (ii) products of continuous UL ($eSoC_s^{\max}, p_s^{\max}$) and continuous DLL ($\underline{\varphi}_{e,t,s}^{eSoC}, \overline{\varphi}_{e,t,s}^{ch}, \overline{\varphi}_{e,t,s}^{dis}$) decision variables in equation (6.30),
- (iii) products of binary UL ($x_{e,t,i}$) and continuous DLL ($\underline{\alpha}_{e,t,i}, \overline{\alpha}_{e,t,i}$) decision variables in equation (6.30).

These three nonlinearities are converted into equivalent mixed-integer linear expressions as explained in Section 6.4.4.

6.4.4 Linearization of the Nonlinear Single-Level Equivalent

6.4.4.1 Linearization of the ES profit constraint

The ES profit in equation (6.4) can be equivalently expressed in terms of other dual variables to linearize it using the complementary slackness conditions of each LL problem. First, using equations (6.25) and (6.26), the ES profit in equation (6.4) for each representative day, e , results in:

$$\sum_{t \in \Omega^T} \sum_{s \in \Omega^S} \lambda_{e,t,s} \cdot (dis_{e,t,s} \cdot \aleph^{\text{dis}} - ch_{e,t,s} / \aleph^{\text{ch}}) = \sum_{t \in \Omega^T} \sum_{s \in \Omega^S} \left[\epsilon_{e,t,s} \cdot \Delta\tau \cdot (ch_{e,t,s} - dis_{e,t,s}) - dis_{e,t,s} \cdot (\underline{\varphi}_{e,t,s}^{\text{dis}} + \overline{\varphi}_{e,t,s}^{\text{dis}}) - ch_{e,t,s} \cdot (\underline{\varphi}_{e,t,s}^{\text{ch}} + \overline{\varphi}_{e,t,s}^{\text{ch}}) \right]. \quad (6.31)$$

Expressing $\Delta\tau \cdot (ch_{e,t,s} - dis_{e,t,s})$ in terms of $eSoC_{e,t,s}$ from (6.15), the first term in the right-hand side of (6.31) (hereinafter denoted as \mathcal{K}_e), can be expressed as:

$$\mathcal{K}_e = \sum_{t \in \Omega^T} \sum_{s \in \Omega^S} \epsilon_{e,t,s} \cdot (eSoC_{e,t,s} - eSoC_{e,t-1,s}). \quad (6.32)$$

The terms in the right-hand side of (6.32) can be rearranged as:

$$\mathcal{K}_e = \sum_{t=1}^{n_T-1} \sum_{s \in \Omega^S} eSoC_{e,t,s} \cdot (\epsilon_{e,t,s} - \epsilon_{e,t+1,s}) + \sum_{s \in \Omega^S} eSoC_{e,n_T,s} \cdot \epsilon_{e,n_T,s}. \quad (6.33)$$

Equation (6.33) can be equivalently expressed in terms of $\bar{\varphi}_{e,t,s}^{eSoC}$ and $\underline{\varphi}_{e,t,s}^{eSoC}$ from (6.27) and (6.28) as:

$$\mathcal{K}_e = \sum_{t \in \Omega^T} \sum_{s \in \Omega^S} eSoC_{e,t,s} \cdot (-\underline{\varphi}_{e,t,s}^{eSoC} - \bar{\varphi}_{e,t,s}^{eSoC}). \quad (6.34)$$

The first term in the right-hand side of (6.31) can be replaced with (6.34), thus equivalently reformulating (6.31) as follows:

$$\begin{aligned} \sum_{t \in \Omega^T} \sum_{s \in \Omega^S} \lambda_{e,t,s} \cdot (dis_{e,t,s} \cdot \aleph^{\text{dis}} - ch_{e,t,s} / \aleph^{\text{ch}}) = & - \sum_{t \in \Omega^T} \sum_{s \in \Omega^S} \left[eSoC_{e,t,s} \cdot (\underline{\varphi}_{e,t,s}^{eSoC} + \bar{\varphi}_{e,t,s}^{eSoC}) + \right. \\ & \left. dis_{e,t,s} \cdot (\underline{\varphi}_{e,t,s}^{\text{dis}} + \bar{\varphi}_{e,t,s}^{\text{dis}}) + ch_{e,t,s} \cdot (\underline{\varphi}_{e,t,s}^{\text{ch}} + \bar{\varphi}_{e,t,s}^{\text{ch}}) \right]. \end{aligned} \quad (6.35)$$

The following equalities can be derived using the complementary slackness conditions associated with constraints (6.16)–(6.18), $\forall t \in \Omega^T, s \in \Omega^S$:

$$dis_{e,t,s} \cdot \bar{\varphi}_{e,t,s}^{\text{dis}} = p_s^{\text{max}} \cdot \bar{\varphi}_{e,t,s}^{\text{dis}}, \quad (6.36)$$

$$ch_{e,t,s} \cdot \bar{\varphi}_{e,t,s}^{\text{ch}} = p_b^{\text{max}} \cdot \bar{\varphi}_{e,t,s}^{\text{ch}}, \quad (6.37)$$

$$eSoC_{e,t,s} \cdot \bar{\varphi}_{e,t,s}^{\text{eSoC}} = eSoC_s^{\text{max}} \cdot \bar{\varphi}_{e,t,s}^{\text{eSoC}}, \quad (6.38)$$

$$ch_{e,t,s} \cdot \underline{\varphi}_{e,t,s}^{\text{ch}} = dis_{e,t,s} \cdot \underline{\varphi}_{e,t,s}^{\text{dis}} = eSoC_{e,t,s} \cdot \underline{\varphi}_{e,t,s}^{\text{eSoC}} = 0. \quad (6.39)$$

After using the equalities (6.36)–(6.39) for the nonlinear terms in (6.35), the ES profits are equivalently rewritten as a nonlinear function depending on the ES power and energy ratings:

$$\sum_{t \in \Omega^T} \sum_{s \in \Omega^S} \lambda_{e,t,s} \cdot (dis_{e,t,s} \cdot \aleph^{\text{dis}} - ch_{e,t,s} / \aleph^{\text{ch}}) = - \sum_{t \in \Omega^T} \sum_{s \in \Omega^S} \left[eSoC_s^{\text{max}} \cdot \bar{\varphi}_{e,t,s}^{\text{eSoC}} + p_s^{\text{max}} \cdot (\bar{\varphi}_{e,t,s}^{\text{ch}} + \bar{\varphi}_{e,t,s}^{\text{dis}}) \right]. \quad (6.40)$$

To equivalently reformulate (6.40) as a linear expression, ES ratings are modeled as:

$$eSoC_s^{\text{max}} = \sum_{q \in Q} \Delta eSOC \cdot u_{s,q}, \forall s \in \Omega^S, \quad (6.41)$$

$$p_s^{\text{max}} = eSoC_s^{\text{max}} \cdot \rho^{-1} = \sum_{q \in Q} \Delta eSOC \cdot \rho^{-1} \cdot u_{s,q}, \forall s \in \Omega^S, \quad (6.42)$$

$$\sum_{q \in Q} u_{s,q} \leq u_s^{\text{max}}, \forall s \in \Omega^S. \quad (6.43)$$

In equations (6.41) and (6.42), it is assumed that at every bus, ES is assembled from standard blocks that have fixed energy ($\Delta eSOC$) and power ($\Delta eSOC \cdot \rho^{-1}$) ratings. For instance, the ratio between these energy and power ratings is assumed constant [48] and the coefficient, ρ , depends on the storage technology [59]. Constraint (6.43) limits the number of blocks that can be installed at each

bus. Using (6.41) and (6.42), the ES profits (6.40) can be equivalently reformulated as:

$$\begin{aligned} & \sum_{t \in \Omega^T} \sum_{s \in \Omega^S} \lambda_{e,t,s} \cdot \left(dis_{e,t,s} \cdot N^{dis} - ch_{e,t,s} / N^{ch} \right) = \\ & - \sum_{t \in \Omega^T} \sum_{s \in \Omega^S} \sum_{q \in \Omega^Q} \Delta eSoC \cdot u_{s,q} \cdot \left(\bar{\varphi}_{e,t,s}^{eSoC} + \rho^{-1} \cdot \left(\bar{\varphi}_{e,t,s}^{ch} + \bar{\varphi}_{e,t,s}^{dis} \right) \right). \end{aligned} \quad (6.44)$$

Expression (6.44) still contains three products of binary and continuous variables that are linearized using the ‘big M’ method [230]. This linearization comes at the expense of auxiliary continuous variables ($a_{e,t,s,q}^1$ and $a_{e,t,s,q}^{2,ch/dis}$) and constraints (6.46)–(6.51). Constraint (6.4) is replaced with the following equivalent:

$$- \sum_{e \in \Omega^E} \omega_e \sum_{t \in \Omega^T} \sum_{s \in \Omega^S} \sum_{q \in \Omega^Q} \left(a_{e,t,s,q}^1 + a_{e,t,s,q}^{2,ch} + a_{e,t,s,q}^{2,dis} \right) \geq \chi \cdot IC, \quad (6.45)$$

and the linear constraints ($\forall e \in \Omega^E, t \in \Omega^T, s \in \Omega^S, q \in \Omega^Q$):

$$-M \cdot (1 - u_{s,q}) \leq \bar{\varphi}_{e,t,s}^{eSoC} \cdot \Delta eSoC - a_{e,t,s,q}^1 \leq 0, \quad (6.46)$$

$$-M \cdot (1 - u_{s,q}) \leq \bar{\varphi}_{e,t,s}^{ch} \cdot \rho^{-1} \cdot \Delta eSoC - a_{e,t,s,q}^{2,ch} \leq 0, \quad (6.47)$$

$$-M \cdot (1 - u_{s,q}) \leq \bar{\varphi}_{e,t,s}^{dis} \cdot \rho^{-1} \cdot \Delta eSoC - a_{e,t,s,q}^{2,dis} \leq 0, \quad (6.48)$$

$$-M \cdot u_{s,q} \leq a_{e,t,s,q}^1 \leq 0, \quad (6.49)$$

$$-M \cdot u_{s,q} \leq a_{e,t,s,q}^{2,ch} \leq 0, \quad (6.50)$$

$$-M \cdot u_{s,q} \leq a_{e,t,s,q}^{2,dis} \leq 0. \quad (6.51)$$

Since the linearization process presented in this subsection is based on algebraic manipulations, complementary slackness conditions, and the ‘big M’ method, the left-hand side in (6.45) is an exact equivalent of the left-hand side in (6.4). Therefore, this linearization does not affect the accuracy of

the solution.

6.4.4.2 Linearization of the strong duality equality

As shown in (6.21), the term OC_e^{DLL} in (6.30) contains several nonlinear terms. The second and third terms in (6.21) are identical to the right-hand side of (6.40) and, thus, the same linearization technique can be applied. The fifth term in (6.21) involving the products $x_{e,t,i} \cdot \bar{\alpha}_{e,t,i} \cdot \bar{G}_i$ and $x_{e,t,i} \cdot \underline{\alpha}_{e,t,i} \cdot \underline{G}_i$ can also be linearized using the ‘big M’ method [230]. Therefore, constraint (6.30) is replaced for each representative day, e , with:

$$OC_e^{\text{PLL}} = \sum_{t \in \Omega^T} \sum_{s \in \Omega^S} \left[\gamma_{e,t,s} \cdot W_{e,t,s} + \lambda_{e,t,s} \cdot (d_{e,t,s} - W_{e,t,s}) + \sum_{q \in Q} \left(a_{e,t,s,q}^1 + a_{e,t,s,q}^{2,\text{ch}} + a_{e,t,s,q}^{2,\text{dis}} \right) \right] \\ + \sum_{t \in \Omega^T} \sum_{i \in \Omega^I} \left[\bar{h}_{e,t,i} + \underline{h}_{e,t,i} + \beta_{e,t,i}^{\text{RU}} \cdot RU_i - \beta_{e,t,i}^{\text{RD}} \cdot RD_i + TSUC_i \cdot y_{e,t,i} + A_i \cdot x_{e,t,i} \right] \\ + \sum_{i \in \Omega^I} (\beta_{e,1,i}^{\text{RU}} + \beta_{e,1,i}^{\text{RD}}) \cdot G_{e,i}^0 + \sum_{t \in \Omega^T} \sum_{l \in \Omega^L} (\bar{\delta}_{e,t,l} - \underline{\delta}_{e,t,l}) \cdot \bar{F}_l, \quad (6.52)$$

$$-M \cdot (1 - x_{e,t,i}) \leq \bar{\alpha}_{e,t,i} \cdot \bar{G}_i - \bar{h}_{e,t,i} \leq 0, \forall t \in \Omega^T, i \in \Omega^I, \quad (6.53)$$

$$0 \leq \underline{\alpha}_{e,t,i} \cdot \underline{G}_i - \underline{h}_{e,t,i} \leq M \cdot (1 - x_{e,t,i}), \forall t \in \Omega^T, i \in \Omega^I, \quad (6.54)$$

$$-M \cdot x_{e,t,i} \leq \bar{h}_{e,t,i} \leq 0, \forall t \in \Omega^T, i \in \Omega^I, \quad (6.55)$$

$$0 \leq \underline{h}_{e,t,i} \leq M \cdot x_{e,t,i}, \forall t \in \Omega^T, i \in \Omega^I. \quad (6.56)$$

The proposed linearization scheme relies on the ‘big M’ method and, thus, requires setting bounds on the LL dual variables, which are known as the ‘big M’ values. The computational performance of the BP can be affected by the selections of the ‘big M’ values, especially when implemented for large-scale systems. This drawback could be overcome either by appropriately selecting the big-M values or by avoiding the use of the ‘big M’ method [231], [232].

6.4.5 MILP Formulation

Using the linearized expressions from Section 6.4.4, the single-level MILP formulation is given as follows:

$$\text{Equation (6.1),} \tag{6.57}$$

subject to:

$$\text{Equation (6.2) – (6.3), (6.5) – (6.9), (6.11) – (6.20), (6.22) – (6.29),} \tag{6.58}$$

$$\text{Equation (6.41) – (6.43), (6.45) – (6.56).} \tag{6.59}$$

In equations (6.57)–(6.59), $\lambda_{e,t,s}$ is modeled as a free variable, which can take arbitrarily high and low values. In practice, individual market participants use their market power to influence LMPs and, hence, maximize their own profit. Therefore, SOs have adopted a set of market power mitigation policies that aim to keep LMPs at a reasonable level to ensure competitive market outcomes [233]. Based on the discussions in [234, 235], the ability of ES to influence LMPs can be limited using ($\forall e \in \Omega^E, t \in \Omega^T, s \in \Omega^S$):

$$(1 - \Delta\lambda) \cdot \bar{\lambda}_{e,t,s} \leq \lambda_{e,t,s} \leq (1 + \Delta\lambda) \cdot \bar{\lambda}_{e,t,s}, \tag{6.60}$$

where $\Delta\lambda$ is a non-negative parameter regulating the range of deviations of the free variable $\lambda_{e,t,s}$ from the reference values $\bar{\lambda}_{e,t,s}$, which are taken as the LMPs in the case without ES. Given constraint (6.60), parameter $\Delta\lambda$ can be interpreted as the maximum deviation of the LMPs from the reference value that ES can achieve by exercising market power. The case study presented in Section 6.5 analyzes the sensitivity of the proposed approach to the value of parameter $\Delta\lambda$.

6.4.6 Computational Complexity

The single-level equivalent presented in Section 6.4.5 is an MILP problem and, therefore, is generally NP-hard. The computational complexity of this problem is characterized by the number of constraints and the number of continuous/binary variables. Table 6.1 summarizes these numbers. Note that the total number of constraints depends on the initial statuses of conventional generators due to constraints (6.7)–(6.9). Hence, Table 6.1 provides an upper bound on the number of such constraints.

Table 6.1. DIMENSION OF THE SINGLE-LEVEL MILP PROBLEM

# of constraints	$4 + n_E + 3n_S + n_{EN}n_T(17n_I + 4n_L + 17n_S + 12n_qn_Q)$
# of continuous variables	$1 + 2n_S + n_{EN}n_T(4n_L + 7n_I + 14n_S + 3n_Sn_Q)$
# of binary variables	$3n_{EN}n_Tn_I + n_Sn_Q$

6.5 Case Study

6.5.1 Test System and Experimental Setup

The single-level MILP problem (6.57)–(6.60) was tested using an 8-zone model of the ISO New England system [220]. This test system covers six US states and is illustrated in Figure 6.2. It includes 76 thermal generators with a total installed capacity of roughly 30 GW. Each zone in this system is numbered in Table 6.2 and is modeled as a separate bus in the proposed BP. In addition to the generation, load, and transmission data given in [220], annual wind generation profiles with an hourly resolution were taken from [236] for a 30% wind penetration level in terms of annual electrical energy produced. Given this data and no ES installed, the UC problem is solved for each day of a given year. The resulting annual operating cost is 2544.5 M\$. The mean hourly average

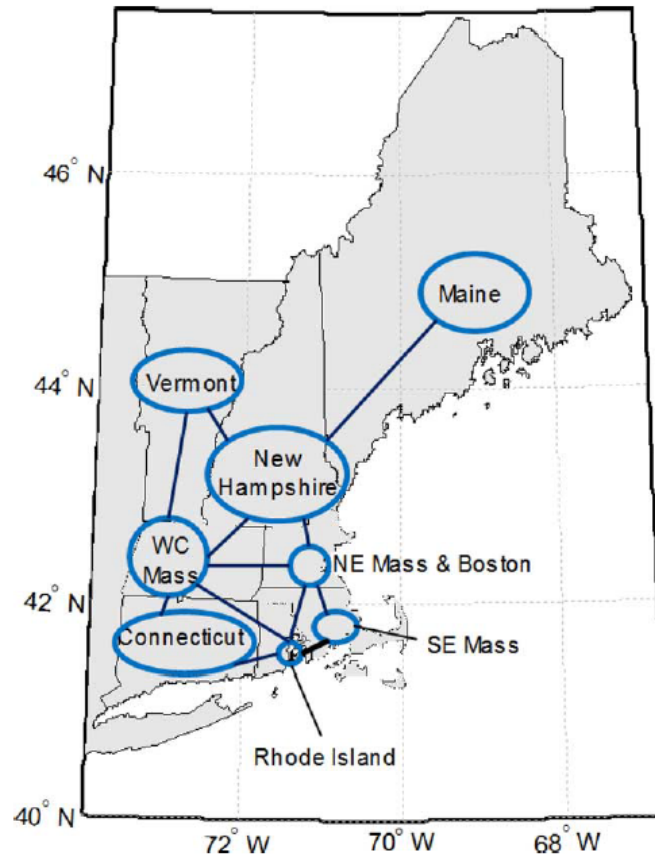


Figure 6.2: A diagram of the ISO NE system described in [220].

Table 6.2. ZONE NUMBERS FOR THE DIAGRAM IN FIGURE 6.2

Region	ME	NH	VT	WC Mass	NE Mass	CT	RI	SE Mass
Zone #	1	2	3	4	5	6	7	8

LMP for each zone and its standard deviation throughout the year are displayed in Figure 6.3. The standard deviation characterizes the range of the LMP distribution over the course of the year and, therefore, gives an indication of LMP variability in each zone.

The recursive hierarchical clustering algorithm described in [237] is used to determine 5 repre-

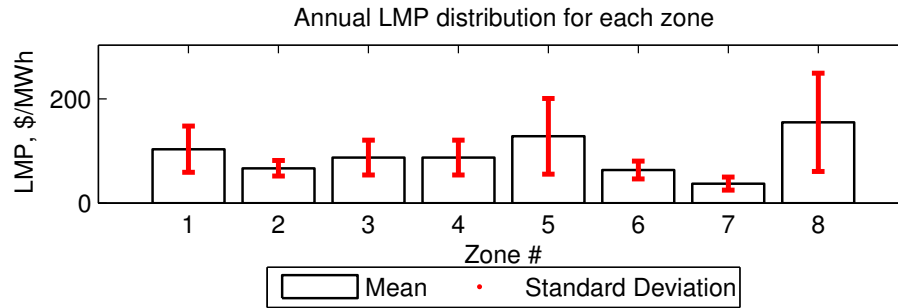


Figure 6.3: The mean and standard deviation of hourly LMPs throughout the considered year in cases without ES.

sentative days and their respective weights from the year-long demand and wind generation profiles. This algorithm is based on a general-to-specific partitioning approach, which recursively combines daily profiles at every bus in a given number of clusters based on user-defined similarity or dissimilarity metrics. The advantage of this algorithm is that it can simultaneously account for the intra-day and seasonal features of these profiles and has a high adaptivity that improves local data quality. However, other clustering techniques can be applied to obtain representative days; interested readers can find the surveys in the detailed literature [237, 238, 239]. Figure 6.4 displays the system-wide aggregated representative load and wind generation profiles for the 5 representative days.

In the following simulations, the value of parameter ρ is set at 6 h, which is a representative energy-to-power ratio for promising ES technologies [47] and is sufficient for providing intra-day energy arbitrage [47, 48]. The charging and discharging efficiency of ES are assumed symmetric with $\eta^{\text{ch}} = \eta^{\text{dis}} = 0.9$, which also falls within the range of prospective ES technologies [47]. Each ES block is assumed to have a $\Delta eSoC = 10$ MW and the maximum number of blocks in each zone, $s(u_s^{\text{max}})$, is set at 300. As in [48], the siting and sizing decisions are analyzed for three capital cost scenarios: low (\$20/kWh and \$500/kW), medium (\$50/kWh and \$1000/kW), and high (\$75/kWh and \$1300/kW). These investment costs are prorated on a daily basis and the values of the c^p and

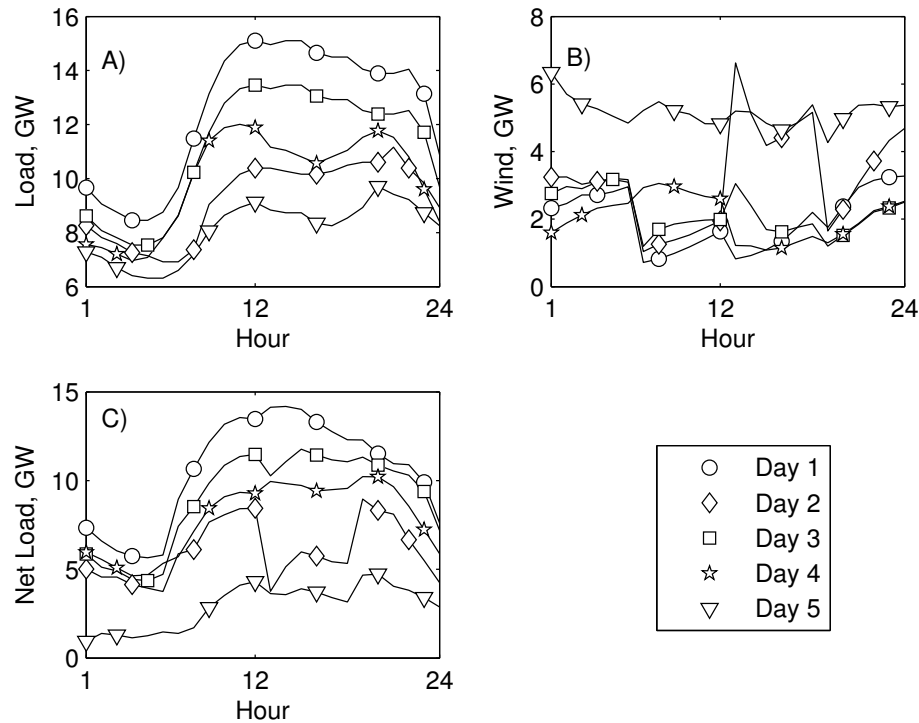


Figure 6.4: The system-wide aggregated representative load (A), wind generation (B), and net load (C) profiles. The net load profile is the difference between the load and wind generation profiles.

e^{SoC} are obtained for each capital cost scenario assuming that the ES lifetime is 10 years and the annual interest rate is 5% (as explained in [48]). The investment budget is $IC^{\text{max}} = \infty$, hence constraint (6.3) is nonbinding, unless stipulated otherwise. Finally, to avoid overestimating the need for ES due to prioritized dispatch of wind generation, the $VoWS$ is set to \$0/MWh.

The dimension of the problem for this case study is 3,633,153 constraints, 947,057 continuous variables, and 29,760 binary variables. All simulations were carried out using CPLEX under GAMS 23.7 [240] on an Intel Xenon 2.55 GHz processor with 32 GB of RAM using the Hyak supercomputer system at the University of Washington [241]. The optimality gap was set at 0.1%. All simulations of the proposed BP with different input parameters presented below were completed within 72 hours.

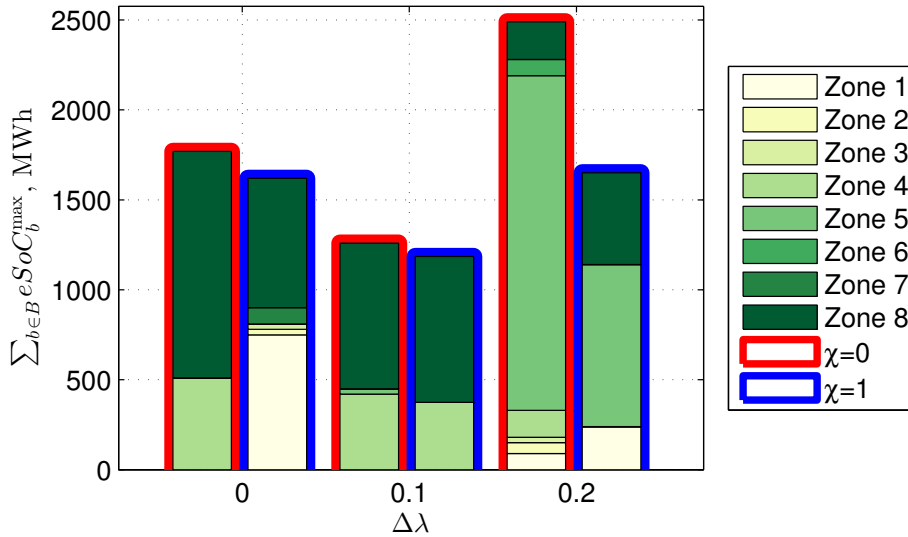


Figure 6.5: Effect of the ES profit constraint (6.4) on the optimized ES siting and sizing decisions for the low capital cost scenario.

6.5.2 Siting and Sizing Decisions

6.5.2.1 Impact of the ES profit constraint

Figure 6.5 displays the optimized siting and sizing decisions² on ES for the low capital cost scenario for different values of χ and $\Delta\lambda$. Regardless of the $\Delta\lambda$ chosen, the ES profit constraint (6.4) affects both the siting and sizing decisions.

If $\Delta\lambda = 0$, i.e., LMPs are not affected by ES installations ($\lambda_{e,t,s} = \bar{\lambda}_{e,t,s}$), siting decisions between the profit-unconstrained ($\chi = 0$) and profit-constrained cases ($\chi = 1$) overlap only in zone 8, which is characterized by the largest variability in LMPs (Figure 6.3). However, as $\Delta\lambda$ increases (i.e., the ES deployment influences LMPs when compared to the case without ES), the number of shared locations between the profit-constrained and unconstrained cases increases. For instance, if $\Delta\lambda = 0.1$, ES are placed in zones 4 and 8 in both cases. If $\Delta\lambda$ is further increased to 0.2, ES are

²Recall that the energy and power ratings of ES are assumed to be proportional (6.42). Therefore, the analyses in Section 6.5.2 discuss the sizing decisions in terms of the energy ratings ($eSOC_s^{\max}$).

installed in zones 1, 5, and 8 for both cases.

Regarding the sizing decisions, the profit-unconstrained case consistently results in larger total energy ratings ($\sum_{s \in \Omega^S} eSoC_s^{\max}$) for any value of $\Delta\lambda$, which also leads to higher investment costs, as illustrated in Figure 6.6A. Figure 6.6B shows that these decisions do not result in sufficient ES profits to recover such high investment costs, thus leading to net monetary losses, i.e., $\Delta < 0$ (Figure 6.6C). Therefore, the profit-unconstrained case overestimates the whole-system need for ES and produces economically nonviable decisions. This conclusion can also be related to the whole-system value of energy storage. As shown in [60], the value of energy storage monotonically reduces as the installed energy storage capacity increases. Thus, larger total energy ratings in profit-unconstrained cases reduce the whole-system value of storage such that ES owners cannot collect sufficient profits to recover their investment costs.

On the other hand, profit-constrained decisions have lower total energy ratings and investment costs, resulting in net monetary gain, i.e., $\Delta > 0$ (Figure 6.6C). This gain ensures the profitability of ES and economic sustainability of these siting and sizing decisions. This difference between the profit-constrained and unconstrained cases can be attributed to different scheduling priorities. In the profit-unconstrained case, ES are installed and scheduled to minimize operating costs, so ES are allowed to incur losses if they reduce operating costs. However, in the profit-constrained case, ES are installed and scheduled to minimize system-wide operating costs as long as the investment costs can be fully recovered.

The common thread of siting decisions in profit-constrained and unconstrained cases is that ES are usually placed in zones with relatively high variability in LMPs (as Figure 6.3 shows). This observation is consistent with the empirical siting rule in [242], suggesting that the most likely profit opportunities for ES in a market environment are at buses with the greatest difference between discharging and charging LMPs. Although the variability in LMPs drives siting decisions, its impact on sizing decisions in the profit-constrained case is not straightforward. For example, Figure 6.3

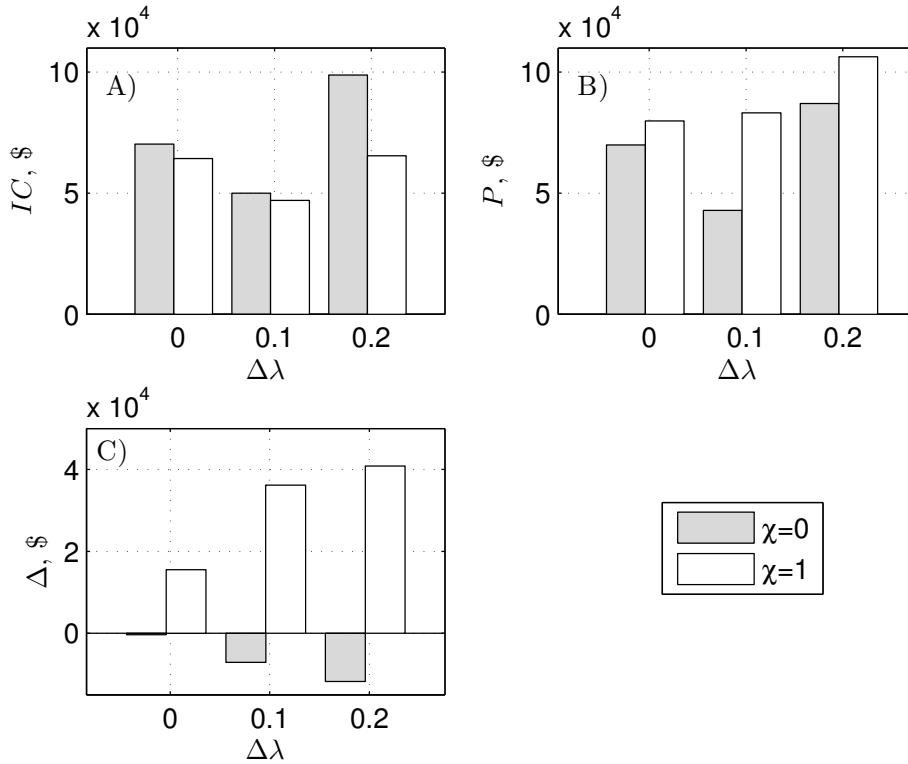


Figure 6.6: Effect of the ES profit constraint (6.4) under the low capital cost scenario on the: A) investment cost of ES (IC), B) expected profit of ES (P), and C) net monetary gain/loss of ES ($\Delta = P - IC$).

shows that the standard deviation of LMPs is larger in zone 8 than in zone 1, but the ES capacity placed in zone 1 is bigger than in zone 8 for $\Delta\lambda = 0$. Similar observations can be made for zones 4, 5, and 8 in cases with $\Delta\lambda = 0.1$ and $\Delta\lambda = 0.2$.

Figures 6.6B and 6.6C show that the regulating parameter $\Delta\lambda$ has a strong correlation with both ES profit and recovery of investment costs, and its effect depends on parameter χ . In the profit-constrained case ($\chi = 1$), increasing $\Delta\lambda$ allows for more intra-day variations in LMPs and, thus, the ES profit (Figure 6.6B) and the net monetary gain (Figure 6.6C) monotonically increases. However, increasing $\Delta\lambda$ would only lead to larger monetary losses in the profit-unconstrained case, i.e., $\chi = 0$ (Figure 6.6C).

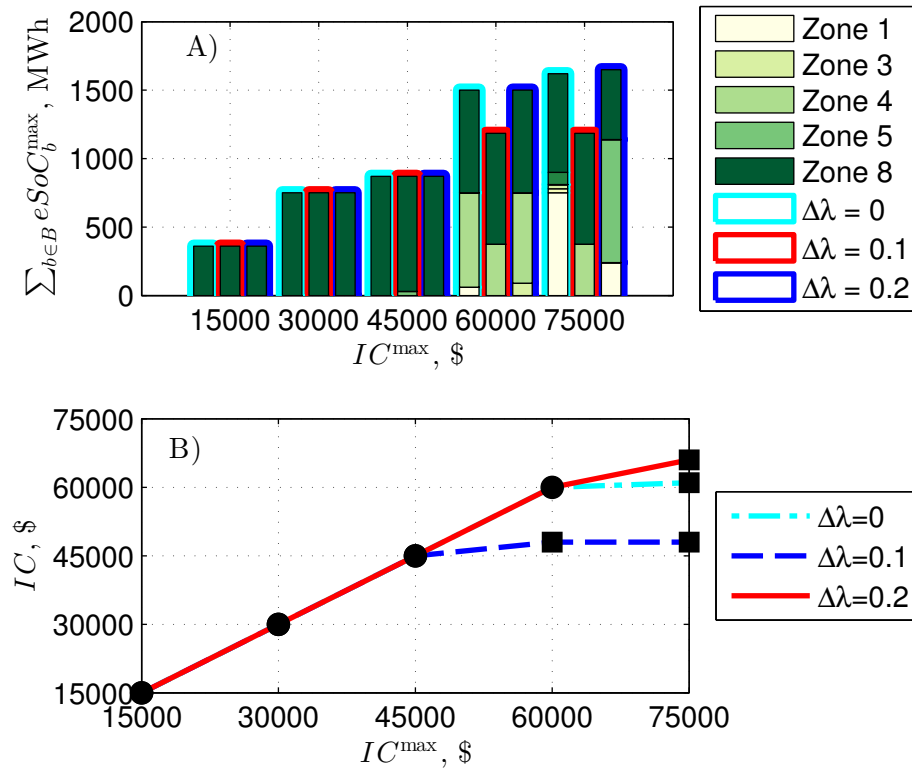


Figure 6.7: Effect of the budget constraint (6.3) under the low capital cost scenario on: A) The optimized ES siting and sizing decisions, B) the relationship between the investment cost and the investment budget. Black circles and squares indicate respectively the cases where the optimization is driven by the binding investment constraint (6.3) and the ES profit constraint (6.4).

Since profit-unconstrained decisions cannot be economically justified, the rest of this case study assumes $\chi = 1$ and examines the profit-constrained case.

6.5.2.2 Effect of the budget constraint

Figure 6.7A illustrates the effect of a finite investment budget on the optimized siting and sizing decisions. For tight investment budgets ($IC^{\max} \leq \$45000$), constraint (6.3) is binding; there is no diversity in ES allocation and energy ratings for different values of $\Delta\lambda$. ES are systematically placed in zone 8 (highest LMP variability, see Figure 6.3) for any value of $\Delta\lambda$. However, as the investment budget increases ($IC^{\max} \geq \$60000$), Figure 6.7A shows that ES are allocated to other

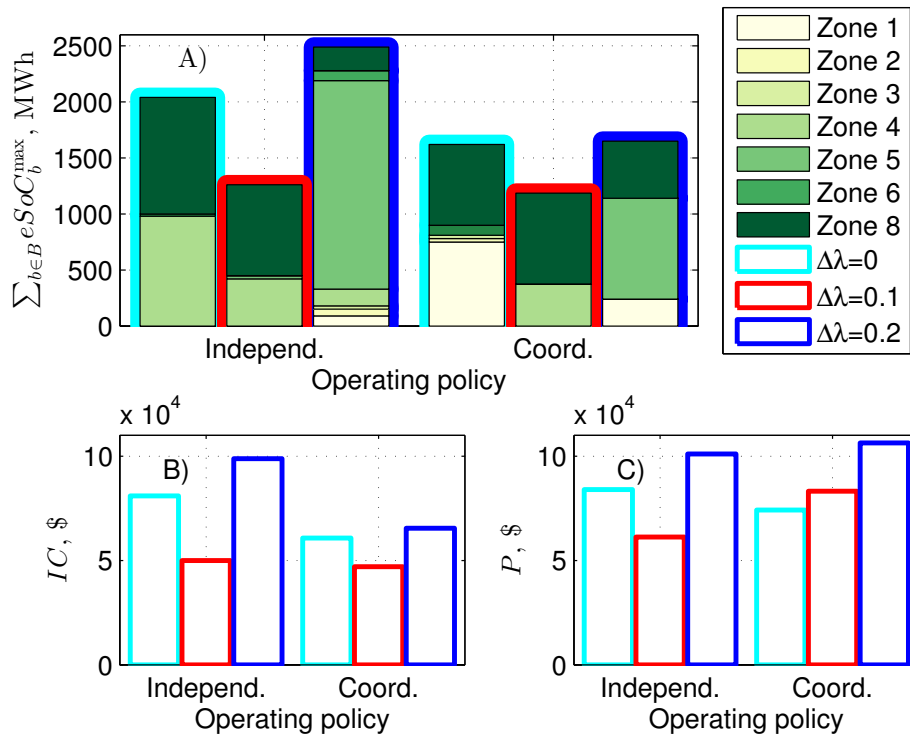


Figure 6.8: Effect of the operating policy under the low capital cost scenario on: A) ES siting and sizing decisions, B) investment cost of ES (IC), and C) profit of ES (P).

zones, resulting in larger total energy ratings. The relationship between the investment cost and the maximum investment budget is shown in Figure 6.7B, which distinguishes cases when the siting and sizing decisions are driven by either the investment budget or the ES profit constraints. When budget constraint (6.3) is nonbinding, the decisions are driven by the binding profit constraint (6.4). The large-scale ES deployment needed to accommodate a high penetration of renewable generation [54] requires large investments and would be driven by the profit constraint, thus showing the importance of the proposed planning method.

6.5.2.3 Effect of the operating policy

Profit constraint (6.4) sums the profits collected by ES in all zones, i.e., it assumes that ES in different zones are operated by the same entity in a *coordinated manner* [177]. In practice, ES located in different zones could be operated by *independent* entities. The independent operating policy can be modeled by replacing (6.4) with nodal ES profit constraints of the following form:

$$\sum_{e \in \Omega^E} \omega_e \cdot \sum_{t \in \Omega^T} \lambda_{e,t,s} \cdot (dis_{e,t,s} \cdot \aleph^{\text{dis}} - ch_{e,t,s} / \aleph^{\text{ch}}) \geq \chi \cdot IC, \quad \forall s \in \Omega^S. \quad (6.61)$$

Figure 6.8A illustrates the difference between ES siting and sizing decisions with the coordinated and independent operating policies. When compared to the independent policy, the coordinated policy consistently results in lower total ES ratings, and it, thus, requires lower investments (Figure 6.8B). On the other hand, despite the lower total ES ratings, the coordinated policy results in higher profits than the independent policy for $\Delta\lambda > 0$. Hence, an ES block installed under the coordinated policy is utilized more efficiently than under the independent policy (when ES deployment influences the LMPs) when compared to the case without ES.

6.5.2.4 Impact of the capital cost

If the capital cost increases, the ES are allocated at fewer zones and their total energy rating decreases (as shown in Figure 6.9) for the coordinated operating policy. Under the high capital cost scenario, ES are only placed at zone 8. Furthermore, there is a relatively small difference between the energy ratings for different values of $\Delta\lambda$. This observation suggests that, as long as the capital cost of ES remains prohibitively expensive, the ability of ES to influence LMPs is insignificant due to their relatively low penetration. However, provided the anticipated ES capital cost reduction,

accounting for impacts of ES on LMPs would be of greater value.

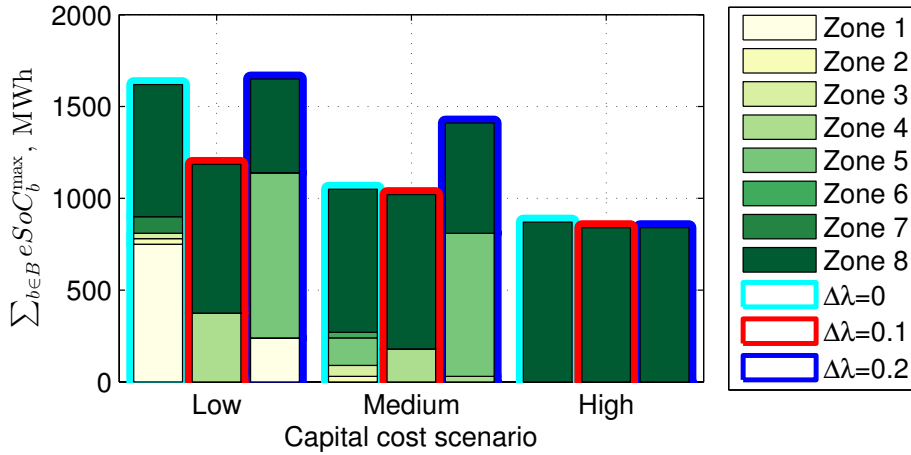


Figure 6.9: Effect of the capital cost on the profit-constrained ES siting and sizing decisions under the coordinated policy.

6.5.3 Evaluation of Costs and Profits

To assess the performance of the system with the various siting and sizing decisions made (as explained above), the UC problem is solved for each day of a given year. This assessment is based on the following metrics: Average daily operating costs for the SO (\overline{OC}^{SO}), average daily cost savings for the SO (\overline{CS}^{SO}) relative to the case without ES, average daily profit for the ES (\overline{P}^{ES}), and average daily wind spillage (\overline{WS}).

Table 6.3 presents the evaluation of the profit-constrained ES siting and sizing decisions made without budget limits and for the low capital cost scenario. It shows that the coordinated operating policy of ES leads to lower annual operating costs and the larger annual cost savings for the SO than the independent operating policy. Similarly, the coordinated operating policy results in larger ES profits. Both the ES and SO metrics are sensitive to the value of $\Delta\lambda$. As $\Delta\lambda$ increases, which translates into larger influence of ES on LMPs, the annual profit of the ES increases. This increase in ES profits comes at the expense of an increase in the annual operating cost and, thus, reduces the

annual cost savings for the SO. The coordinated operating policy reduces the annual wind spillage by a factor of two as compared to the independent operating policy. Notably, parameter $\Delta\lambda$ marginally affects the annual wind spillage for a given policy.

Table 6.4 presents the evaluation of the profit-constrained ES siting and sizing decisions made without budget limits with the coordinated operating policy under different capital cost scenarios. As in Table 6.3, all metrics are sensitive to $\Delta\lambda$. However, this sensitivity varies with capital costs. As the capital cost increases, the difference in cost savings between cases with $\Delta\lambda = 0$ and $\Delta\lambda = 0.2$ reduces. Similarly, the difference in ES profits between those cases non-monotonically decreases. Thus, the ES ability to influence LMPs would chiefly affect ES profit and SO savings when the ES capital cost is lower. If the capital cost is relatively high, the influence of ES on LMPs would have a moderate impact on these metrics. Also, as the capital cost decreases, more ES capacity is installed, which leads to lower annual wind spillage.

Table 6.3. ANNUAL ASSESSMENT OF THE ES SITING AND SIZING DECISIONS FOR DIFFERENT OPERATING POLICIES AND VALUES OF $\Delta\lambda$

Metric	Operating policy	$\Delta\lambda$		
		0	0.1	0.2
\overline{OC}^{SO} , M\$	Coordinated	2,439.7	2,449.8	2,455.0
	Independent	2,439.9	2,457.8	2,461.3
\overline{CS}^{SO} , M\$	Coordinated	104.8	94.6	89.2
	Independent	104.6	86.7	83.2
\overline{P}^{ES} , M\$	Coordinated	267.6	275.8	286.5
	Independent	234.1	239.1	247.2
\overline{WS} , MWh	Coordinated	51.5	52.1	52.7
	Independent	98.7	96.4	96.1

Table 6.4. ANNUAL ASSESSMENT OF THE ES SITING AND SIZING DECISIONS FOR DIFFERENT CAPITAL COSTS AND VALUES OF $\Delta\lambda$

Metric	Capital cost	$\Delta\lambda$		
		0	0.1	0.2
\overline{OC}^{SO} , M\$	Low	2,439.7	2,449.8	2,455.0
	Medium	2,480.4	2,486.4	2,488.9
	High	2,491.3	2,495.4	2,495.8
\overline{CS}^{SO} , M\$	Low	104.8	94.6	89.2
	Medium	64.1	58.1	55.6
	High	53.2	49.1	48.7
\overline{P}^{ES} , M\$	Low	267.6	275.8	286.5
	Medium	216.7	241.2	247.4
	High	209.3	216.2	216.2
\overline{WS} , MWh	Low	51.5	52.1	52.7
	Medium	64.7	70.5	79.2
	High	87.4	101.4	101.4

6.6 Conclusion

The proposed bilevel program for the optimally siting and sizing of ES accounts for the perspectives of both the SO and the owners of ES devices. The results indicate that optimal ES siting and sizing decisions are sensitive to the minimum profit constraint. This constraint represents a linear relationship between the short-term operational profit and long-term investment cost of merchant ES. If the profitability requirement is not accounted for (i.e. if the parameter χ is set to 0), ES owners would not be able to recover their investment costs, leading to economically nonviable siting and sizing decisions. The case study also reveals the sensitivity of the profit-constrained siting and sizing decisions to:

- Operating policy: Enabling coordinated ES operations at different buses increases ES profits and SO cost savings, as well as reduces wind spillage;

- Ability to influence LMPs: Merchant ES can extract additional profits by influencing LMPs, which comes at the expense of the system-wide operating costs;
- Capital cost: As the capital cost of ES remains prohibitively expensive, ES cannot take advantage of the coordinated operating strategy and influencing LMPs.

Part IV
CONCLUSIONS

Chapter 7

CONCLUSIONS

7.1 Conclusions

This dissertation has emphasized the importance of sustainable practices—a generic set of decision-making rules and methods that support the adoption of new technological means of reducing the usage of non-renewable resources and gas emissions, while providing universal access to energy at socially acceptable costs—for the optimal operation and expansion of real-life power systems in the presence of high penetration levels of renewable generation. It has been demonstrated that the transition to a sustainable power system can be achieved by revising existing operational policies and by strategic investments in ultra-flexible generation resources. These tasks require striking trade-offs between different performance metrics, such as cost and reliability, and can be dealt with by using the appropriate optimization techniques.

Specifically, this dissertation describes how explicit modeling of the uncertainty imposed by renewable generation requires intelligent risk-averse operation in the least-cost fashion. However, potential benefits that can be attained from revising the operational policies are finite. Therefore, this dissertation describes an approach to optimizing investments in ES devices to provide additional support for the integration of renewable generation.

In addition to the detailed conclusions given in each chapter, a number of generalizations can be drawn from this dissertation:

- Even though it is commonly accepted that deterministic reserve policies are less cost efficient and reliable than stochastic, robust, and interval equivalents, this dissertation has shown that a combination of non-deterministic UC techniques yields more cost savings and reliability

benefits than every non-deterministic technique taken individually. These benefits, whether in terms of cost or reliability, facilitate further integration of renewable generation at a lower cost and are achieved through the higher utilization of renewable generation by minimizing its spillage.

- In addition to the techno-economic assessment of different non-deterministic UC techniques, this dissertation has scrutinized their computational performance—an additional component to a traditional cost-reliability assessment. Numerical experiments have illustrated the importance of this component when choosing between different non-deterministic UC techniques. For example, numerical results reveal that some non-deterministic UC techniques have comparable cost and reliability performances, but their computing times vary by orders of magnitude. These results suggest that, in sustainable power systems, decision-making tools should also be ranked based on their feasibility for a specific application.
- Renewable generation (which has been traditionally considered as a negative load) can be an active producer that adjusts its production to minimize system-wide costs, thus alleviating the reliability implications of its stochastic nature. This dissertation has demonstrated that active renewable generation is capable of simultaneously providing flexibility and reducing system-wide flexibility requirements. Controlling injections of renewable generation can be used to re-enforce environmental benefits of emission-free renewable generation by reducing the unnecessary cycling of fossil-fired generators.
- Since power system expansion requires capital intensive investments, the ability to integrate new generation and transmission assets (e.g., energy storage) into existing power systems is in question due to their uncertain benefits. This dissertation has proposed and validated a general framework that can be adopted for assessing the economic viability and potential of any innovative technology in electricity markets. Case studies using this framework on a model

of an actual power system have demonstrated that accommodating for high penetration levels of renewable generation requires ES devices and that there are enough profit opportunities to ensure the long-term viability of these devices.

7.2 *Future Work*

7.2.1 *General modeling enhancements*

The modeling and experimental contributions of this dissertation warrant the further refinements of some modeling assumptions, even though these assumptions are customary to similar publications on short- and long-term planning problems and can further be extended should these revisions be computationally tractable. The following enhancements are suggested:

- **Improved network representation:** All of the models presented in this work rely on decoupled direct current (DC) power flows, thus simplifying the non-linear and, most importantly, non-convex physics of the underlying alternating current (AC) power flows. While this assumption is rather common for both short- and long-term planning problems, recent advances in modeling and solving computationally efficient models based on AC power flows can be used to improve the quality of solutions obtained with the proposed models. Incorporating AC constraints into the proposed models will enable accounting for reactive power flows and nodal voltages, which may lead to more accurate scheduling and dispatch decisions on conventional generators.

Modeling reactive power flows and nodal voltages and explicitly enforcing limits on these variables will also lay out a framework for assessing the technical and economic impacts that uncertain and variable renewable power generation will impose on the provision of ancillary reactive power and voltage control services. Currently, these impacts are neglected, but since renewable penetration levels are expected to grow, it will be important to ensure that the system has enough resources to be AC-feasible. Furthermore, these modeling enhancements

can be used to assess the monetary value that providers of ancillary reactive power and voltage control services have to the system and enable advanced market-based provision mechanisms for these services.

Modeling AC power flows may be unnecessary for long-term studies, but may be crucial for resource adequacy studies, especially given the limitations of some renewable generation technologies to provide reactive power and voltage control services.

- **System dynamics:** The models presented in this dissertation implicitly assume that the power system is in the steady state both pre- and post-disturbance. Although this assumption is sufficient for the analyses carried out in this dissertation, it unavoidably disregards that the system continuously evolves from one state to another, thus exhibiting a quasi-state behavior. Including AC power flow constraints, thus revealing reactive power and voltage variables (as explained above), will enable modeling of the system dynamics and accounting for the limitations of available control means to prevent emergencies (e.g. voltage collapse) and violating security margins during commutations (e.g. transmission switching and switching on/off generators). These modeling extensions will also enable considering dynamic power flow limits, in addition to thermal power flow limits, which can be of use in power systems spreading over wide areas.

Accounting for the system dynamics will require improved modeling of existing control means. Specifically, there is a need to model the non-linear P-Q characteristics of conventional generators, which are currently simplified to "box constraints" on active and reactive power outputs. The improved modeling of P-Q characteristics will also produce more realistic scheduling and dispatch decisions and enable better awareness of the feasibility boundaries.

- **Data-driven analytics:** The case studies presented in this dissertation parametrize uncertainty and variability of renewable generation using various statistical hypotheses enabled

by processing large archives of historical observations. The accuracy of these hypotheses can be improved if they also account for the physical processes driving atmospheric flows that essentially determine the output of wind and PV generation, thus enabling more accurate operational and planning decisions. This suggestion paves the way to the integration of NOAA-hosted mesoscale weather prediction models with the prediction tools used in power system applications.

Accounting for data-driven rather than statistical uncertainty and variability of renewables can be used to improve the accuracy of scheduling and dispatch decisions at sub-hourly resolutions, which are often hidden from existing decision-making tools.

7.2.2 Suggested Enhancements to Operational Planning

The UC models presented in Chapters 3-5 of this dissertation have demonstrated that both reliability and cost performance of power system operations could be improved if a combination of optimization frameworks is used. However, further modifications are needed to facilitate real-life implementations of these models:

- **Coordination with electricity markets:** The proposed UC models assume a vertically integrated power system, so future investigations are needed to implement these models within a market environment. This research should address the problem of minimizing the difference between market-based decisions (fundamentally driven by a time variable power supply and demand equilibrium) and reliability-based decision (enforced due to the physical and security limitations of power system operations). Specifically, this research will require an explicit co-optimization of the total operating costs and uplift and lost opportunity costs of generators that provide spare capacity for dealing with the uncertainty and variability of renewable generation.

- **Integration of different decision-making stages:** The proposed UC models are designed for a day-ahead planning framework and require further integration with hour-ahead planning tools to minimize the need for post-day-ahead corrective actions. This could be achieved if the modeling multi-stage recourse (hour-ahead) decisions were improved in the proposed models.
- **Improved modeling of ramping events:** In addition to adopting the data-driven analytics described in Section 7.2.1, the proposed UC models could benefit from a better modeling of ramping events. Even though the ramping scenarios proposed in Chapter 3 approximate stochastic scenarios to avoid modeling unnecessarily conservative ramping requirements, there is a need to relax these scenarios further. This relaxation can be attained by accounting for correlations between upward and downward ramping scenarios and by modeling sub-hourly dynamics.
- **Non-affine ramp policy of generators:** The proposed UC models assume that generators ramp up and down their power output according to a given affine policy with constant ramp up and down rates. This assumption could be further refined if more accurate (e.g. triangulation-based) policies are modeled, thus more accurately quantifying the flexibility available on the supply side.
- **Demand-side flexibility:** The proposed UC models consider electrical loads as being inelastic and uncontrollable. In reality, this is likely to change as more communication infrastructure is installed to harvest demand-side flexibility. Therefore, this flexibility must also be integrated with the proposed UC models and co-optimized with other generation resources.

7.2.3 *Suggested Enhancements to Storage Siting and Sizing*

The bilevel model presented in Chapter 6 for the siting and sizing of ES devices has been used to demonstrate that arbitrage opportunities in an actual power system with a large penetration of renewable generation provide enough profit to recover ES investment costs of independently owned ES devices fully. This model, however, can be further extended as follows:

- **Scalability:** While the proposed model is tested on a realistic model of the ISO-NE test system, the dimensions of the problem remain rather compact, and it can be solved using off-the-shelf optimization solvers. Should the proposed model be applied to a larger test system (e.g., WECC-240), the model is likely to become computationally intractable and, therefore, one may need to develop a decomposition technique to speed up the computations.
- **Investment model:** The proposed model assumes that the investment model is static, i.e., all investments are optimized for a target year. Further refinement should account for multiple decision-making stages, i.e., a dynamic investment model, with potentially mixed-integer resource decisions. Such optimization problems are extremely computationally challenging, and the implementation of this modeling enhancement depends on future advances in operation research and applied optimization methods.
- **Profitability:** The notion of profitability adopted in the proposed model is based on the expected profit. However, siting and sizing decisions can also be made more robust against additional risk metrics that would account for operational conditions probabilistically remote from the expected value, e.g., worst case scenarios. This can be achieved by means of considering conditional values at risk or robust optimization. However, besides the obvious extra computational complexity, these approaches are notorious for their conservatism; therefore, one needs to develop reliable heuristics to trade-off the expected value and worst case scenario.

- **Market design and profit adequacy:** This dissertation assumes that profits collected by energy storage in day-ahead electricity markets are calculated using a locational marginal pricing scheme. However, recently, it has been observed that, as more renewable generation resources are integrated into existing power systems, the locational marginal prices decrease, thus gradually eliminating arbitrage opportunities for ES devices and making it harder to recover their investment costs. This trend suggests that market designs should be changed in such a way that guarantees revenue adequacy for all market participants, including ES devices. Since the shape of these market designs is yet unknown and any potential changes are likely to be driven by political (rather than analytical) decisions, it is impossible to anticipate how it would affect the proposed model. However, one needs to take into account this ‘regulatory’ uncertainty.

A potential resolution of the ES storage profit adequacy problem could be found by exploring a trade-off between the profits of ES devices in the short-term (e.g., day- and hour-ahead) markets and long-term (e.g., capacity) markets. Since ES devices are not physical producers, an approach to quantify the ES device contributions to capacity markets is needed.

- **Multi-service ES operation:** In the proposed model, ES devices are assumed to provide spatiotemporal arbitrage services only. However, in practice, ES devices can provide other services (e.g., frequency and voltage support), regulation and load following services, as well as contingency mitigation. These services entitle ES owners to larger profits. Ideally, all available profit opportunities should be co-optimized to determine the optimal blend of services that would maximize ES profits and SO savings. This co-optimization is a particularly challenging task because ES devices are not physical producers; therefore, one needs to carefully coordinate the utilization of their energy and power capacities.

To explore the ability of ES devices to provide some services (e.g., voltage support) one may

first need to improve the network representation for long-term planning applications as is discussed in Section 7.2.1.

- **Competition:** The proposed model assumes that ES devices are the only generation technology that may affect market-clearing outcomes; other generation technologies follow an honest bidding/offering strategy. However, in practice, other generation technologies will also affect the market-clearing outcomes. In this environment, it will be important to assess the impact of energy storage siting and sizing on competition. This task will require converting the proposed model into an equilibrium program with equilibrium constraints (EPEC) and developing a computationally tractable solution technique.
- **Techno-economic assessment of different ES technologies:** The case studies in this dissertation assume generic battery ES devices with cost and technical parameters that fall within a broad range of various technologies. However, the proposed model can be tailored to better represent specific features of a particular technology (e.g., degradation characteristics, charging/discharging losses, and self-discharge) and assess the ability of that technology to provide specific services. This modeling improvement will enable techno-economic assessments of different ES technologies on the operational and market conditions of a given power system.

Part V

SUPPLEMENTARY MATERIALS

Appendix A
NOTATION

A.0.3.1 Sets

Ω^B	Set of piecewise linear segments of each generating unit's cost curve, indexed by b .
Ω^E	Set of typical days, indexed by e .
Ω^I	Set of generating units, indexed by i .
Ω^J	Set of generating units' start-up costs, indexed by j .
Ω^L	Set of transmission lines, indexed by l .
Ω^R	Set of uncertainty for the RUC, indexed by r .
Ω^S	Set of buses, indexed by s .
Ω^{S_I}	Set of buses that host generators, indexed by s .
Ω^{S_w}	Set of buses that host wind farms, indexed by s .
Ω^T	Set of hours, indexed by t . Note that $\Omega^T = \Omega^{T^{SUC}} \cup \Omega^{T^{IUC}}$.
$\Omega^{T^{SUC}}$	Set of hours solved by the SUC formulation.
$\Omega^{T^{IUC}}$	Set of hours solved by the IUC formulation.
Ω^Q	Set of ES blocks, indexed by q .

Ω^U	Set of scenarios, indexed by u .
Ω^X	Set of feasible dispatch solutions for fixed commitment decisions \mathbf{x} , such that $\mathbf{x} = \{x_{t,i}\}, \forall t \in \Omega^T, i \in \Omega^I$.
Ω^W	Set of wind farms, indexed by w .

A.0.3.2 Binary variables

$q_{t,i,j}$	Generator start-up cost identification matrix (1 if generator i is started up during hour t after being off for $\underline{T}_{i,j}$ to $\bar{T}_{i,j}$ hours, 0 otherwise).
$u_{s,q}$	Binary variable corresponding to the placement decision of ES block q at bus s .
$x_{e,t,i}$	Generator on/off status (1 if generator i is on during hour t , 0 otherwise). Index e is only used for storage siting and sizing.
$y_{e,t,i}$	Generator start-up status (1 if generator i is started up during hour t , 0 otherwise). Index e is only used for storage siting and sizing.
$z_{e,t,i}$	Generator shut down status (1 if generator i is shut down during hour t , 0 otherwise). Index e is only used for storage siting and sizing.

A.0.3.3 Continuous non-negative variables

CoU	Cost of Unhedged Uncertainty (\$).
$c_{t,w,u}$	Power curtailment of wind farm w under scenario u during hour t (MW).
$c_{e,t,s}$	Power curtailment of wind farm at bus s during hour t on representative day e (MW).

$ch_{e,t,s}$	ES charging rate at bus b during time interval t on representative day e , MW.
$dis_{e,t,s}$	ES discharging rate at bus b during time interval t on representative day e , MW.
$eSoC_{e,t,s}$	State-of-charge of ES at bus b at the end of time interval t on representative day e , MWh.
$eSoC_s^{\max}$	Maximum state-of-charge of the ES at bus s , MWh.
$g_{t,i,u}$	Power output of generator i under scenario u during hour t (MW).
$g_{e,t,i}$	Power output of generator i during hour t on representative day e (MW).
$g_{t,i,b,u}^{\text{seg}}$	Power output on segment b of generator i under scenario u during hour t (MW).
IC	Investment cost, \$.
OC_e^{PLL}	Objective function of the PLL problem on representative day e , \$.
OC_e^{DLL}	Objective function of the DLL problem on representative day e , \$.
p_s^{\max}	Maximum power rating of ES at bus s , MW.
$su_{t,i}$	Start-up cost of generator i during hour t (\$).
SC	Security cost (\$).
t^{sw}	Switching time between the SUC and IUC formulations (h).

A.0.3.4 Continuous variables

- $\theta_{t,s,u}$ Voltage angle at bus s under scenario u during hour t (rad).
- $\theta_{e,t,s}$ Voltage angle at bus s during hour t on representative day e (rad).
- $f_{e,t,l}$ Power flow in transmission line l during time interval t on representative day e , MW.

A.0.3.5 Dual Continuous Variables

Dual variables associated with the PLL problem constraints:

- $\underline{\alpha}_{e,t,i}, \bar{\alpha}_{e,t,i}$ Min/max power output of conventional generators, eq. (6.11).
- $\beta_{e,t,i}^{RD/RU}$ Ramp down/up limit of conventional generators, eq. (6.12).
- $\xi_{e,t,l}$ Power flow, eq. (6.13).
- $\underline{\delta}_{e,t,l}, \bar{\delta}_{e,t,l}$ Power flow limits, eq. (6.14).
- $\epsilon_{e,t,s}$ State-of-charge of ES, eq. (6.15).
- $\bar{\varphi}_{e,t,s}^{ch/dis}, \underline{\varphi}_{e,t,s}^{ch/dis}$ Charging/discharging limits of ES, eq. (6.16)–(6.17).
- $\bar{\varphi}_{e,t,s}^{eSoC}, \underline{\varphi}_{e,t,s}^{eSoC}$ State-of-charge limits of ES, eq. (6.18).
- $\lambda_{e,t,s}$ Nodal power balance, eq. (6.19).
- $\gamma_{e,t,s}$ Upper bound on the wind spillage, eq. (6.20).

A.0.3.6 Auxiliary variables

$a_{e,t,s,q}^1, a_{e,t,s,q}^{2, \text{ch/dis}}$ Auxiliary variables used for linearization of eq. (6.4).

$\underline{h}_{e,t,i}, \bar{h}_{e,t,i}$ Auxiliary variables used for linearization of eq. (6.30).

A.0.3.7 Parameters

A_i No-load cost of generator i (\$).

B_{sm} Admittance of line connecting nodes s and m (S).

$c^{e\text{SoC}}$ Capital cost of ES per MWh (\$/MWh).

c^p Capital cost of ES per MW (\$/MW).

CC Committed capacity (MW).

$D_{t,s}$ Load at bus s during hour t (MW).

DT_i Generator i minimum down time (h).

\bar{G}_i Maximum power output of generator i (MW).

\underline{G}_i Minimum power output of generator i (MW).

$G_{e,i}^0$ Initial power output of conventional generator i on representative day e (MW). Index e is only used for storage siting and sizing.

IC^{max} Investment budget, \$.

$K_{i,b}$ Slope of the b -th segment of the cost curve of generator i (\$/MW).

\bar{K}_i	One-segment incremental cost of generator i (\$/MW).
$\bar{L}_{e,i}$	Minimum up time of generator i (h). Index e is only used for storage siting and sizing.
$\underline{L}_{e,i}$	Minimum down time of generator i (h). Index e is only used for storage siting and sizing.
\bar{F}_l, \bar{F}_{sm}	Power flow limit of line l connecting nodes s and m (MW).
M	Sufficiently large positive number.
n_E	Number of representative days in set Ω^E .
n_I	Number of conventional generators in set Ω^I .
n_L	Number of transmission lines in set Ω^L .
n_S	Number of buses in set Ω^S .
n_T	Number of time intervals in set Ω^T .
n_Q	Number of ES blocks in set Ω^Q .
RD_i	Ramp down limit of generator i (MW/h).
RU_i	Ramp up limit of generator i (MW/h).
$SUC_{i,j}$	Cost of segment j of the stepwise start-up cost curve of generator i (\$).
$\bar{T}_{i,j}$	Upper limit of segment j of the stepwise start-up cost curve of generator i (h).

$\underline{T}_{i,j}$	Lower limit of segment j of the stepwise start-up cost of generator i curve (h).
$TSUC_i$	Total start-up cost of generator i from the cold-start state (\$).
u_s^{\max}	Maximum number of ES blocks that can be installed at bus s .
UT_i	Generator i minimum up time (h).
$W_{t,w,u}$	Available wind power at wind farm w under scenario u during hour t (MW).
$W_{e,t,s}$	Available wind power at bus s during hour t on representative day e (MW).
$VoLL$	Value of lost load, \$/MWh.
$VoWS$	Value of wind spillage, \$/MWh.
x_l	Reactance of transmission line l .
$X_{e,i}^0$	Initial commitment of conventional generator i on representative day e . Index e is only used for storage siting and sizing.
$\Delta eSoC$	Energy rating of the single ES block, MWh.
$\Delta\lambda$	Parameter modeling the deviation of the LMP from the no-ES case.
$\Delta\tau$	Duration of time interval t , h.
π_u	Probability of scenario u (used only in the SUC).
χ	Parameter relating the investment cost of ES and their expected profit.
ω_e	Weight of representative day e .

ρ Energy-to-power ratio of ES, h.

η^{ch} Charging efficiency of ES.

η^{dis} Discharging efficiency of ES.

Appendix B

MAP OF THE IEEE RELIABILITY TEST SYSTEM

Appendix C

AUTHOR'S VITA

Yury Dvorkin received the B.S.E.E. degree with the highest honors from Moscow Power Engineering Institute (Technical University), Moscow, Russia, in 2011. He is currently a Ph.D. candidate in electrical engineering at the Renewable Energy Analysis Laboratory (University of Washington, Seattle).

Previously, Yury was a graduate student researcher at Los Alamos National Laboratory's Center for Nonlinear Studies (2014). His research interests include short- and long-term planning in power systems with renewable generation, power system economics and policy. Yury is a recipient of the Clean Energy Institute's Graduate Fellowship (2013-2014) and the Clean Energy Institute's Student Training & Exploration Grant (2014-2015). In 2014 and 2015 Yury was recognized as the Outstanding Reviewer by both the IEEE Transactions on Power Systems and IEEE Transactions on Sustainable Energy.

Appendix D

AUTHOR'S BIBLIOGRAPHY*D.0.3.8 Selected Journal Publications*

1. **Y. Dvorkin**, R. Fernandez-Blanco, D. S. Kirschen, H. Pandzic, J.-P. Watson, and C. A. Silva Monroy, "Ensuring Profitability of Energy Storage," *IEEE Transactions on Power Systems*, early access, 2016..
2. T. Qiu, B. Xu, Y. Wang, **Y. Dvorkin**, and D. Kirschen, "Stochastic Multi-Stage Co-Planning of Transmission Expansion and Energy Storage," *IEEE Transactions on Power Systems*, early access, 2016.
3. **Y. Dvorkin**, M. Ortega-Vazquez, and R. Fernandez-Blanco, "Probabilistic Security-Constrained Unit Commitment with Generation and Transmission Contingencies," *IEEE Transactions on Power Systems*, early access, 2016. [**pdf**]
4. **Y. Dvorkin**, P. Henneaux, D. Kirschen, and H. Pandzic, "Optimizing Primary Response in Preventive Security-Constrained Optimal Power Flow," *IEEE Systems Journal*, early access 2016. [**pdf**]
5. M. Lubin, **Y. Dvorkin**, and S. Backhaus, "A Robust Approach to Chance Constrained Optimal Power Flow with Renewable Generation," *IEEE Transactions on Power Systems*, early access, 2016. [**pdf**]
6. M. Sarker, **Y. Dvorkin**, and M. Ortega-Vazquez, "Optimal Participation of an Electric Vehicle

- Aggregator in Energy and Reserve Markets,” *IEEE Transactions on Power Systems*, early access, 2016. [pdf]
7. **Y. Dvorkin**, M. Lubin, S. Backhaus, and M. Chertkov, “Uncertainty Sets for Wind Power Generation,” *IEEE Transactions on Power Systems*, early access, 2016. [pdf]
 8. K. Bruninx, **Y. Dvorkin**, E. Delarue, H. Pandzic, W. Dhaeseleer and D. S. Kirschen, “Coupling Pumped Hydro Energy Storages with Unit Commitment,” *IEEE Transactions on Sustainable Energy*, Vol. 7, No. 2, pp. 786 - 796, 2016. [pdf]
 9. H. Pandzic, **Y. Dvorkin**, Y. Wang, and D. S. Kirschen, “Toward Cost-Efficient and Reliable Unit Commitment under Uncertainty,” *IEEE Transactions on Power Systems*, Vol. 31, No. 2, pp. 970 - 982, 2016. [pdf]
 10. **Y. Dvorkin**, M. A. Ortega-Vazquez, and D. S. Kirschen, “Wind Generation As a Reserve Provider,” *IET on Generation, Transmission and Distribution*, Vol. 8, No. 9, pp. 779 - 787, 2015. [pdf]
 11. H. Pandzic, Y. Wang, T. Qiu, **Y. Dvorkin**, and D. S. Kirschen, “Near-Optimal Method for Siting and Sizing of Distributed Storage in a Transmission Network,” *IEEE Transactions on Power Systems*, early access, pp. 1-13, 2015. [pdf]
 12. **Y. Dvorkin**, H. Pandzic, M. A. Ortega-Vazquez, and D. S. Kirschen, “A Hybrid Stochastic/Interval Approach to Transmission-Constrained Unit Commitment with Uncertainty,” *IEEE Transactions on Power Systems*, Vol. 30, No. 2, pp. 621 - 631, 2015. [pdf]
 13. **Y. Dvorkin**, M. A. Ortega-Vazquez, D. S. Kirschen, “Assessing Flexibility Requirements in Power Systems,” *IET on Generation, Transmission and Distribution*, Vol. 8, No. 11, pp. 1820 - 1830, 2014. [pdf]

D.0.3.9 Selected Conference Publications

1. B. Xu, **Y. Dvorkin**, D. Kirschen, J-P. Watson, and C. Silva-Monroy, “A Comparison of Policies on the Participation of Storage in U.S. Frequency Regulation Markets,” accepted for publication in Proc. of the 2016 IEEE PES General Meeting, 2016.
2. M. Almassalkhi, **Y. Dvorkin**, J. Felder, R. Fernández-Blanco, I. Hiskens, D. Kirschen, J. Martin, H. Pandžić, Ting Qiu, M. Sarker, M. Vrakopoulou, Y. Wang, M. Xue, “Incorporating Storage as a Flexible Transmission Asset in Power System Operation Procedure,” accepted for publication in Proc. of the 19th Power Systems Computation Conference (PSCC 2016), 2016.
3. H. Pandzic, **Y. Dvorkin**, Y. Wang, and D. Kirschen, “Effect of Time Resolution on Unit Commitment Decisions in Systems with High Wind Penetration,” in Proc. of *2014 IEEE PES General Meeting*, Washington DC, 2014. [[pdf](#)] (*Best paper*)
4. **Y. Dvorkin**, H. Pandzic, Y. Wang, and D. Kirschen, “Comparison of Scenario Reduction Techniques for the Stochastic Unit Commitment,” in Proc. of *2014 IEEE PES General Meeting*, Washington DC, 2014. [[pdf](#)]
5. **Y. Dvorkin**, E. Pepin, G. Kychyakoff, and A. Mamishev, “Improved Efficiency of Energy-Intensive Processes through Control of Build-Up on Critical Heat-Transfer Surfaces,” Proc. of *American Council for an Energy-Efficient Economy Conference on Energy Efficiency in Industry*, Niagara Falls, NY, 2011. [[pdf](#)]

BIBLIOGRAPHY

- [1] P. G. Hill, *Power generation: resources, hazards, technology, and costs*. Cambridge, MA, USA: The MIT Press, 1977.
- [2] D. Bodansky, "Electricity Generation Choices for the Near Term," *Science*, Vol. 207 no. 4432 pp. 721-728, Feb. 1980.
- [3] V. Smil, "Renewable energies: how much and how renewable," *Bulletin of Atmospheric Sciences*, vol. 35, no. 10, pp. 12-19, December 1979.
- [4] J. E. J. Cottrill, "Economic assessment of the renewable energy sources," *Physical Science, Measurement and Instrumentation, Management and Education - Reviews, IEE Proceedings A*, vol. 127, pp. 279-288, 1980.
- [5] A. Verbruggen, "Renewable and nuclear power: A common future?," *Energy Policy*, vol. 36, pp. 4036-4047, Nov. 2008.
- [6] J. P. Holdren, G. Morris, and I. Mintzer, "Environmental Aspects of Renewable Energy Sources," *Annual Review of Energy*, vol. 5, pp. 241-291, 1980.
- [7] S. Silva, I. Soares, and O. Afonso, "Economic and environmental effects under resource scarcity and substitution between renewable and non-renewable resources," *Energy Policy*, Vol. 54, pp. 113-124, Mar. 2013.
- [8] F. C. Menz, "Green electricity policies in the United States: case study," *Energy Policy*, vol. 33, pp. 2398-2410, Dec. 2005.
- [9] P. Komor and M. Bazilian, "Renewable energy policy goals, programs, and technologies," *Energy Policy*, vol. 33, pp. 1873-1881, Sep. 2005.
- [10] Konrad Prandecki, "Theoretical Aspects of Sustainable Energy", *Energy and Environmental Engineering*, vol. 2, no. 4, pp. 83-90, 2014
- [11] R. Haas, C. Panzer, G. Resch, M. Ragwitz, G. Reece, and A. Held, "A historical review of promotion strategies for electricity from renewable energy sources in EU countries," *Renewable and Sustainable Energy Reviews*, vol. 15, pp. 1003-1034, Feb. 2011.
- [12] T. J. Foxon, R. Gross, A. Chase, J. Howes, A. Arnall, and D. Anderson, "UK innovation systems for new and renewable energy technologies: drivers, barriers and systems failures," *Energy Policy*, vol. 33, pp. 2123-2137, Nov. 2005.

- [13] R. Saidur, M. R. Islam, N. A. Rahim, and K. H. Solangi, "A review on global wind energy policy," *Renewable and Sustainable Energy Reviews*, vol. 14, pp. 1744-1762, Sep. 2010.
- [14] J. I. Lewis and R. H. Wiser, "Fostering a renewable energy technology industry: An international comparison of wind industry policy support mechanisms," *Energy Policy*, vol. 35, pp. 1844-1857, Mar. 2007.
- [15] R. H. Wiser and S. J. Pickle, "Financing investments in renewable energy : the impacts of policy design," *Renewable and Sustainable Energy Reviews*, vol. 2, pp. 361-386, Dec. 1998.
- [16] A. Aslani and K.-F. V. Wong, "Analysis of renewable energy development to power generation in the United States," *Renewable Energy*, vol. 63, pp. 153-161, Mar. 2014.
- [17] F. R. Pazheri, M. F. Othman, and N. H. Malik, "A review on global renewable electricity scenario," *Renewable and Sustainable Energy Reviews*, vol. 31, pp. 835-845, Mar. 2014.
- [18] A. J. Wood and B. F. Wollenberg, *Power Generation, Operation, and Control*. Hoboken, NJ, USA: Wiley, 1984.
- [19] ERCOT, *ERCOT Methodologies for Determining Ancillary Service Requirements*, 2010. [Online]. Available: <http://www.ercot.com/content/mktinfo/services/kd/2010%20Methodologies%20for%20Determining%20AS%20Requirements.pdf>
- [20] PJM, *Manual 12: Balancing Operations - PJM.com*, 2015. [Online]. Available at: <http://www.pjm.com/~media/documents/manuals/m12.ashx>
- [21] B. Pitt, "Applications of data mining techniques to electric load profiling", *Ph.D. thesis*, University of Manchester, UK, 2000. [Online]. Available at: http://www.ee.washington.edu/research/real/Library/Thesis/Barnaby_PITT.pdf
- [22] M. Moghavvemi and F. M. Omar, "Technique for contingency monitoring and voltage collapse prediction," *IEE Proceedings-Generation, Transmission and Distribution*, Vol. 145, pp. 634-640, 1998.
- [23] V. Terzija, G. Valverde, C. Deyu, P. Regulski, V. Madani, J. Fitch, et al., "Wide-Area Monitoring, Protection, and Control of Future Electric Power Networks," *Proceedings of the IEEE*, Vol. 99, pp. 80-93, 2011.
- [24] T. T. Warner, R. A. Peterson, and R. E. Treadon, "A Tutorial on Lateral Boundary Conditions as a Basic and Potentially Serious Limitation to Regional Numerical Weather Prediction," *Bulletin of the American Meteorological Society*, Vol. 78, pp. 2599-2617, 1997.

- [25] C. Monteiro, R. Bessa, V. Miranda, A. Botterud, J. Wang, and G. Conzelmann, "Wind Power Forecasting: State-of-the-Art 2009," Technical report. [Online]. Available: <http://www.ipd.anl.gov/anlpubs/2009/11/65613.pdf>, 2009.
- [26] M. Lange, "Analysis of the uncertainty of wind power predictions," *Ph.D. dissertation*, Fakultet Mathematik und Naturwissenschaften, Carl von Ossietzky Universitt, Oldenburg, Germany, 2003.
- [27] FERC Order No. 764. [Online]. Available at: www.ferc.gov/whatsnew/comm-meet/2012/062112/E-3.pdf
- [28] E. Ela and M. O'Malley, "Studying the Variability and Uncertainty Impacts of Variable Generation at Multiple Timescales," *IEEE Transactions on Power Systems*, vol. 27, no. 3, pp. 1324-1333, Aug. 2012.
- [29] Y. Dvorkin, D. S. Kirschen, and M. A. Ortega-Vazquez, "Assessing flexibility requirements in power systems," *IET on Generation, Transmission & Distribution*, Vol. 8, pp. 1820-1830, 2014.
- [30] Y. Dvorkin, M. Lubin, S. Backhaus, and M. Chertkov, "Uncertainty Sets for Wind Power Generation", *IEEE Trans. Power Syst.*, early access, 2015.
- [31] Y. V. Makarov, C. Loutan, M. Jian, and P. de Mello, "Operational Impacts of Wind Generation on California Power Systems," *IEEE Transactions on Power Systems*, vol. 24, no. 2, pp. 1039-1050, May 2009.
- [32] M. A. Ortega-Vazquez and D. S. Kirschen, "Estimating the Spinning Reserve Requirements in Systems With Significant Wind Power Generation Penetration," *IEEE Transactions on Power Systems*, Vol. 24, pp. 114-124, 2009.
- [33] M. A. Ortega-Vazquez and D. S. Kirschen, "Assessing the Impact of Wind Power Generation on Operating Costs," *IEEE Transactions Smart Grid*, Vol. 1, pp. 295-301, 2010.
- [34] N. Troy, E. Denny, and M. O'Malley, "Base-Load Cycling on a System With Significant Wind Penetration," *IEEE Transactions on Power Systems*, Vol. 25, pp. 1088-1097, 2010.
- [35] D. S. Kirschen, J. Ma, V. Silva, and R. Belhomme, "Optimizing the flexibility of a portfolio of generating plants to deal with wind generation," in *Proceedings of the 2011 IEEE Power and Energy Society General Meeting*, 2011, pp. 1-7.
- [36] J. Ma, V. Silva, R. Belhomme, D. S. Kirschen, and L. F. Ochoa, "Evaluating and Planning Flexibility in Sustainable Power Systems," *IEEE Transactions on Sustainable Energy*, Vol. 4, pp. 200-209, 2013.

- [37] M. Huber, D. Dimkova, and T. Hamacher, "Integration of wind and solar power in Europe: Assessment of flexibility requirements," *Energy*, Vol. 69, pp. 236-246, 2014.
- [38] N. Troy, D. Flynn, M. Milligan, and M. O'Malley, "Unit Commitment With Dynamic Cycling Costs," *IEEE Transactions on Power Systems*, Vol. 27, pp. 2196-2205, 2012.
- [39] E. Denny and M. O'Malley, "The impact of carbon prices on generation cycling costs," *Energy Policy*, vol. 37, no. 4, pp. 1204-1212, 2009.
- [40] D. Lew, G. Brinkman, N. Kumar, P. Besuner, D. Agan, and S. Lefton, "Impacts of Wind and Solar on Fossil-Fueled Generators," in *Proceedings of the 2012 IEEE Power and Energy Society General Meeting*, 2012, pp. 1-8.
- [41] K. Studarus and R. D. Christie, "A deterministic metric of stochastic operational flexibility," in *Proc. of 2013 IEEE Power and Energy Society General Meeting*, 2013, pp. 1-4.
- [42] R. Dominguez, A. J. Conejo, and M. Carrion, "Toward Fully Renewable Electric Energy Systems," *IEEE Transactions on Power Systems*, Vol. 30, pp. 316-326, 2015.
- [43] E. Y. Bitar, R. Rajagopal, P. P. Khargonekar, K. Poolla, and P. Varaiya, "Bringing Wind Energy to Market," *IEEE Transactions on Power Systems*, Vol. 27, pp. 1225-1235, 2012.
- [44] J. C. Ketterer, "The impact of wind power generation on the electricity price in Germany," *Energy Economics*, Vol. 44, pp. 270-280, 2014.
- [45] R. Baldick, "Wind and Energy Markets: A Case Study of Texas," *IEEE Systems Journal*, Vol. 6, pp. 27-34, 2012.
- [46] D. Lin, B. F. Hobbs, and P. Renson, "What is the Cost of Negative Bidding by Wind? A Unit Commitment Analysis of Cost and Emissions," *IEEE Transactions on Power Systems*, Vol. 30, pp. 1805-1814, 2015.
- [47] B. Dunn, H. Kamath, and J.-M. Tarascon, "Electrical energy storage for the grid: A battery of choices," *Science*, vol. 334, no. 6058, pp. 928-935, Nov. 2011.
- [48] H. Pandžić *et al.*, "Near-optimal method for siting and sizing of distributed storage in a transmission network," *IEEE Transactions on Power Systems*, vol. 30, no. 5, pp. 2288-2300, Sep. 2015.
- [49] D. Gayme and U. Topcu, "Optimal power flow with large-scale storage integration," *IEEE Transactions on Power Systems*, vol. 28, no. 2, pp. 709-717, May 2013.
- [50] Y. V. Makarov *et al.*, "Sizing energy storage to accommodate high penetration of variable energy resources," *IEEE Transactions on Sustainable Energy*, vol. 3, no. 1, pp. 34-40, Jan. 2012.

- [51] B. M. Grainger *et al.*, "Power Electronics for Grid-Scale Energy Storage," *Proc. of the IEEE*, Vol. 102, No. 6, pp. 1000-1013, 2014.
- [52] L. S. Vargas, G. Bustos-Turu, and F. Larrain, "Wind power curtailment and energy storage in transmission congestion management considering power plants ramp rates," *IEEE Trans. Power Syst.*, vol. 30, no. 5, pp. 2498–2506, Sep. 2015.
- [53] S. Zakaib, "The need for fast responding energy storage: benefits today and ensuring grid stability in the future," in *Proceedings of the IET Conference on Power in Unity: a Whole System Approach*, 2013, pp. 1-28.
- [54] A. A. Solomon, D. M. Kammen, and D. Callaway, "The role of large-scale energy storage design and dispatch in the power grid," *Applied Energy*, vol. 134, pp. 75–89, Dec. 2014.
- [55] CPUC Decision 13-10-040, "Order Instituting Rulemaking Pursuant to Assembly Bill 2514 to Consider the Adoption of Procurement Targets for Viable and Cost-Effective Energy Storage Systems". [Online]. Available at: https://www.sce.com/wps/wcm/connect/435ea164-60d5-433f-90bc-b76119ede661/R1012007_StorageOIR_D1310040_AdoptingEnergyStorageProcurementFrameworkandDesignProgram.pdf?MOD=AJPERES
- [56] M. C. W. Kintner-Meyer *et al.*, "Energy storage for power systems applications: A regional assessment for the Northwest Power Pool," Technical report, 2010. [Online]. Available at: http://www.pnl.gov/main/publications/external/technical_reports/PNNL-19300.pdf
- [57] "Advancing and maximizing the value of energy storage technology," Technical report, 2014. [Online]. Available at: <http://www.caiso.com/documents/advancing-maximizingvalueofenergystoragetechology-californiaroadmap.pdf>
- [58] FERC Order No. 792, "Small Generator Interconnection Agreements and Procedures". [Online]. Available at: <https://www.ferc.gov/whats-new/comm-meet/2013/112113/E-1.pdf>
- [59] S. Wogrin and D. F. Gayme, "Optimizing storage siting, sizing, and technology portfolios in transmission-constrained networks," *IEEE Transactions on Power Systems*, early access, pp. 1–10, Nov. 2015.
- [60] D. Pudjianto *et al.*, "Whole-systems assessment of the value of energy storage in low-carbon electricity systems," *IEEE Transactions on Smart Grid*, vol. 5, pp. 1098–1109, 2014.
- [61] C. Goebel, D. S. Callaway, and H. A. Jacobsen, "The Impact of State of Charge Management When Providing Regulation Power With Energy Storage," *IEEE Transactions on Power Systems*, Vol. 29, pp. 1433-1434, 2014.

- [62] CAISO, “Non-Generator Resource Regulation Energy Management Project,” *Implementation Plan*. [Online]. Available at: <http://www.caiso.com/Documents/Non-GeneratorResourceRegulationEnergyManagementImplementationPlan.pdf>, 2012.
- [63] H. Kissinger, *Diplomacy*. New York, NY, USA: Simon and Schuster, 2012.
- [64] Bryan Palmintier, “Incorporating operational flexibility into electric generation planning: impacts and methods for system design and policy analysis,” *Ph.D. thesis, Massachusetts Institute of Technology*, USA, 2013. [Online]. Available at: <http://dspace.mit.edu/handle/1721.1/79147>.
- [65] Pearl Donohoo, “Design of wide-area electric transmission networks under uncertainty: methods for dimensionality reduction,” *Ph.D. thesis, Massachusetts Institute of Technology*, USA, 2013. [Online]. Available at: <http://dspace.mit.edu/handle/1721.1/90160>.
- [66] A. J. Ardakani and F. Bouffard, “Acceleration of Umbrella Constraint Discovery in Generation Scheduling Problems,” *IEEE Transactions on Power Systems*, Vol. PP, pp. 1-10, 2014.
- [67] A. J. Ardakani and F. Bouffard, “Identification of Umbrella Constraints in DC-Based Security-Constrained Optimal Power Flow,” *IEEE Transactions on Power Systems*, Vol. 28, pp. 3924-3934, 2013.
- [68] G. Box and N. Draper, *Empirical Model Building and Response Surfaces*, John Wiley & Sons, New York, NY, 1987.
- [69] B.-M. Hodge, A. Florita, J. Sharp, M. Margulis and D. McCreavy, “The Value of Improved Short-Term Wind Power Forecasting,” Technical Report. [Online]. Available at: <http://www.nrel.gov/docs/fy15osti/63175.pdf>, 2015.
- [70] A. Greenhaul, “Wind Scenarios for Stochastic Energy Scheduling,” *Ph.D. thesis, University of Washington*, UK, 2000. [Online]. Available at: https://digital.lib.washington.edu/researchworks/bitstream/handle/1773/23516/Greenhall_washington_0250E_11735.pdf?sequence=1
- [71] A. I. Negash, A. Hooshmand, and R. Sharma, “A wavelet-based method for high resolution multi-step PV generation forecasting,” the Proc. of the *2014 IEEE PES T&D Conference and Exposition*, 2014, pp. 1-5.
- [72] S. Sperati, S. Alessandrini, P. Pinson, and G. Kariniotakis, “The “Weather Intelligence for Renewable Energies” Benchmarking Exercise on Short-Term Forecasting of Wind and Solar Power Generation,” *Energies*, Vol. 8, 2015.

- [73] Rapid Refresh (RAP). [Online]. Available at: <http://rapidrefresh.noaa.gov/>, 2015.
- [74] P. Pinson, C. Chevallier, and G. N. Kariniotakis, "Trading Wind Generation From Short-Term Probabilistic Forecasts of Wind Power," *IEEE Transactions on Power Systems*, Vol. 22, pp. 1148-1156, 2007.
- [75] T. Gneiting, F. Balabdaoui, and A. E. Raftery, "Probabilistic forecasts, calibration and sharpness," *Journal of the Royal Statistical Society: Series B (Statistical Methodology)*, Vol. 69, pp. 243-268, 2007.
- [76] P. Pinson, J. Juban, and G. N. Kariniotakis, "On the Quality and Value of Probabilistic Forecasts of Wind Generation," in Proc. of the *International Conference on Probabilistic Methods Applied to Power Systems*, 2006.
- [77] P. Pinson, H. Madsen, H. A. Nielsen, G. Papaefthymiou, and B. Klckl, "From probabilistic forecasts to statistical scenarios of short-term wind power production," *Wind Energy*, Vol. 12, pp. 51-62, 2009.
- [78] J. Tastu, P. Pinson, E. Kotwa, H. Madsen, H. Nielsen, "Spatio-temporal analysis and modeling of wind power forecast errors," *Wind Energy*, Vol. 14, No. 1, 2011, pp. 4360.
- [79] E. M. Constantinescu, V. M. Zavala, M. Rocklin, L. Sangmin, and M. Anitescu, "A Computational Framework for Uncertainty Quantification and Stochastic Optimization in Unit Commitment With Wind Power Generation," *IEEE Transactions on Power Systems*, Vol. 26, pp. 431-441, 2011.
- [80] H. Pandzic, Y. Dvorkin, T. Qiu, Y. Wang, and D. S. Kirschen, "Toward Cost-Efficient and Reliable Unit Commitment Under Uncertainty," *IEEE Transactions on Power Systems*, early access, pp. 1-13, 2015.
- [81] Y. Dvorkin, H. Pandzic, M. A. Ortega-Vazquez, and D. S. Kirschen, "A Hybrid Stochastic/Interval Approach to Transmission-Constrained Unit Commitment," *IEEE Transactions on Power Systems*, Vol. 30 No. 2, 2014.
- [82] H. Pandzic, Y. Dvorkin, Y. Wang, T. Qiu, and D. S. Kirschen, "Effect of Time Resolution on Unit Commitment Decisions in Systems with High Wind Penetration," in Proc. of the 2014 IEEE PES General Meeting — Conference & Exposition, pp. 1-5, 2014.
- [83] Y. Dvorkin, W. Yishen, H. Pandzic, and D. S. Kirschen, "Comparison of scenario reduction techniques for the stochastic unit commitment," in Proc. of the 2014 IEEE PES General Meeting — Conference & Exposition, pp. 1-5, 2014.
- [84] Y. Dvorkin, M. A. Ortega-Vazquez, and D. S. Kirschen, "Wind generation as a reserve provider," *IET on Generation, Transmission & Distribution*, Vol. 9, pp. 779-787, 2015.

- [85] H. Pandzic, Y. Wang, T. Qiu, Y. Dvorkin, and D. S. Kirschen, "Near-Optimal Method for Siting and Sizing of Distributed Storage in a Transmission Network," *IEEE Transactions on Power Systems*, early access, pp. 1-13, 2015.
- [86] Y. Dvorkin, R. Fernandez-Blanco, D. S. Kirschen, H. Pandzic, J.-P. Watson, C. A. Silva Monroy, "Ensuring Profitability of Energy Storage," submitted to *IEEE Transactions on Power Systems*, 2015.
- [87] E. Ela and B. Kirby, "ERCOT Event on February 26, 2008: Lessons Learned", 2008, [Online]. Available at: <http://www.nrel.gov/docs/fy08osti/43373.pdf>
- [88] PJM, "PJM Manual 11: Energy & Ancillary Services Market Operations". [Online]. Available at: <http://www.pjm.com/~media/documents/manuals/m11.ashx>, 2015.
- [89] ISO New England, "ISO New England Manual for Market Operations". [Online]. Available at: http://www.iso-ne.com/static-assets/documents/2015/05/m_11_market_operations_revision_49_05_27_15.doc
- [90] CAISO, "Business Practice Manual for Market Operations". [Online]. Available: http://bpmcm.caiso.com/BPM%20Document%20Library/Market%20Operations/BPM_for_Market%20Operations_V44_redline.pdf
- [91] ERCOT, "Day-Ahead Market Operating Procedure Manual". [Online]. Available: <http://www.ercot.com/content/mktrules/bpm/1430343354410.doc>
- [92] A. J. Conejo, M. Carrion, and J. M. Morales. *Decision making under uncertainty in electricity markets*. Springer, 2010.
- [93] B. Stott and E. Hobson, "Power System Security Control Calculations Using Linear Programming, Part I," *IEEE Transactions on Power Apparatus and Systems*, Vol. PAS-97, pp. 1713-1720, 1978.
- [94] B. Stott and E. Hobson, "Power System Security Control Calculations Using Linear Programming, Part II," *IEEE Transactions on Power Apparatus and Systems*, Vol. PAS-97, pp. 1721-1731, 1978.
- [95] John A. Muckstadt and Sherri A. Koenig, "An Application of Lagrangian Relaxation to Scheduling in Power-Generation Systems," *Operations Research*, Vol. 25, No. 3, pp. 387 - 403, 1977.
- [96] J. Carpentier, "Optimal power flows," *International Journal of Electrical Power & Energy Systems*, Vol. 1, pp. 3-15, 1979.

- [97] S.J. Wang, M. Shahidehpour, D.S. Kirschen, S. Mokhtari, and G.D. Irisarri, "Short-term generation scheduling with transmission and environmental constraints using an augmented Lagrangian relaxation," *IEEE Transactions on Power Systems*, Vol. 10, No. 3, pp. 1294-1301, 1995
- [98] X. Guan, Q. Zhai, A. Papalexopoulos, "Optimization based methods for unit commitment: Lagrangian relaxation versus general mixed integer programming," in the 2003 IEEE Power Engineering Society General Meeting, 2003, pp. 13-17 July, 2003.
- [99] A. J. Wood and B. F. Wollenberg, *Power generation, operation, and control*, Wiley, 1984.
- [100] Y. G. Rebours, D. S. Kirschen, M. Trotignon, and S. Rossignol, "A Survey of Frequency and Voltage Control Ancillary Services. Part I: Technical Features," *IEEE Trans. Power Syst.*, vol. 22, no. 1, pp. 350-357, Feb. 2007.
- [101] Y. G. Rebours, D. S. Kirschen, M. Trotignon, and S. Rossignol, "A Survey of Frequency and Voltage Control Ancillary Services. Part II: Economic Features," *IEEE Trans. Power Syst.*, vol. 22, no. 1, pp. 358-366, Feb. 2007.
- [102] *ERCOT Methodologies for Determining Ancillary Service Requirements*, 2012. [Online] Available at: www.ercot.com/meetings/wms/keydocs/2004/0819/WMS08192004-3.doc
- [103] R. Piwko, K. Clark, L. Freeman, G. Jordan, and N. Miller, "Western wind and solar integration study," 2010.
- [104] ISO New England, "Operating Procedure No. 8 Operating Reserve and Regulation", [Online]. Available at: http://www.iso-ne.com/rules_proceeds/operating/isone/op8/op8_rto_final.pdf
- [105] F. Bouffard, F. D. Galiana, and A. J. Conejo, "Market-clearing with stochastic security-part I: formulation," *IEEE Trans. Power Syst.*, vol. 20, no. 4, pp. 1818-1826, Nov. 2005.
- [106] F. Bouffard, F. D. Galiana, and A. J. Conejo, "Market-clearing with stochastic security-part II: case studies," *IEEE Trans. Power Syst.*, vol. 20, no. 4, pp. 1827-1835, Nov. 2005.
- [107] S. Takriti, J. R. Birge, and E. Long, "A stochastic model for the unit commitment problem," *IEEE Trans. Power Syst.*, vol. 11, no.3, pp. 1497-1508, Aug. 1996.
- [108] P. Carpentier, G. Gohen, J. C. Culioli, and A. Renaud, "Stochastic optimization of unit commitment: a new decomposition framework," *IEEE Trans. Power Syst.*, vol. 11, no. 2, pp. 1067-1073, May 1996.
- [109] J. Wang, M. Shahidehpour, and Z. Li, "Security-Constrained Unit Commitment With Volatile Wind Power Generation," *IEEE Trans. Power Syst.*, vol. 23, no.3 pp. 1319-1327, Aug. 2008.

- [110] L. Wu and M. Shahidehpour, "Accelerating the Benders decomposition for network-constrained unit commitment problems," *Energy Systems*, vol. 1, no. 3, pp. 339-376, 2010.
- [111] J. M. Morales, R. Minguez, and A. J. Conejo, "A methodology to generate statistically dependent wind speed scenarios," *Appl. Energy*, vol. 87, no. 3, pp. 843-855, March 2010.
- [112] L. Wu, M. Shahidehpour, and T. Li, "Stochastic Security-Constrained Unit Commitment," *IEEE Trans. Power Syst.*, vol. 22, no. 2, pp. 800-811, May 2007.
- [113] A. Papavasiliou, S. S. Oren, and B. Rountree, "Applying High Performance Computing to Transmission-Constrained Stochastic Unit Commitment for Renewable Energy Integration," *IEEE Transactions on Power Systems*, Vol. PP, pp. 1-12, 2015.
- [114] J. Dupačová, N. Gröwe-Kuska, and W. Römisch, "Scenario reduction in stochastic programming," *Math. Program.*, vol. 95, pp. 493-511, Feb. 2003.
- [115] H. Heitsch and W. Römisch, "Scenario Reduction Algorithms in Stochastic Programming," *Comput. Optim. Appl.*, vol. 24, no. 2-3, pp. 187-206, Feb. 2003.
- [116] J. M. Morales, S. Pineda, A. J. Conejo, and M. Carrion, "Scenario Reduction for Futures Market Trading in Electricity Markets," *IEEE Trans. Power Syst.*, vol. 24, no. 2, pp. 878-888, May 2009.
- [117] L. Wu, M. Shahidehpour, and Z. Li, "Comparison of Scenario-Based and Interval Optimization Approaches to Stochastic SCUC," *IEEE Trans. Power Syst.*, vol. 27, no. 2, pp. 913-921, May 2012.
- [118] D. Arthur and S. Vassilvitskii, "K-means++: the advantages of careful seeding," in *Proc. of 18th Annual ACM-SIAM Symposium on Discrete Algorithms*, pp. 1027-1035, New Orleans, Louisiana, 2007.
- [119] J. Dupacova, N. Growe-Kuska, and W. Romisch, "Scenario reduction in stochastic programming: An approach using probability metrics," *Math. Program.*, Vol. 95, pp. 493-511, 2003.
- [120] H. Heitsch and W. Romisch, "Scenario Reduction Algorithms in Stochastic Programming," *Comput. Optim. Appl.*, Vol. 24, No. 2-3, pp. 187-206, 2003.
- [121] J. M. Morales, S. Pineda, A. J. Conejo, M. Carrion, "Scenario Reduction for Futures Market Trading in Electricity Markets," *IEEE Trans. Power Syst.*, Vol. 24, No. 2, pp. 878-888, 2009.
- [122] A. Papavasiliou and S. S. Oren, "Multiarea Stochastic Unit Commitment for High Wind Penetration in a Transmission Constrained Network," *Operations Research*, Vol. 61, No. 3, pp. 578-592, 2013.

- [123] Y. Dvorkin, Y. Wang, H. Pandžić, and D. S. Kirschen, "Comparison of Scenario Reduction Techniques for the Stochastic Unit Commitment," in *Proc. of IEEE PES General Meeting 2014*, pp. 1-5, July 2014.
- [124] A. Papavasiliou, S. S. Oren, and B. Rountree, "Applying High Performance Computing to Transmission-Constrained Stochastic Unit Commitment for Renewable Energy Integration," *IEEE Transactions on Power Systems*, Vol. PP, pp. 1-12, 2015.
- [125] L. Wu, M. Shahidehpour, and Z. Li, "Comparison of Scenario-Based and Interval Optimization Approaches to Stochastic SCUC," *IEEE Trans. Power Syst.*, vol. 27, no. 2, pp. 913-921, May 2012.
- [126] Y. Wang, Q. Xia, and C. Kang, "Unit Commitment With Volatile Node Injections by Using Interval Optimization," *IEEE Trans. Power Syst.*, Vol. 26, No. 3, pp. 1705-1713, 2011.
- [127] J. W. Chinneck and K. Ramadan, "Linear Programming with Interval Coefficients," *JORS*, Vol. 51, No. 2, pp. 209-220, 2000.
- [128] P. B. Luh, Y. Yaowen, Z. Bingjie, E. Litvinov, Z. Tongxin, Z. Feng, et al., "Grid Integration of Intermittent Wind Generation: A Markovian Approach," *IEEE Transactions on Smart Grid*, Vol. 5, pp. 732-741, 2014.
- [129] Y. Yu, P. B. Luh, E. Litvinov, T. Zheng, J. Zhao, and F. Zhao, "Grid Integration of Distributed Wind Generation: Hybrid Markovian and Interval Unit Commitment," *IEEE Transactions on Smart Grid*, early access, 2015.
- [130] D. Bertsimas, E. Litvinov, X. A. Sun, Z. Jinye, and Z. Tongxin, "Adaptive Robust Optimization for the Security Constrained Unit Commitment Problem," *IEEE Transactions on Power Systems*, Vol. 28, pp. 52-63, 2013.
- [131] A. Lorca and X. A. Sun, "Adaptive Robust Optimization With Dynamic Uncertainty Sets for Multi-Period Economic Dispatch Under Significant Wind," *IEEE Trans. Power Syst.*, Vol. PP, No. 99, pp. 1-12, 2014.
- [132] R. Jiang, M. Zhang, G. Li, and Y. Guan, "Two-stage network constrained robust unit commitment problem," *Eur. J. Oper. Res.*, vol. 234, no. 3, pp. 751-762, May 2014.
- [133] R. Jiang, J. Wang, M. Zhang, and Y. Guan, "Two-Stage Minimax Regret Robust Unit Commitment," *IEEE Trans. Power Syst.*, vol. 28, no. 3, pp. 2271-2282, Aug. 2013.
- [134] R. Jiang, J. Wang, and Y. Guan, "Robust Unit Commitment With Wind Power and Pumped Storage Hydro," *IEEE Trans. Power Syst.*, vol. 27, no. 2, pp. 800-810, May 2012.

- [135] B. Zheng and L. Zhao, "Robust unit commitment problem with demand response and wind energy," in *Proc. IEEE PES General Meeting 2012*, San Diego, USA, July 2012, pp. 1-8.
- [136] B. Zeng and L. Zhao, "Solving two-stage robust optimization problems using a column-and-constraint generation method," *Operations Research Letters*, Vol. 41, No. 5, pp. 457-461, 2013.
- [137] J. Lavaei and S. H. Low, "Zero Duality Gap in Optimal Power Flow Problem," *IEEE Transactions on Power Systems*, Vol. 27, pp. 92-107, 2012.
- [138] Q. Wang, Y. Guan, and J. Wang, "A Chance-Constrained Two-Stage Stochastic Program for Unit Commitment With Uncertain Wind Power Output," *IEEE Transactions on Power Systems*, Vol. 27, pp. 206-215, 2012.
- [139] D. Bienstock, M. Chertkov, and S. Harnett, "Chance-Constrained Optimal Power Flow: Risk-Aware Network Control under Uncertainty," *SIAM Review*, Vol. 56, pp. 461-495, 2014.
- [140] M. Lubin, Y. Dvorkin, and S. Backhaus, "A Robust Approach to Chance Constrained Optimal Power Flow with Renewable Generation," submitted to *IEEE Transactions on Power Systems*, 2015, [Online]. Available at: <http://arxiv.org/abs/1504.06011>.
- [141] O. Leitmann and J. L. Kirtley, "Energy storage for use in load frequency control," in *Proc. of the 2010 IEEE Conference on Innovative Technologies for an Efficient and Reliable Electricity Supply (CITRES)*, 2010, pp. 292-296.
- [142] Sandia National Laboratory, "Energy Storage". [Online]. Available at: http://www.sandia.gov/ess/tech_batteries.html, 2015.
- [143] Energy Storage Association, "Energy Storage Technology". [Online]. Available at: <http://energystorage.org/energy-storage/energy-storage-technologies>, 2015.
- [144] D.O. Akinyele and R.K. Rayudu, "Review of energy storage technologies for sustainable power networks", *Sustainable Energy Technologies and Assessments*, Vol. 8, 2014, pp. 74-91.
- [145] A. Castillo and D. F. Gayme, "Grid-scale energy storage applications in renewable energy integration: A survey", *Energy Conversion and Management*, Vol. 87, 2014, pp. 885-894.
- [146] M. A. Ortega-Vazquez, "Optimal scheduling of electric vehicle charging and vehicle-to-grid services at household level including battery degradation and price uncertainty," *IET on Generation, Transmission & Distribution*, Vol. 8, pp. 1007-1016, 2014.

- [147] J. T. Pieronek, D. Decker, A.K. Spector, "Spacecraft flywheel systems benefits and issues," in Proc. of the *IEEE National Aerospace and Electronics Conference*, Dayton, USA, 1997, pp. 589-593.
- [148] H. Liu and J. Jiang, "Flywheel energy storage An upswing technology for energy sustainability", *Energy and Buildings*, Vol. 39, No. 5, 2007, pp. 599-604.
- [149] Atul Sharma, V.V. Tyagi, C.R. Chen, D. Buddhi, "Review on thermal energy storage with phase change materials and applications" *Renewable and Sustainable Energy Reviews*, Vol. 13, No. 2, 2009, pp. 318-345.
- [150] S. Shoenung, "Energy Storage Systems Cost Update," *Technical report*. [Online]. Available at: <http://prod.sandia.gov/techlib/access-control.cgi/2011/112730.pdf>, 2011.
- [151] J. Eyer and G. Corey, "Energy Storage for the Electricity Grid: Benefits and Market Potential Assessment Guide," *Technical report*. [Online]. Available at: http://www.storagealliance.org/sites/default/files/whystorage/Sandia_Energy_Storage_Guide.pdf, 2010.
- [152] J. A. Taylor, S. V. Dhople, and D. S. Callaway, "Power Systems Without Fuel". [Online]. Available at: <http://arxiv.org/abs/1506.04799>, 2015.
- [153] S. M. Ryan, J. D. McCalley, and D. L. Woodruff, "Long Term Resource Planning for Electric Power Systems Under Uncertainty". [Online]. Available at: http://works.bepress.com/cgi/viewcontent.cgi?article=1027&context=sarah_m_ryan, 2011.
- [154] Yang Gu, "Long-term power system capacity expansion planning considering reliability and economic criteria," *Ph.D. thesis, Iowa State University, USA*, 2011. [Online]. Available at: <http://lib.dr.iastate.edu/cgi/viewcontent.cgi?article=1125&context=etd>.
- [155] Yanyi He, "Analysis of investment decision making in power systems under environmental regulations and uncertainties," *Ph.D. thesis, Iowa State University, USA*, 2013. [Online]. Available at: <http://lib.dr.iastate.edu/cgi/viewcontent.cgi?article=4554&context=etd>.
- [156] Conrado Borraz-Sanchez, Russell Bent, Scott Backhaus, Hassan Hijazi, and Pascal Van Hentenryck, "Convex Relaxations for Gas Expansion Planning," Submitted to *INFORMS Journal on Computing*, 2015. [Online]. Available at: <http://arxiv.org/pdf/1506.07214v1.pdf>.
- [157] S. Misra; M.W. Fisher; S. Backhaus; R. Bent; M. Chertkov; F. Pan, "Optimal Compression in Natural Gas Networks: A Geometric Programming Approach," *IEEE Transactions on Control of Network Systems*, vol.2, no.1, pp. 47-56, March 2015.

- [158] S. Rinaldi, J. Peerenboom, and T. Kelly, "Identifying, Understanding, and Analyzing Critical Infrastructure Interdependencies," *IEEE Control Systems Magazine*, vol.21, no.6, pp. 11-25, Dec 2001.
- [159] M. A. Ortega-Vazquez, F. Bouffard, and V. Silva, "Electric Vehicle Aggregator/System Operator Coordination for Charging Scheduling and Services Procurement," *IEEE Transactions on Power Systems*, Vol. 28, pp. 1806-1815, 2013.
- [160] Y. Feng and S. M. Ryan, "Scenario construction and reduction applied to stochastic power generation expansion planning", *Computers & Operations Research*, Vol. 40, No. 1, pp. 9-23, 2013.
- [161] S. Jin, S.M. Ryan, J.P. Watson, and D.L. Woodruff, "Modeling and solving a large-scale generation expansion planning problem under uncertainty", *Energy Systems*, Vol. 2, No. 3, pp. 209242, 2011.
- [162] B. F. Hobbs, "Optimization methods for electric utility resource planning," *European Journal of Operational Research*, Vol. 83, pp. 1-20, 1995.
- [163] C. Ruiz and A. J. Conejo, "Robust transmission expansion planning," *European Journal of Operational Research*, Vol. 242, pp. 390-401, 2015.
- [164] Garce, x, L. P. s, A. J. Conejo, R. Garcia-Bertrand, and R. Romero, "A Bilevel Approach to Transmission Expansion Planning Within a Market Environment," *IEEE Transactions on Power Systems*, Vol. 24, pp. 1513-1522, 2009.
- [165] S. Wogrin, E. Centeno, and J. Barquin, "Generation Capacity Expansion in Liberalized Electricity Markets: A Stochastic MPEC Approach," *IEEE Transactions on Power Systems*, Vol. 26, pp. 2526-2532, 2011.
- [166] S. J. Kazempour, A. J. Conejo, and C. Ruiz, "Strategic Generation Investment Using a Complementarity Approach," *IEEE Transactions on Power Systems*, Vol. 26, pp. 940-948, 2011.
- [167] L. Baringo and A. J. Conejo, "Wind power investment within a market environment," *Applied Energy*, Vol. 88, pp. 3239-3247, 2011.
- [168] S. de la Torre, A. J. Conejo, and J. Contreras, "Transmission Expansion Planning in Electricity Markets," *IEEE Transactions on Power Systems*, Vol. 23, pp. 238-248, 2008.
- [169] J. Shan and S. M. Ryan, "Capacity Expansion in the Integrated Supply Network for an Electricity Market," *IEEE Transactions on Power Systems*, Vol. 26, pp. 2275-2284, 2011.
- [170] S. J. Kazempour and A. J. Conejo, "Strategic Generation Investment Under Uncertainty Via Benders Decomposition," *IEEE Transactions on Power Systems*, Vol. 27, pp. 424-432, 2012.

- [171] A. Motamedi, H. Zareipour, M. O. Buygi, and W. D. Rosehart, "A Transmission Planning Framework Considering Future Generation Expansions in Electricity Markets," *IEEE Transactions on Power Systems*, Vol. 25, pp. 1987-1995, 2010.
- [172] A. Castillo and D. F. Gayme, "Profit maximizing storage allocation in power grids," in Proc. of the 2013 *IEEE 52nd Annual Conference on Decision and Control (CDC)*, 2013, pp. 429-435.
- [173] D. Pudjianto, M. Aunedi, P. Djapic, and G. Strbac, "Whole-Systems Assessment of the Value of Energy Storage in Low-Carbon Electricity Systems," *IEEE Transactions on Smart Grid*, Vol. 5, pp. 1098-1109, 2014.
- [174] P. Denholm, J. Jorgenson, M. Miller, and E. Zhou, "Methods for Analyzing the Economic Value of Concentrating Solar Power with Thermal Energy Storage," 2015. [Online]. Available at: <http://www.nrel.gov/docs/fy15osti/64256.pdf>.
- [175] . P. Denholm, J. Jorgenson, M. Hummon, T. Jenkin, D. Palchak, B. Kirby, O. Ma, and M. O'Malley, "The Value of Energy Storage for Grid Applications," 2013. [Online]. Available at: <http://www.nrel.gov/docs/fy13osti/58465.pdf>.
- [176] H. Mohsenian-Rad, "Optimal Bidding, Scheduling, and Deployment of Battery Systems in California Day-Ahead Energy Market," *IEEE Transactions on Power Systems*, Vol. PP, pp. 1-12, 2015.
- [177] H. Mohsenian-Rad, "Coordinated Price-Maker Operation of Large Energy Storage Units in Nodal Energy Markets," *IEEE Transactions on Power Systems*, Vol. PP, pp. 1-12, 2015.
- [178] C. G. Baslis and A. G. Bakirtzis, "Mid-Term Stochastic Scheduling of a Price-Maker Hydro Producer With Pumped Storage," *IEEE Transactions on Power Systems*, Vol. 26, pp. 1856-1865, 2011.
- [179] J. A. M. Sousa, F. Teixeira, and S. Faias, "Impact of a price-maker pumped storage hydro unit on the integration of wind energy in power systems," *Energy*, Vol. 69, pp. 3-11, 5/1/ 2014.
- [180] L. Tao and M. Shahidehpour, "Dynamic Ramping in Unit Commitment," *IEEE Transactions on Power Systems*, Vol. 22, pp. 1379-1381, 2007.
- [181] D. Rajan and S. Takriti, "Minimum Up/Down Polytopes of the Unit Commitment Problem with Start-Up Costs," *IBM Research Report*, Jun. 2005.
- [182] "Resolving Infeasibilities & High Spring Washer Price situations – An Overview," Transpower, *Technical Report*, 2010. [Online]. Available at: <http://tinyurl.com/ndqoy8f>

- [183] "The IEEE Reliability Test System - 1996," A report prepared by the Reliability Task Force of the Application of Probability Methods Subcommittee, *IEEE Trans. Power Syst.*, vol. 14, no. 3, pp. 1010-1020, Aug. 1999.
- [184] "REAL Library," University of Washington. [Online] Available at: www.ee.washington.edu/research/real/library.html
- [185] H. Pandžić, T. Qiu, and D. Kirschen, "Comparison of State-of-the-Art Transmission Constrained Unit Commitment Formulations," in *Proc. of IEEE PES General Meeting 2013*, Vancouver, Canada, July 2013, pp. 1-5.
- [186] M. Ortega-Vazquez, *Optimizing the Spinning Reserve Requirements*, PhD dissertation, University of Manchester, May 2006.
- [187] P. Pinson and H. Madsen, "Ensemble-based probabilistic forecasting at Horns Rev," *Wind Energy*, vol. 12, no. 2, pp. 137-155, 2009.
- [188] R. Jursa, "Wind power prediction with different artificial intelligence models," in *Proceedings of the 2007 European Wind Energy Conference*, Milan, Italy, May 2007.
- [189] T. Hastie, R. Tibshirani, and J. Friedman. *The Elements of Statistical Learning: Data Mining, Inference and Prediction*. Springer, second ed., 2009.
- [190] A. J. Smola and B. Schölkopf, "A Tutorial on Support Vector Regression," *Stat. Comput.*, vol. 14, no. 3, pp. 199-222, Aug. 2004.
- [191] G. Giebel, "The State of the Art in Short-Term Prediction of Wind Power - A Literature Review, 2nd Edition," 2011. [Online] Available at: www.prediktor.dk/publ/GGiebelEtAl-StateOfTheArtInShortTermPrediction_ANEMOSplus_2011.pdf
- [192] L. Breiman, "Random Forests," *Mach. Learn.*, vol. 45, no. 1, pp. 5-32, Oct. 2001.
- [193] P. Pinson and G. Kariniotakis, "Conditional Prediction Intervals of Wind Power Generation," *IEEE Trans. Power Syst.*, Vol. 25, No. 4, pp. 1845-1856, 2010.
- [194] N. Growe-Kuska, H. Heitsch, and W. Romisch, "Scenario reduction and scenario tree construction for power management problems," in *Proc. 2003 IEEE Power Tech Conference*, Bologna, Italy, June 2003, pp. 1-7.
- [195] C. W. Potter, D. Lew, J. McCaa, S. Cheng, S. Eichelberger, and E. Gritmit, "Creating the Dataset for the Western Wind and Solar Integration Study," in *Proc. of the 7th International Workshop on Large Scale Integration of Wind Power and on Transmission Networks for Off-shore Wind Farms*, Madrid, Spain, May 2008, pp. 1-7.

- [196] B.M. Hodge and M. Milligan, "Wind Power Forecasting Error Distributions over Multiple Timescales," in *Proc. of IEEE PES General Meeting 2011*, Michigan, Detroit, July 24-29, 2011.
- [197] M. S. Nazir and F. Bouffard "Intra-hour wind power characteristics for flexible operations," in *Proc. of IEEE PES General Meeting 2012*, San Diego, CA, July 2012, pp. 1-8.
- [198] G. J. Hahn and S. S. Shapiro. *Statistical Models in Engineering*. John Wiley & Sons, 1967.
- [199] Q. Zheng, J. Wang, M. and A. Liu, "Stochastic Optimization for Unit Commitment – A Review," *IEEE Trans. Power Syst.*, early access.
- [200] A. Papavasiliou and S. S. Oren, "A comparative study of stochastic unit commitment and security-constrained unit commitment using high performance computing," in *Proc. of 2013 European Control Conference (ECC)*, 2013, pp. 2507-2512.
- [201] V. Zavala, M. Anitescu, A. Kannan, C. Petr, "On the Convergence of Day-Ahead and Real-Time Electricity Markets," *FERC*. [Online]. Available at: <http://www.ferc.gov/CalendarFiles/20110628130756-Jun28-SesC3-Zavala-Argonne.pdf>, 2011.
- [202] G. Anders, "Commitment Techniques for Combined-Cycle Generating units," *NYISO*. [Online]. Available at: <http://tinyurl.com/kw5w517>, 2005.
- [203] P. Bendotti, C. D'Ambrosio, G. Doukopoulos, A. Lenoir, L. Liberti, and Y. Sahraoui, "MILP model for a real-world hydro-power unit-commitment problem," *2014 Mixed Integer Programming Workshop*. [Online]. Available at: <http://tinyurl.com/lyu5bca>, 2014.
- [204] K. K. Kariuki and R. N. Allan, "Evaluation of reliability worth and value of lost load," *IEE Proceedings – Gener. Transm. Distrib.*, Vol. 143, No. 2, pp. 171-180, 1996.
- [205] J. G. Deqiang and E. Litvinov, "Energy and reserve market designs with explicit consideration to lost opportunity costs," *IEEE Trans. Power Syst.*, Vol. 18, No. 1, pp. 53-59, 2003.
- [206] E. Saiz-Marin, J. Garcia-Gonzalez, J. Barquin, and E. Lobato, "Economic Assessment of the Participation of Wind Generation in the Secondary Regulation Market," *IEEE Trans. Power Syst.*, Vol. 27, No. 2, pp. 866-874, 2012.
- [207] J. M. Morales, A. J. Conejo, and J. Perez-Ruiz, "Economic Valuation of Reserves in Power Systems With High Penetration of Wind Power," *IEEE Trans. Power Syst.*, Vol. 24, No. 2, pp. 900-910, 2009.
- [208] M. Lange, "Analysis of the uncertainty of wind power predictions," Ph.D. dissertation, Fakultt Mathematik und Naturwissenschaften, Carl von Ossietzky Universitt, Oldenburg, Germany, 2003.

- [209] M. Lange, "On the Uncertainty of Wind Power Predictions Analysis of the Forecast Accuracy and Statistical Distribution of Errors," *Journal of Solar Energy Engineering*, Vol. 127, No. 2, pp. 177-184, 2005.
- [210] R. P. Brent, "Algorithms for Minimization Without Derivatives", *Dover Publications*, 1973.
- [211] J. Kim, Ph.D. Thesis, "Iterated Grid Search Algorithm on Unimodal Criteria," Virginia Polytechnic Institute and State University, 1997.
- [212] M. A. Ortega-Vazquez and D. S. Kirschen, "Optimizing the Spinning Reserve Requirements Using a Cost/Benefit Analysis," *IEEE Transactions on Power Systems*, Vol. 22, No. 1, pp. 24-33, 2007.
- [213] ERCOT, Day-ahead Market Information, [Online]. Available at: www.ercot.com/mktinfo/dam/
- [214] M. A. Ortega-Vazquez and D. S. Kirschen, "Should the spinning reserve procurement in systems with wind power generation be deterministic or probabilistic?" in *Proc. of SUPERGEN '09. International Conference on Sustainable Power Generation and Supply*, pp. 1-9, 2009.
- [215] J. Aho, A. Buckspan, L. Pao, and P. Fleming, "Active Power Control System for Wind Turbines Capable of Primary and Secondary Frequency Control for Supporting Grid Reliability," in *Proc. of 2012 AIAA/ASME Wind Symposium*, Grapevine, TX, 2012.
- [216] Z. S. Zhang, Y. Z. Sun, and L. Cheng, "Potential of trading wind power as regulation services in the California short-term electricity market," *Energy Policy*, Vol. 59, pp. 885-897, 2013.
- [217] M. A. Ortega-Vazquez, D. S. Kirschen, "Optimising the spinning reserve requirements considering failures to synchronise," *IET on Generation, Transmission, and Distribution*, Vol. 2, No. 5, pp. 655-665, 2008
- [218] G. Liu and K. Tomsovic, "Quantifying Spinning Reserve in Systems with Significant Wind Power Penetration," *IEEE Trans. Power Syst.*, Vol. 27, No. 4, pp. 2385-2393, 2012.
- [219] K. Dvijotham, M. Chertkov, and S. Backhaus, "Storage Sizing and Placement through Operational and Uncertainty-Aware Simulations," in *Proc. of the 47th HI Int. Conf. on Syst. Sc.*, pp. 2408-2416, 2014.
- [220] D. Krishnamurthy, W. Li, and L. Tesfatsion, "An 8-zone test system based on ISO New England data: Development and application," *IEEE Trans. Pwr. Syst.*, early access, pp. 1-12, 2015.
- [221] J. M. Arroyo, "Bilevel programming applied to power system vulnerability analysis under multiple contingencies," *IET Gener. Transm. Distrib.*, vol. 4, pp. 178-190, 2010.

- [222] S. A. Gabriel, A. J. Conejo, D. Fuller, B. F. Hobbs, and C. Ruiz, “Complementarity Modeling in Energy Markets,” *Springer: International Series in Operation Research & Management Science*, New York, USA, 2012.
- [223] R. Fernández-Blanco, J. M. Arroyo, and N. Alguacil, “A unified bilevel programming framework for price-based market clearing under marginal pricing,” *IEEE Trans. Power Syst.*, vol. 27, no. 1, pp. 517–525, Feb. 2012.
- [224] L. Baringo and A. J. Conejo, “Strategic wind power investment,” *IEEE Trans. Power Syst.*, vol. 29, no. 3, pp. 1250–1260, May 2014.
- [225] S. Tegen, E. Lantz, M. Hand, B. Maples, A. Smith, and P. Schwabe, “2011 Cost of Wind Energy: Review,” National Renewable Energy Laboratory, 2011. [Online]. Available at: <http://www.nrel.gov/docs/fy13osti/56266.pdf>
- [226] P. D. Easton, “PE ratios, PEG ratios, and estimating the implied expected rate of return on equity capital,” *The Accounting Review*, vol. 79, no. 1, pp. 73–95, Jan. 2004.
- [227] A. L. Motto, J. M. Arroyo, and F. D. Galiana, “A mixed-integer LP procedure for the analysis of electric grid security under disruptive threat,” *IEEE Trans. Power Syst.*, vol. 20, no. 3, pp. 1357–1365, Aug. 2005.
- [228] C. Ruiz and A. Conejo, “Pool strategy of a producer with endogenous formation of LMPs,” *IEEE Trans. Power Syst.*, vol. 24, no. 4, pp. 855–866, Nov. 2009.
- [229] R. Fernández-Blanco, J. M. Arroyo, and N. Alguacil, “Bilevel programming for price-based electricity auctions: A revenue-constrained case,” *EURO J. Comput. Optim.*, vol. 3, no. 3, pp. 163–195, Apr. 2015.
- [230] C. A. Floudas, *Nonlinear and Mixed-Integer Optimization: Fundamentals and Applications*. New York, NY, USA: Oxford University Press, 1995.
- [231] J. F. Bard and J. T. Moore, “A branch and bound algorithm for the bilevel programming problem,” *SIAM J. Sci. Statist. Comput.*, vol. 11, no. 2, pp. 281–292, 1990.
- [232] J. Hu, J. E. Mitchell, J.-S. Pang, K. P. Bennett, and G. Kunapuli, “On the global solution of linear programs with linear complementarity constraints,” *SIAM J. Optim.*, vol. 19, no. 1, pp. 445–471, 2008.
- [233] Federal Energy Regulatory Commission (FERC), “Price Formation in Organized Wholesale Electricity Markets: Staff Analysis of Energy Offer Mitigation in RTO and ISO Markets,” 2014. [Online]. Available at: <https://www.ferc.gov/legal/staff-reports/2014/AD14-14-mitigation-rto-iso-markets.pdf>

- [234] R. O'Neill, D. Mead, and P. Malvadkar, "On market clearing prices higher than the highest bid and other almost paranormal phenomena," *The Electricity Journal*, vol. 18, no. 2, pp. 19–27, Mar. 2005.
- [235] F. Wolak, "Diagnosing the California electricity crisis," *The Electricity Journal*, vol. 16, no. 7, pp. 11–37, Aug.-Sep. 2003.
- [236] Eastern Wind Dataset, *National Renewable Energy Laboratory*, 2012. [Online]. Available at: http://www.nrel.gov/electricity/transmission/eastern_wind_methodology.html
- [237] B. Pitt, "Applications of data mining techniques to electric load profiling", *PhD thesis*, University of Manchester, UK, 2000. [Online]. Available at: http://www.ee.washington.edu/research/real/Library/Thesis/Barnaby_PITT.pdf
- [238] S. Wogrin, D. Galbally, and J. Reneses, "Optimizing storage operations in medium- and long-term power system models," *IEEE Trans. Power Syst.*, early access, pp.1–10, 2015.
- [239] D. Getman, A. Lopez, T. Mai, and M. Dyson, "Methodology for Clustering High-Resolution Spatiotemporal Solar Resource Data," Technical report, 2015. [Online]. Available at: <http://www.nrel.gov/docs/fy15osti/63148.pdf>
- [240] R. E. Rosenthal, "GAMS – A Users Guide", GAMS Corp., 2013.
- [241] Hyak Supercomputer, 2015. [Online]. Available at: <http://escience.washington.edu/content/hyak-0>
- [242] V. Krishnan and T. Das, "Optimal allocation of energy storage in a co-optimized electricity market: Benefits assessment and deriving indicators for economic storage ventures", *Energy*, vol. 815, pp. 175–188, Mar. 2015.